

THESIS

REACTIVE TRANSPORT MODELING OF NUTRIENTS IN ARCTIC TUNDRA  
STREAMS

Submitted by

Woochul Kang

Department of Civil and Environmental Engineering

In partial fulfillment of the requirements

For the Degree of Master of Science

Colorado State University

Fort Collins, Colorado

Fall 2014

Master's Committee:

Advisor: Michael N. Gooseff

Jorge A Ramirez

Ryan Bailey

Tim Covino

Copyright by Wochul Kang 2014

All Rights Reserved

## ABSTRACT

### REACTIVE TRANSPORT MODELING OF NUTRIENTS IN ARCTIC TUNDRA STREAMS

The one dimensional solute transport inflow and storage (OTIS) model is used to simulate the transport of non-conservative and conservative solutes in arctic tundra streams. Field research was conducted in I8 Inlet and Outlet streams,(in Northern Alaska) which are located upstream and downstream of I8 Lake between June and September 2010 and 2011 (thaw season) and these two streams are classified as alluvial, low gradient, headwater tundra streams. Repeat solute injections were conducted on both streams. Two sets of solute injections were made, Injection A is sodium chloride (NaCl) and phosphate ( $\text{PO}_4$ ) and Injection B is sodium chloride (NaCl) and ammonium ( $\text{NH}_4$ ). The NaCl is conservative and other two solutes are non-conservative solutes.

With the observed concentration data, OTIS-P was used to estimate the model parameters values related to transport (dispersion and advection), transient storage and nutrient uptake mechanisms, by nonlinear least squares fit. The dispersion coefficient and main channel cross-sectional area parameters represented transport, storage zone cross-sectional area and exchange coefficient parameters represent transient storage, and 1<sup>st</sup> order decay coefficient in main channel and storage zone represent nutrient uptake. Additionally, transport and uptake metrics were calculated with estimated parameters. We assumed discharge, stream water temperature, and date (as a surrogate for thaw depth beneath the stream) were potential control variables on transport, transient storage, and nutrient uptake processes.

Linear regression was conducted to identify potential relationships between these estimated parameters and metrics and control variables. Hydraulic controls are positively correlated with transport and transient storage mechanisms and stream temperature has positive relationships with nutrient uptake of non-conservative solutes ( $\text{NH}_4$  and  $\text{PO}_4$ ). Although, this study did not find direct influence of date (indicator of thaw depth) as a control, active layer condition is an important factor in solute transport dynamics in arctic region. Moreover, additional controls should be considered to explain solute transport dynamics more exactly. Beyond the scope of this study, for example, stream ecosystem status or activity may more directly explain  $\text{NH}_4$  and  $\text{PO}_4$  uptake variability.

## TABLE OF CONTENTS

Abstract .....	ii
1. Introduction.....	1
2. Study Site / Method.....	4
2.1 Study Site .....	4
2.1.1 Overview of the TOOLIK region.....	4
2.2 Field Data Collection .....	5
2.2.1 Solute Injection .....	5
2.2.2 Gauging and Monitoring .....	6
2.3 Modeling Method .....	8
2.3.1 OTIS .....	9
2.3.2 Metrics Characterizing Transient Storage.....	10
2.3.3 Modeling OTIS and OTIS-P.....	11
2.3.4 Output of OTIS and OTIS-P.....	13
3. Results .....	15
3.1 Three Potential Control Variables .....	15
3.2 Discharge and Hydraulic Controls on Solute Transport Dynamics.....	18
3.2.1 I8 Inlet .....	18
3.2.2 I8 Outlet.....	23
3.3 Date and Thaw Depth .....	28
3.3.1 I8 Inlet .....	28
3.3.2 I8 Outlet.....	32
3.3 The Ratio non-conservative to conservative masses and Mass loss.....	37
3.3.1 I8 Inlet .....	37
3.3.2 I8 Outlet.....	40
3.4 Stream Water Temperature as a Potential Control on the fate of PO <sub>4</sub> and NH <sub>4</sub> .....	42
3.4.1 I8 Inlet .....	42
3.4.2 I8 Outlet.....	47
4. Discussion.....	45
4.1 OTIS-P and Uncertainty.....	53
4.2 Relationship between each parameter and control variable .....	54
4.3 Other control variables effects on solute transport dynamics .....	56
5. Conclusion .....	59
Reference.....	60

Appendix 1 .....	66
Appendix 2 .....	80
Appendix 3 .....	86
Appendix 4 .....	87

## 1 Introduction

The transient storage model has been used in many studies of stream solute transport, as it served to present the delay of downstream transport in the small eddies, pools and hyporheic zones of streams. The most popular mathematical transient storage model accounts for conservative and non-conservative transport, OTIS-P. Several studies have found that reactive terms were related to the rates of chemical and microbial processes and these have a first order dependence on the concentration of reactant [Mcknight et al., 2004; Gooseff et al., 2004]. Many studies have found that transient storage in the hyporheic zone resulted in biochemical transformations such as nutrient uptake and cycling, regeneration of inorganic nutrients and organic matter mineralization and these processes have great importance on ecosystem [D'Angelo et al., 1993; Lyons et al., 1998; Edward et al., 2003; Gooseff et al., 2004]. Thus, stream solute transport dynamics are important to stream ecosystem function and processes.

Because of the increasing attention paid to the effects of solute transport (transient storage and chemical reaction), numerous studies have focused on Interpretation of model parameters. Various studies conducted investigations on the relationship between transport and transient storage and hydraulic parameters such as discharge, velocity and channel cross-sectional area [Legrand-Marcq & Laudelout, 1985; Wondzell & Swanson, 1996]. Additionally, other controls (e.g. morphology, sediments characteristics, etc) have been considered to identify controls or relationships to transport and transient storage mechanisms [Leopold & Maddock, 1953; Kasahara & Wondzell, 2003]. Characteristics and control variables (e.g climatic variation, nutrient cycling and dynamics) of the transport and uptake of non-conservative solutes have been also studied [Mullholland et al., 1997; Hall et al., 2002].

Arctic tundra streams are underlain by permafrost, yet they exchange water with thaw bulbs that surround the stream during the thaw season. Bradford et al. [2005] found that the active layer of a peat bed arctic stream was thicker than the terrestrial environments in the same region. Various studies conducted investigations on the characteristics of the thaw bulb. The active layer development and how it affects stream processes depend on surface energy balance, and in a typical season, the thaw depth increases rapidly in early summer, and then becomes fairly consistent by middle to late summer [Sturm et al., 2005; Zarnetskt et al., 2007]. When the streambeds thaw, and streams are flowing, there is an opportunity for hyporheic exchange to occur [Bradford et al., 2005]. Several studies of streams in permafrost regions have proposed that, the thaw bulb development during the summer thaw season influences hyporheic exchange, and therefore stream ecosystems, in addition to channel morphology [Edwardson et al., 2003; Gooseff et al., 2004; Zarnetske et al., 2007; Gooseff et al., 2004]. In addition to hyporheic exchange controls by thaw bulb development, stream nutrient uptake may also be influenced by water temperature, as stream ecosystem demands change with water temperature.

In this study, I evaluate the stream solute transport dynamics in two arctic streams to explore the controls of hydraulics (discharge), thaw bulb development (date), and stream temperature on three processes: (transport, transient storage and nutrient uptake, Figure 1-1). Repeat instantaneous stream tracer experiments were simulated with OTIS-P to estimate model parameters which represent transport processes. Parameter optimization was conducted using a nonlinear least squares fitting of simulated values to observations. Dispersion coefficient ( $D$ ) and main stream cross-sectional area ( $A$ ) are parameters related to transport process, storage zone cross-sectional area ( $A_s$ ) and exchange coefficient ( $\alpha$ ) are parameter values that represent transient storage processes, and 1<sup>st</sup> order decay coefficient in the main channel ( $\lambda$ ) and 1<sup>st</sup> order decay coefficient in the storage zone ( $\lambda_s$ ) are parameters

related to nutrient uptake of  $\text{NH}_4$  and  $\text{PO}_4$ . In addition, discharge, date (as a surrogate for thaw bulb development) and average stream water temperature, which were acquired from field studies, represent each control variable (hydraulic conditions, thaw depth and stream temperature). Linear regression is conducted with these data to identify relationships between model parameters and three solute transport and fate processes. It is expected that hydraulic conditions control transport and transient storage mechanisms, that transient storage is related to thaw depth, and that stream water temperature has a significant correlation to the fate of non-conservative solutes.

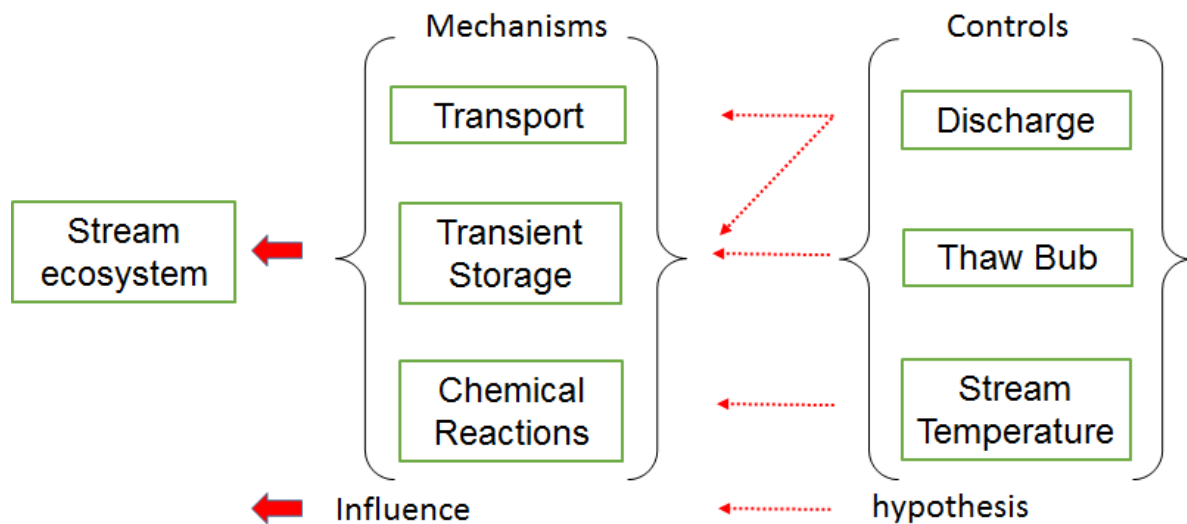


Figure 1-1 Expected relationships between controls on solute transport and fate mechanisms in streams, and their ultimate influence on the stream ecosystem.

## 2 Study site/Method

### 2.1 Study Site

#### 2.1.1 Overview of the TOOLIK Region

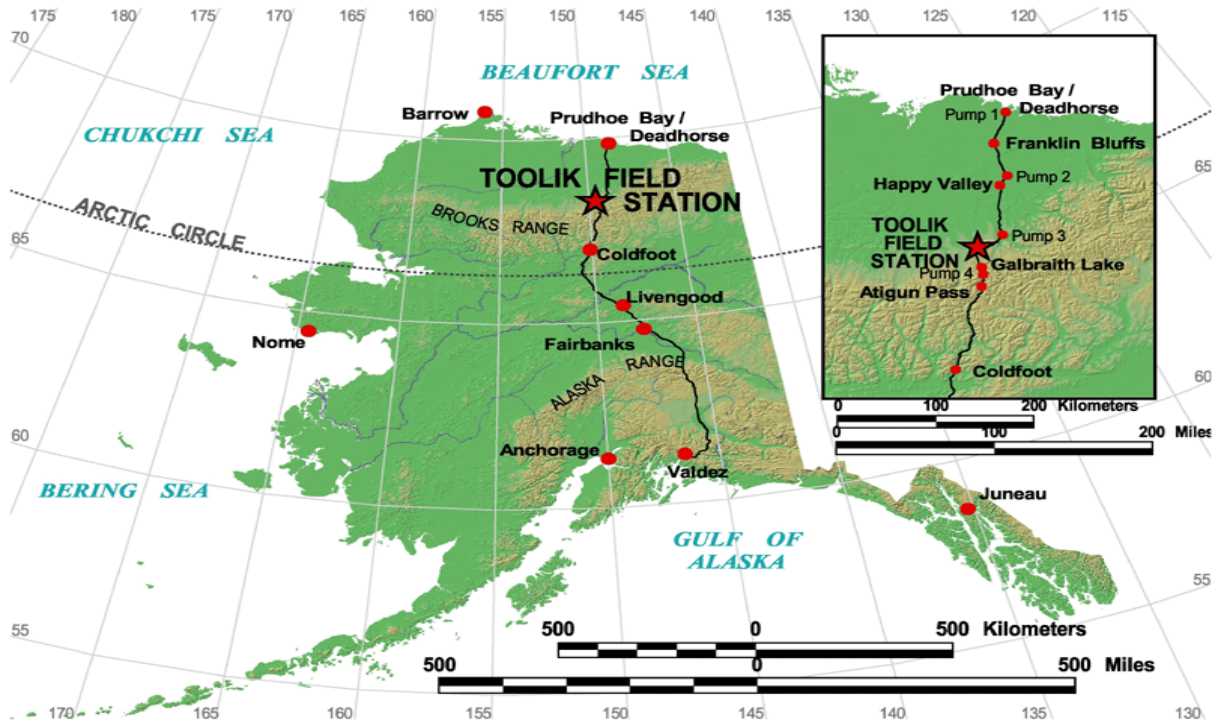


Figure 2-1 Map of Toolik Region. Field research was conducted in the vicinity of Toolik field station. <http://toolik.alaska.edu/gis/maps/maps.php?category=general>

The study area was located in the North Slope of Alaska's Brooks Range, within the Toolik Research Natural Area (Figure 2-1). Glacial sediments from the greater Wisconsinian glaciations established river drainages and stream side vegetation consists dominantly of sedges, grasses and mixed dwarf birch. The regional hydrology is dominated by spring snow melt and this initiates a brief surface flow period from May through late September [Kane et al., 1989]. This region is high polar desert due to small average annual rainfall, 18cm which occurs during thaw season [Kane et al., 1989; McNamara et al., 1997, 1998]. Streams of this region are underlain by continuous permafrost. Thus, stream water can be connected to shallow groundwater, but not deep groundwater. Stream water exchange results in exchange of heat between the stream channel and streambed [Brosten et al., 2006, 2009]. Two streams

were selected for this study, I8 Inlet and I8 Outlet, located upstream and downstream of I8 Lake, respectively (Figure 2-2). Both two streams were divided into 2 reaches with a single upstream injection point, and 2 sampling stations downstream (Table 2-1). We assume that each reach is an appropriate representation of stream morphology and hydrologic features. Both streams drain tundra-covered foothills of North Slope and are meandering streams with gravel and cobble beds. Due to these geomorphic characteristics, they were classified as alluvial, low gradient, headwater tundra streams.

Stream Name	Year	Sub-reach 1 [m]	Sub-reach 2 [m]	Total-reach
I8 Inlet	2010	340	160	550
	2011	340	215	555
I8 Outlet	2010, 2011	260	100	360

Table 2-1 Characteristics of Stream reaches, I8 Inlet and I8 Outlet

## 2.2 Field Data Collection

### 2.2.1 Solute Injection

All stream tracer experiments in this study were conducted using the instantaneous solute injection (SI) technique, in which a known mass of dissolved tracer is directly applied to streams. Between June and September 2010 and 2011, two sets of solute slugs were released on both I8 Inlet and I8 Outlet in a day; Injection A (sodium chloride (NaCl), phosphate (PO<sub>4</sub>) and Nitrate (NO<sub>3</sub>)) and Injection B (sodium chloride (NaCl) and ammonium (NH<sub>4</sub>)). From the Injection A results, NO<sub>3</sub> did not show uptake, and therefore ignored in analysis. The information about each injection, such as solute masses and time of release, were used to define stream boundary condition in the solute transport modeling. Cl is non-reactive solute, considered a tracer for solute transport, and PO<sub>4</sub> and NH<sub>4</sub> are reactive solutes. Non-reactive and reactive solutes were simulated to characterize conservative and

non-conservative transport of fate processes. At each sampling location for each injection simple mass balance calculations were made by integrating under the solute concentration breakthrough curves (BTCs). The ratio conservative (Cl) masses to non-conservative (PO<sub>4</sub> and NH<sub>4</sub>) masses were estimated to assess proportions or percentages of loss, when compared the ratio of injected masses

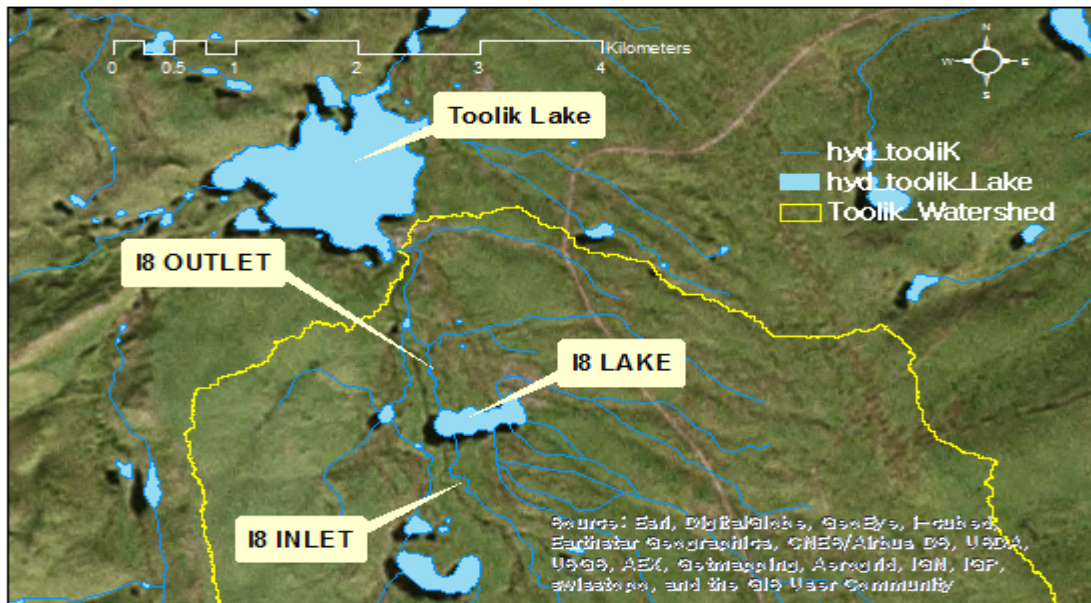


Figure 2-2 Location of experimental two reaches I8 Inlet and Outlet (map modified from <http://toolik.alaska.edu/gis/maps/maps.php?category=general>)

### 2.2.2 Gauging and Monitoring

Discharge was measured by the dilution gauging technique using NaCl and high frequency specific conductance (SC) measurements by HOBO U24-001 conductivity logger record. Monitored specific conductivity translated to concentration by calibration curves which by correcting for background SC [Gooseff & McGlynn, 2005; Payn et al., 2009].

Discharge is quantified with using following equation.

$$Q [L^3/T] = \frac{M}{\int_0^t C(t)} \left[ \frac{M}{(M/L^3) \times [T]} \right] \quad (2 - 1)$$

Where, Q is discharge [L/s], M is the injected mass [g], C is concentration, t is time [s] and

$\int_0^t C(t)$  is 0<sup>th</sup> moment, integrating area under a curve of BTC. Moreover, any observed difference discharge between injection and monitoring points were treated as lateral inflow or outflow in the transient storage modeling (Appendix 1).

In a few cases, dilution gauging discharge was not conducted or had a poor result. When this occurred, discharge in the model was taken from a seasonal record of discharge at a long-term monitoring station at the end of each reach. These records were developed by relating discrete discharge measurements to continuously measured stage data (HOBO U20 water Level Data Logger which was located in deep-pool location).

$$Q = Cd^b \quad (2 - 2)$$

Where, d is depth (m), and c and b are constants. For I8 Inlet c= 45607 and b=5.8 and I8 Outlet, c=18640 and b=6.81. These relationships were used to transform continuous stage measurements into continuous discharge measurements.

Stream temperatures and temperature at 1m depth beneath stream bed were also monitored continuously at I8 Inlet and I8outlet with Campbell Scientific CR1000 data loggers, at 3-hour interval. Non-conservative ( $PO_4$ ) concentrations were measured by analyzing for dissolved orthophosphate from filtered through Glass Fiber Filters. The  $PO_4^{3-}$  reacts with ammonium molybdate and antimony potassium tartrate under acidic conditions to form a antimony-phosphomolybdate complex. This complex is reduced with ascorbic acid to form a blue complex which absorbs light at 880 nm. The absorbance is proportional to the concentration of  $PO_4^{3-}$  in the digested sample. In the case of ammonia, when it is heated with salicylate and hypochlorite in an alkaline phosphate buffer an emerald green color is produced which is proportional to the ammonia concentration. This color is intensified by the addition of sodium nitroprusside. In addition, if distillation is required, the sample is buffered at a pH of 9.5 with a borate buffer to decrease hydrolysis of cyanates and organic nitrogen compounds, and is distilled into a dilute solution of sulfuric acid.

## 2.3 Modeling Method

### 2.3.1 OTIS (One-dimensional Solute Transport with Inflow and Storage)

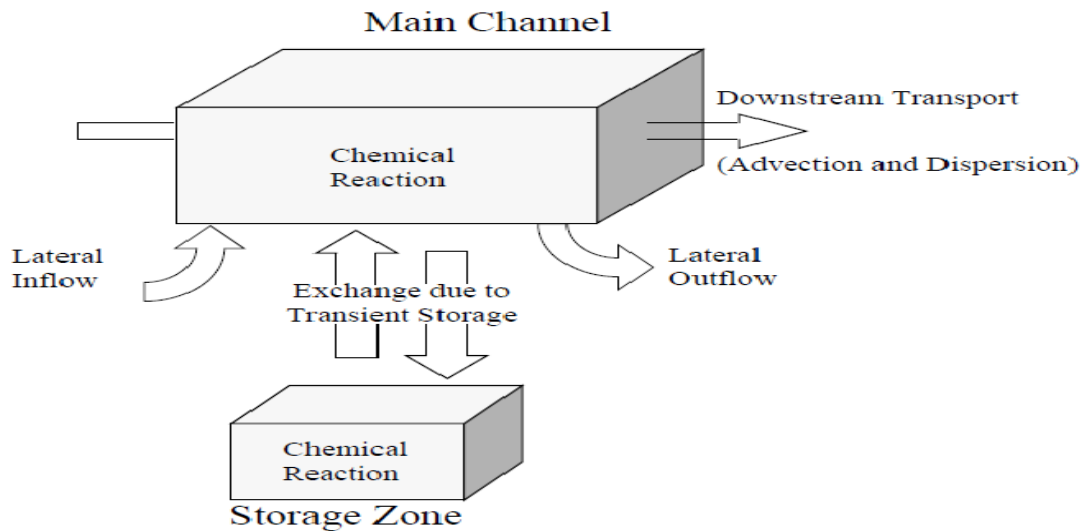


Figure 2-3 Conceptual model which include the main channel and the storage zone. Source : One-Dimensional Transport with Inflow and Storage (OTIS): A Solute Transport Model for Streams and Rivers, by Runkel, R. L. (1998), U.S. Geological Survey Water-Resources Investigations Report 98-4018, p. 3.

The OTIS model simulates stream solute transport in streams and includes not only advection and dispersion in main channel, but also exchange of solute with storage zones. Storage zones are all lumped in the model, but may be stagnant zones in the stream channel or exchange through the subsurface. This model is referred to as transient storage model [Bencala & Walter, 1983]. Processes that affect solute concentrations within the stream solute models are depicted in Figure 2-3. Solutes in main channels are transported downstream by advection and dispersion. However, these two transport mechanisms are not included in the storage zone. Lateral inflow is incoming water to main channel such as overland flow, inter flow and ground-water discharge and lateral outflow represents additional water discharging from the main channel to the surrounding watershed. Transient solute exchanges between the main channel and the storage zone and chemical reactions can be represented to occur in the

main channel and storage zone. Stream reach and storage zone are represented with finite difference elements. In this study, length of all finite difference elements is set as 1m.

Observed tracer concentration data from non-reactive solute was simulated with OTIS. The governing equations for this model are organized by writing mass balance equations for two conceptual areas [Runkel & Broshears, 1991]. The main channel and the storage zone

$$\frac{\partial C}{\partial t} = -\frac{Q}{A} \frac{\partial C}{\partial x} + \frac{1}{A} \frac{\partial}{\partial x} \left( AD_x \frac{\partial C}{\partial x} \right) + \frac{q_{LIN}}{A} (C_L - C) + \alpha (C_s - C) \quad (2-3)$$

$$\frac{\partial C_s}{\partial t} = \partial \frac{A}{A_s} (C - C_s) \quad (2-4)$$

Where Q is stream discharge (m<sup>3</sup>/s), C is main channel solute concentration (mg/m<sup>3</sup>), C<sub>s</sub> is the storage zone solute concentration (mg/L), C<sub>L</sub> is the lateral inflow solute concentration (mg/m<sup>3</sup>), A is main channel area (m<sup>2</sup>), A<sub>s</sub> is the storage zone area (m<sup>2</sup>), D<sub>x</sub> is the dispersion coefficient (m<sup>2</sup>/s), q<sub>LIN</sub> is the lateral inflow rate (m<sup>3</sup>/s), and α is the main channel – storage zone exchange rate (1/s).

In case of non-conservative solutes, chemical reaction should be considered. OTIS-P can simulate sorption and first-order decay. However, sorption would be ignored in this modeling because nutrient uptake can be well represented by 1<sup>st</sup> order decay, which can be represented by adding terms to equations (2-3) and (2-4).

$$\frac{\partial C}{\partial t} = L(C) + -\lambda C \quad (2-5)$$

$$\frac{\partial C_s}{\partial t} = S(C_s) + -\lambda_s C_s \quad (2-6)$$

Where L(C) and S(C<sub>s</sub>) are physical processes in the main channel and storage zone (equation 2-3 and 2-4), λ is main channel first order decay coefficient (1/s), λ<sub>s</sub> is storage zone first order decay coefficient (1/s). For the reason of accuracy, efficiency and stability, the Crank-Nicolson techniques are used for these differential equations (equation 2-3 ~ 2-6). In this

study, the integration of time steps within time-variable solution is set to be 0.004 (and 0.005 if simulation results were unstable with the smaller time step)

### 2.3.2 Metrics Characterizing Transient Storage

Several metrics have been developed to characterize transient storage. One common metric is turnover length  $L_s$  [Mulholland et al., 1994]

$$L_s = \frac{u}{\alpha} \quad (2 - 7)$$

Stream velocity,  $u$  is computed by dividing the stream volumetric flow rate by stream cross-sectional area. The turnover length characterizes how far a solute travels in the main channel before entering the storage zone. After traveling a distance  $L_s$ , the molecule remains in storage zone for an average time given by  $t_s$  [Thackston & Schnelle, 1970].

$$t_s = \frac{A_s}{\alpha A} \quad (2 - 8)$$

An additional metric is the storage exchange flux,

$$q_s = \alpha A \quad (2 - 9)$$

Which is reported in  $m^3/s/m^2$ . In addition, reaction significance factor (RSF) describes the effect of chemical reactions in storage zone from the stream-tracer injections and simulation.

$$RSF = \frac{\lambda_s t_s L}{L_s} \quad (2 - 10)$$

Where,  $\lambda_s$  is the reaction rate constant in the storage zone,  $t_s$  is the hydrologic residence time in the storage zone, and  $L$  is the length of the stream reach under consideration. When the values of RSF are greater than 0.2, it is suggested that chemical reactions in the storage zone are fast and flow through the storage zone significant enough to exert a cumulative influence on downstream chemistry.

### 2.3.3 Modeling OTIS and OTIS-P

A goal of this solute transport study is quantifying transport parameters by simulating observed concentrations. In field research, sodium chloride (NaCl) is subject to the physical processes of advection, dispersion and transient storage. We therefore want to estimate area of main channel and storage zone ( $A$  and  $A_s$ ) and coefficient of dispersion and storage ( $D$  and  $\alpha$ ). The  $\text{PO}_4$  and  $\text{NH}_4$  are simulated with fixed transport parameters to estimate 1<sup>st</sup> order decay coefficient in main channel and storage zone ( $\lambda$  and  $\lambda_s$ ). Estimation of these parameters was conducted by Nonlinear Least Squares (NLS) via a trial and error procedure using OTIS-P. The procedure starts with initial parameter estimates and the initial size of the trust region and then determines the simulated main-channel concentration corresponding to the observed concentration by equation (2-5) and (2-6). The observed solute concentration may be expressed as the sum of simulated concentration and a random error term.

$$C_k = f(\zeta, \vec{\theta}) + \varepsilon_k \quad K = 1..N \quad (2 - 11)$$

Where  $N$  is the number of observation,  $NP$  is the number of model parameter,  $c_k$  is the observed main channel solute concentration,  $f(\zeta + \vec{\theta})_k$  is a nonlinear function that simulates the  $k$ th observation,  $\zeta$  is time in time-variable problem and distance is steady-state problem,  $\vec{\theta}$  is a vector length  $NP$  containing the parameter estimates ( $D, A, A_s, \alpha, \lambda, \lambda_s$ ) and  $\varepsilon_k$  is random error associated with  $k$ th observation. The goal of NLS is to determine the vector of parameter estimate that minimized by

$$\text{RSS}(\vec{\theta}) = \sum_{k=1}^N \{ \omega_k [c_k - f(\zeta, \vec{\theta})]^2 \} = \sum_{k=1}^N (\omega_k \varepsilon_k^2) \quad (2 - 12)$$

Where  $\text{RSS}(\vec{\theta})$  is weighted residual sum of squares,  $w_k$  is weighting factor. NLS minimizes  $\text{RSS}(\vec{\theta})$  by an iterative process. During this process, parameter estimates updated by

$$\vec{\theta}_{m+1} = \vec{\theta}_m - (J^T W J + s + Y)_m^{-1} J_m^T W_m \vec{\varepsilon}_m^T \quad (2 - 13)$$

With condition

$$\sqrt{\sum_{l=1}^{NP} \left[ \frac{(\theta_{m+1,l} - \theta_{m,l})}{SCALE_l} \right]^2} \leq d_m \quad (2 - 14)$$

Where, S is NP by NP matrix, SCALE is typical size of parameter, W is N by N diagonal matrix of weighting factors, Y is NP by NP matrix which satisfied equation (2-14), d is size of trust region, l is quantities corresponding to lth parameter, m is the number of iteration,  $\vec{\epsilon}$  is vector of length N of residuals,  $\theta$  is estimates of lth parameter at mth iteration and J is N by NP matrix with  $J_{k,l}$  defined by

$$J_{k,l} = \frac{\partial f(\zeta, \vec{\theta})_k}{\partial \theta_l} \quad (2 - 15)$$

The iterative procedure continued until satisfying one of two criteria: 1) the relative change in parameters

$$\frac{\max \left[ \frac{|\theta_{m+1,l} - \theta_{m,l}|}{SCALE_l} \right]}{\max \left[ |\theta_{m+1,l}| - \frac{|\theta_{m,l}|}{SCALE_l} \right]} \leq STOPP, \quad l = 1, N \quad (2 - 16)$$

2) the change of the residual sum of squares.

$$\frac{fcst[RSS(\vec{\theta})]}{RSS(\vec{\theta}_m)} < STOPSS \quad (2 - 17)$$

Where, STOPP and STOPSS are convergence criteria and  $fcst[RSS(\vec{\theta})]$  is the expected change in the residual sum of squares.

Additionally, the time-variable upstream boundary condition was characterized.

There are 3 options (Fig 2-4) which can be used to simulate boundary condition (IBOUND):

1) Concentration-Step (IBOUND=1), 2) Flux-Step (IBOUND=2) and 3) Concentration-Continuous (IBOUND=3).

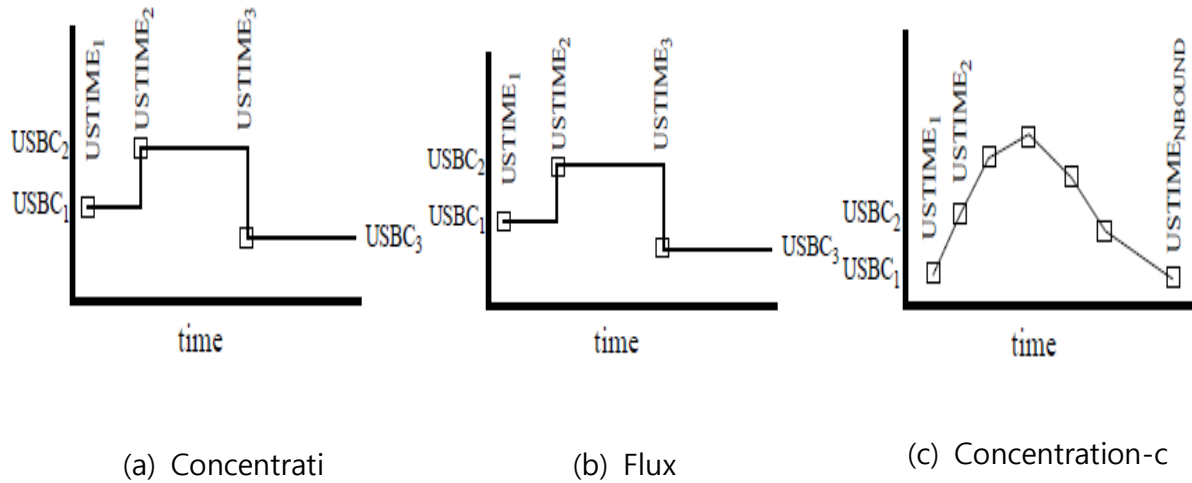


Figure 2-4 Upstream boundary condition options (a) Concentration-Step (b) Flux-Step (c) Concentration-Continuous Source : One-Dimensional Transport with Inflow and Storage (OTIS): A Solute Transport Model for Streams and Rivers, by Runkel, R. L. (1998), U.S. Geological Survey Water-Resources Investigations Report 98-4018, p. 36.

In this research, the concentration-step option was used for upstream boundary conditions. Under this option, boundary value corresponds to the upstream boundary concentration and this subsequently updated at appropriate time. Slug injections were simulated to occur over 3 or 4 time steps (0.005 hours)

$$C_{bc} = \frac{\text{mass injection}}{Q \times t_{inj}} \quad (2 - 18)$$

Where,  $C_{bc}$  is boundary concentration [mg/L],  $t_{inj}$  is time for conducting injection [s].

### 2.3.4 Output of OTIS and OTIS-P

The simulation models created 3 output files: 1) solute output file 2) parameter output file and 3) STARPAC output file. The breakthrough curves of simulated solutes from solute output files compare with observed concentration at monitoring points. Coefficients of determination ( $R^2$ ) are used for goodness of fit evaluation between observed concentrations and the simulated concentration.

$$R^2 = \frac{SS_{\text{reg}}}{SS_{\text{tot}}} = 1 - \frac{SS_{\text{res}}}{SS_{\text{tot}}} = \frac{\sum(y_i - \hat{y}_i)^2}{1 - \sum(y_i - \bar{y})^2} \quad (2 - 19)$$

Where,  $SS_{\text{tot}}$  is the total sum of squares (proportional to the sample variance),  $SS_{\text{reg}}$  is the regression sum of squares, also called the explained sum of squares and  $SS_{\text{res}}$  is the regression sum of squares, also called the unexplained sum of squares. The output files for solutes and coefficients of determinations are provided in the Appendix. STARPAC output file contains initial conditions and the statistical interpretation of results related to observed data and the NLS procedure (section 2.3.3). This output file also contains the upper and lower boundary value related to 95% confidence limits determined by NLS procedure. Additionally, since all transport parameters could not be negative value, estimated error terms below zero were ignored.

### 3 Results

#### 3.1 Three Potential Control Variables

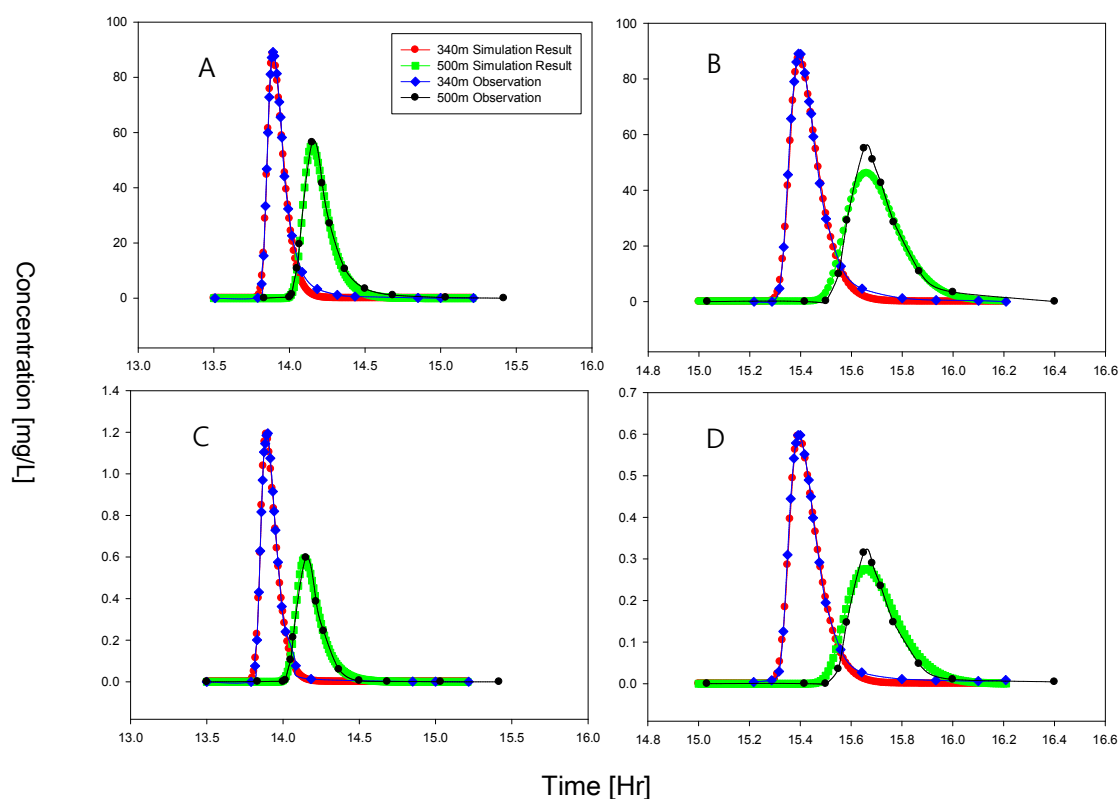


Figure 3-1 Break through curves from simulation result. A is Cl from injection A, B is Cl from injection B, C is PO<sub>4</sub> from injection A and D is NH<sub>4</sub> from injection B

The simulated and observed concentrations of conservative and non-conservative solutes were typically in excellent agreement (e.g. Figure3-1). The mass of solute injected and the masses which passed the sampling locations are presented in Table3-1. In most cases, calculated mass passing, as calculated from simulated and observed solute concentrations, were less than actual injected masses.

All transport and fate parameters were estimated by OTIS-P and they were related to the three control variables. The linear regression to determine whether there was a significant relationship. When a statistically significant regression was identified ( $P < 0.1$ ), the regression is displayed in the graph with solid line, otherwise, relationship is presented as a dashed line.

Stream	Date	Reach	Cl A [g]			Cl B [g]			PO <sub>4</sub> -P [g]			NH <sub>4</sub> -N [g]			
			Inj Mass	Sim Mass	OBS Mass	Inj Mass	Sim Mass	OBS Mass	Inj Mass	Sim Mass	OBS Mass	Inj Mass	Sim Mass	OBS Mass	
18 In	20100721	Reach 1	12237.0	11340.2	12758.2	12473.4	10835.2	11768.1	113.8	62.8	98.5	104.7	80.9	100.7	
		Reach 2	12237.0	11340.2	10919.7	12473.4	10835.2	11601.9	113.8	61.6	68.9	104.7	76.2	107.5	
	20100728	Reach 1	4864.1	4864.1	5066.8	4923.6	4903.8	4827.7	28.4	13.4	14.3	26.2	17.9	19.3	
		Reach 2	4864.1	4836.3	5629.9	4923.6	4127.9	4194.0	28.4	6.7	6.9	26.2	10.1	9.2	
	20100918	Reach 1	10077.8	9850.5	10851.0	10330.5	10098.1	10835.8	158.7	126.3	132.8	71.5	66.0	74.4	
		Reach 2	10077.8	9290.2	9962.1	10330.5	9515.7	10208.1	158.7	91.3	88.0	71.5	52.4	52.8	
	20100925	Reach 1	3584.7	4762.1	4843.0	3709.5	3709.5	4369.9	57.0	36.0	33.2	25.5	24.8	28.0	
		Reach 2	3584.7	3791.2	3761.1	3709.5	3707.7	4806.5	57.0	20.0	18.3	25.5	16.7	19.2	
	20110606	Reach 1	1232.6	1117.2	954.3	1305.6	1183.8	1185.7	108.2	44.8	46.7	27.1	14.1	11.0	
		Reach 2	1232.6	862.5	861.6	1305.6	676.3	788.2	108.2	11.7	12.6	27.1	3.1	4.1	
	20110612	Reach 1	1781.1	1687.4	1660.0	1880.8	1781.4	1812.2	51.7	7.8	7.6	14.5	3.2	3.7	
		Reach 2	1781.1	1255.2	1358.2	1880.8	1079.1	1092.1							
	20110719	Reach 1	4562.0	4561.6	4372.5	4693.2	5722.7	4594.0	68.9	29.8	28.6	33.3	15.0	14.8	
	20100719	Reach 1	3648.8	3648.8	4411.8	3008.3	3808.2	4167.5	51.0	20.4	33.8	52.3	30.1	34.3	
		Reach 2	3648.8	3648.8	3938.6				51.0	12.8	14.5				
	18 Out	20100726	Reach 1	6037.4	4520.8	4808.9	6167.9	4593.9	5099.8	45.5	14.9	16.2	39.3	20.8	25.3
			Reach 2	6037.4	4505.3	5437.3	6167.9	4556.6	5046.9	45.5	8.7	9.3	39.3	15.3	18.0
		20100916	Reach 1	4818.4	4689.2	4375.3	4938.0	4770.5	4409.6	74.7	33.2	33.3	33.6	24.3	27.4
Reach 2			4818.4	4686.0	4780.6	4938.0	4719.4	4747.5	74.7	19.5	28.3	33.6	21.0	22.4	
20110604		Reach 1	4224.4	4221.7	4162.2	3724.6	3724.4	4047.2	66.5	25.9	27.8	33.1	15.3	16.5	
		Reach 2	4224.4	4099.9	4213.3	3724.6	3689.6	4188.7	66.5	15.3	18.5	33.1	9.6	17.4	
20110610		Reach 1	4321.1	3941.7	3918.5	4407.0	3839.5	3876.9	74.9	13.2	14.9	34.5	11.3	11.5	
		Reach 2	4321.1	3426.6	3509.6	4407.0	3514.3	3547.0				34.5	3.7	4.1	
20110716		Reach 1	8380.7	7723.2	7046.4	8111.6	7512.5	7272.5	52.3	13.3	13.0	45.5	17.8	18.0	
20110902		Reach 1	2437.7	2403.0	2285.2	2476.1	2374.0	2182.6	17.8	1.7	1.7	20.8	17.2	16.5	

Table 3-1 Injected Mass and Mass Calculation Result from Simulation and Observation Data

Transport parameters estimated by OTIS-P are expected to be controlled by channel hydraulics. Therefore, they have been related to stream discharge. Although other studies suggest many other physical characteristics should be considered (e.g., geomorphology, flow and substrate), we expect that discharge is the master hydraulic variable [D' Angelo et al., 1993; Runkel et al., 2002]. In addition, transport metrics and fate parameters are also considered to assess relationship with discharge and  $A_s/A$  (the ratio of storage zone size to main channel size) is considered to assess potential for storage of solute during transport.

Depth of thaw beneath and adjacent to stream channels increases rapidly in early summer and slows by middle to late summer in these arctic tundra season [Zarnetsket et al., 2007]. Further, the energy of water in active layer extends beneath streambed creating thawed bulb [Brosten et al., 2006] and thawed sediment creates opportunity for hyporheic exchange in tundra streams. Although thaw depth was not monitored directly, it has an intimate relationship with seasonal change [Osterkamp & Romanovsky, 1999]. So we assumed date is reasonable surrogate for thaw depth influence on solute transport, namely storage parameters ( $A_s, \alpha$ ).

Chemical reactions which occur in main stream and storage zone are likely associated with biological processes in solute transport dynamics. These processes are important to ecosystem function [Lyons et al., 1998]. Nutrient uptake is also affected by other control variables like permeability of sediments and hyporheic processes. Temperature also has vital role in biological processes, generally positively correlated. Hence, temperature may be related to nutrient uptake rates ( $\lambda, \lambda_s$ ) to determine if it is a control on fate of  $\text{NH}_4$  and  $\text{PO}_4$ .

Although, I8 Inlet and I8 outlet have similar conditions such as alluvial, low gradient, headwater tundra streams, it has been found that there is a potential influence of Lake I-8 which results in different solute transport mechanisms in the two streams [Wlostoski, 2012]. He suggested that I8 Inlet had wider and shallower channel structure with fine particles and

different shallow groundwater dynamics. I8 Lake affects seasonal stream flow dynamics in I8 Outlet, buffering sharp inflows to the lake. Because of this reason, the controls in both streams are analyzed separately. The hydrographs of two streams in 2011 indicate different of flow regime in the two streams (Figure 3-2).

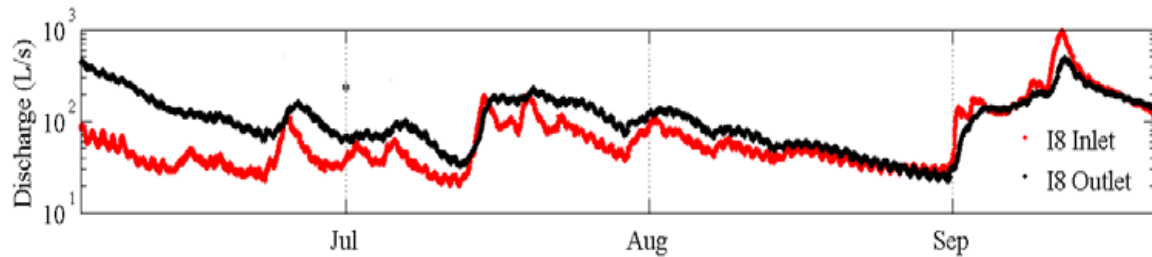


Figure 3-2 Hydrographs of 2011 from I8 Inlet and I8 Outlet Source: “Solute transport dynamics in alaskan arctic tundra streams” by Wlostoski N. Adam. (2012) Master’s thesis, Pennsylvania State University

### 3.2 Discharge and Hydraulic controls on solute transport dynamics

#### 3.2.1 I8Inlet

Interpretation of dispersion coefficient and main stream cross sectional area is related to dispersion and advection mechanisms. Discharge is positively correlated with these mechanisms. In the case of longitudinal dispersion which was only considered in the OTIS, it seems positive correlation could not be approached by uncertainty (Figure 3-3). However, main stream cross sectional area is highly correlated with discharge (Figure 3-4,  $p < 0.001$  Reach 1 Injection A,  $p = 0.002$  Reach 1 Injection B,  $p = 0.002$  Reach 2 Injection A and  $p = 0.03$  Reach 2 Injection B). In addition, both parameters have slightly different correlations in reach 1 and 2. This suggests that there are small changes through downstream transport characteristic such as presence of obstructions, stream size, slope, etc.

To determine whether there is a hydraulic control on transient storage, storage zone cross-sectional area and exchange coefficient are also related to discharge. In the figure 3-5, storage zone cross sectional area display positive correlation in reach 1, with only a

significant relationship for injection A ( $p < 0.001$  Reach 1 Injection A), and negative correlations in reach 2 (not significant trends). The exchange coefficient linearly increased when discharge increased (Figure, 3-6,  $p = 0.001$  Reach 1 Injection A,  $p = 0.001$  Reach 1 Injection B,  $p = 0.003$  Reach 2 Injection A and  $p = 0.005$  Reach 2 Injection B) In addition, transient storage zone are as a proportion of stream cross sectional area is not correlated with discharge (Figure 3-7).

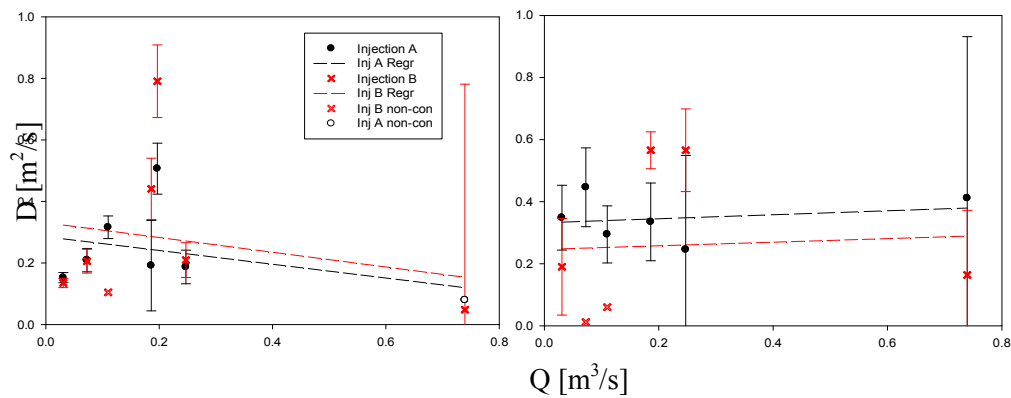


Figure 3-3 Linear regression between Dispersion coefficient (D) and Discharge (Q) with 95% confidence limits, left is Reach 1, right is Reach 2 at I8 Inlet

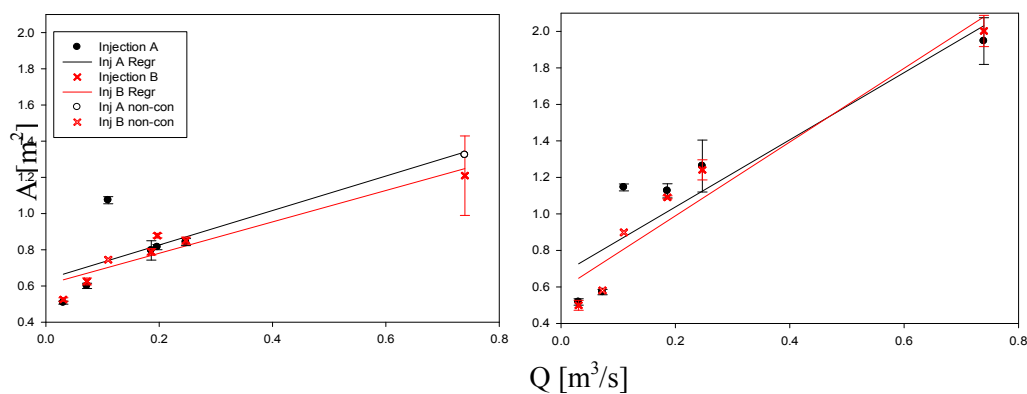


Figure 3-4 Linear regression between Main stream area (A) and Discharge (Q) with 95% confidence limits, left is Reach 1, right is Reach 2 at I8 Inlet

Three metrics – turnover length, mean storage residence time and storage exchange flux – were related to discharge to further determine the potential influence of discharge on transient storage (Figure 3-8 ~ 3-10). Turnover length and average storage zone residence time appear to decrease when discharge increased. However, none of these relationships are significant. Thus, we should consider other factors which may affect solute transport

dynamics. Storage exchange flux has strong correlation with discharge (Fig 3-9,  $p < 0.001$  Reach 1 Injection A,  $p < 0.001$  Reach 1 Injection B,  $p < 0.001$  Reach 2 Injection A and  $p = 0.001$  Reach 2 Injection B). Storage exchange flux is strongly related to discharge, likely due to the fact that discharge is strongly related to cross-sectional area (Figure 3-4) which is constituent of the exchange flux metric (equation 2-9).

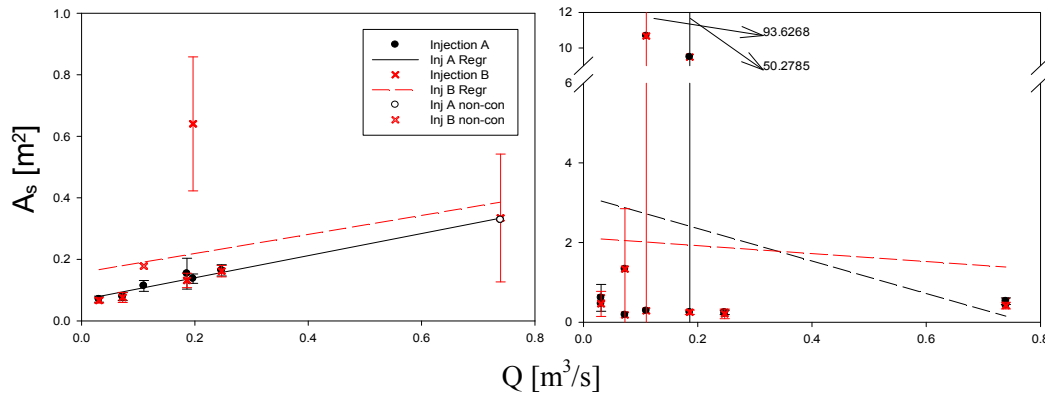


Figure 3-5 Linear regression between Storage zone stream area ( $A_s$ ) and Discharge ( $Q$ ) with 95% confidence limits, left is Reach 1, right is Reach 2 at I8 Inlet

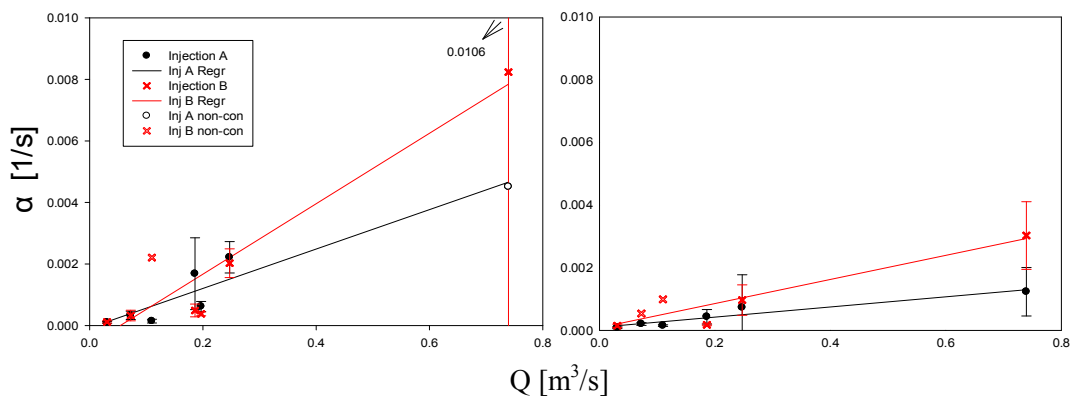


Figure 3-6 Linear regression between Exchange coefficient ( $\alpha$ ) and Discharge ( $Q$ ), left is Reach 1, right is Reach 2 at I8 Inlet

To determine whether discharge has an influence on the fate of  $\text{NH}_4$  and  $\text{PO}_4$ , values of the 1<sup>st</sup> order decay coefficient in main channel and storage zone and the RSF metric (which describes relative chemical reaction rate occurring in the main channel and storage zone area) are also related to stream discharge. None of these three parameters were significantly related to discharge in any of the reaches (Figure 3-10, 3-11 and 3-12). When we consider model structure, we estimated transport parameters first and then 1<sup>st</sup> order decay parameters in two

conceptual zones, so biogeochemical processes were simulated separate from transport processes.

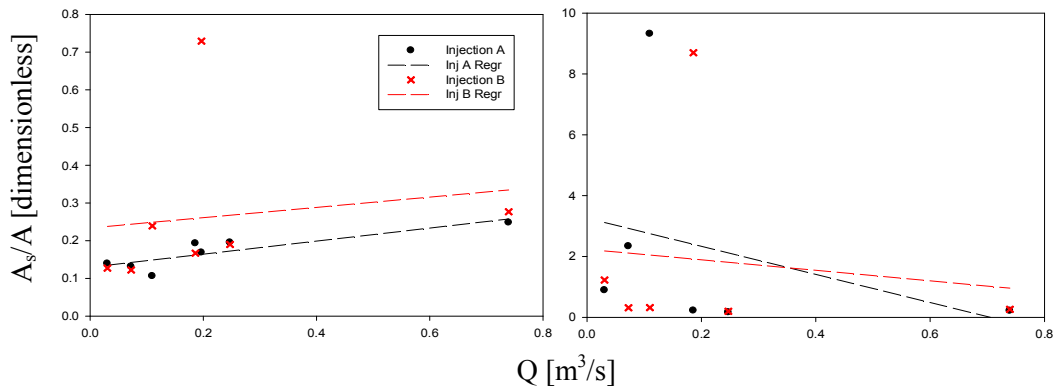


Figure 3-7 Linear regression between  $A_s/A$  and Discharge ( $Q$ ), left is Reach 1, right is Reach 2 at I8 Inlet

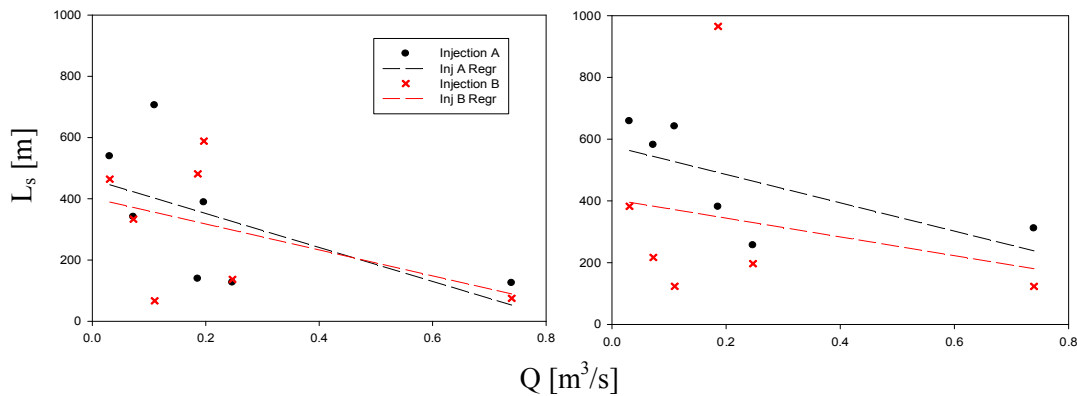


Figure 3-8 Linear regression between Turn over length ( $L_s$ ) and discharge ( $Q$ ), left is Reach 1, right is Reach 2 at I8 Inlet

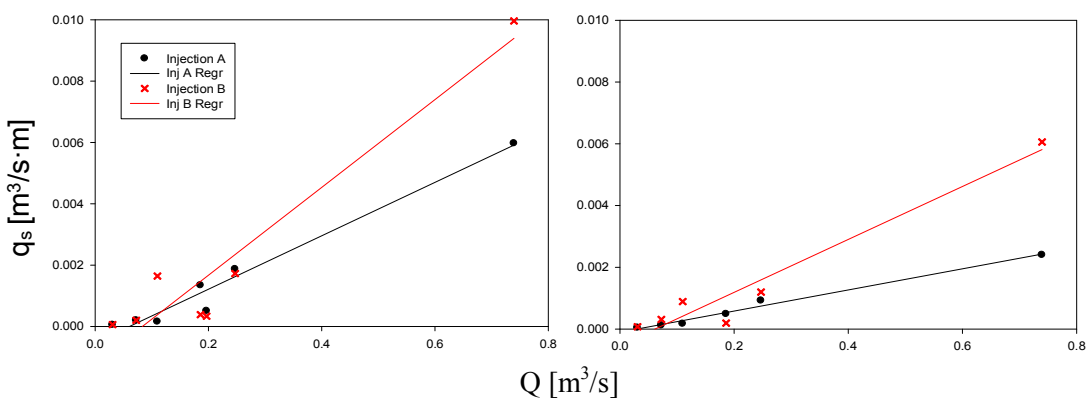


Figure 3-9 Linear regression between Storage exchange flux ( $q_s$ ) and Discharge ( $Q$ ), left is Reach 1, right is Reach 2 at I8 Inlet

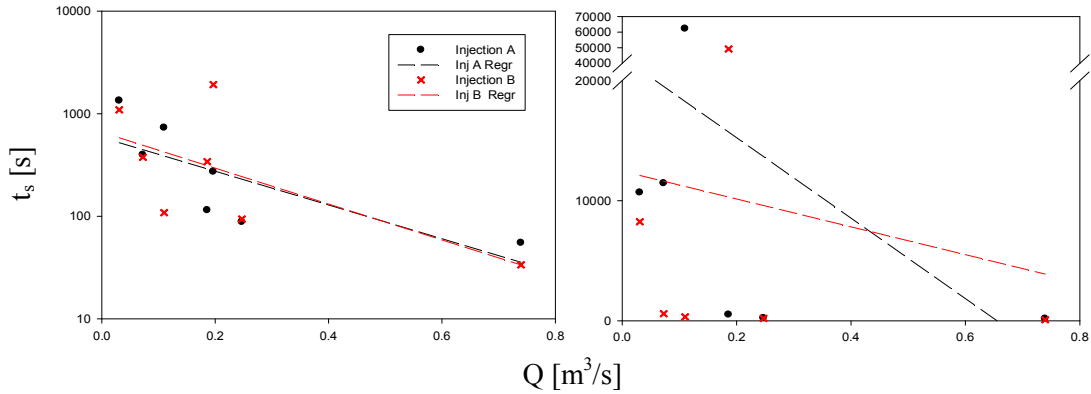


Figure 3-10 Linear regression between Average residence time in storage zone ( $t_s$ ) and discharge ( $Q$ ), left is Reach 1, right is Reach 2 at I8 Inlet

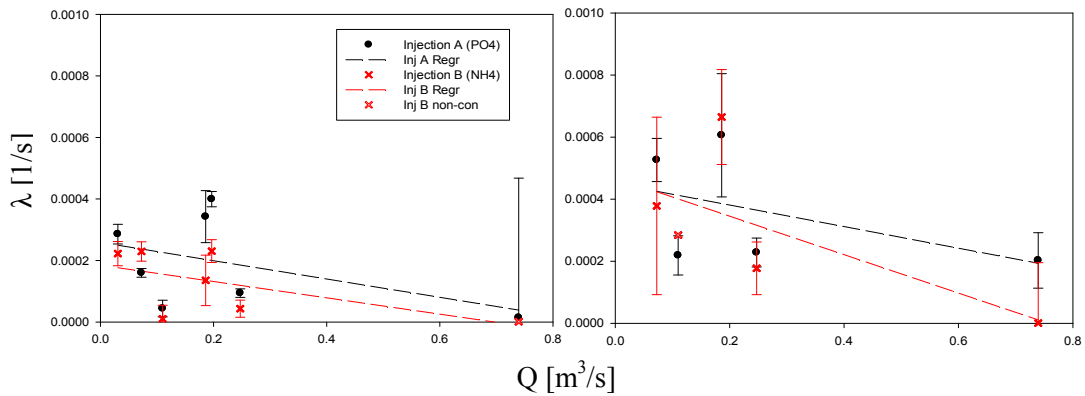


Figure 3-11 Linear regression between Decay coefficient in main channel ( $\lambda$ ) and Discharge ( $Q$ ) with 95% confidence limits, left is Reach 1, right is Reach 2 at I8 Inlet

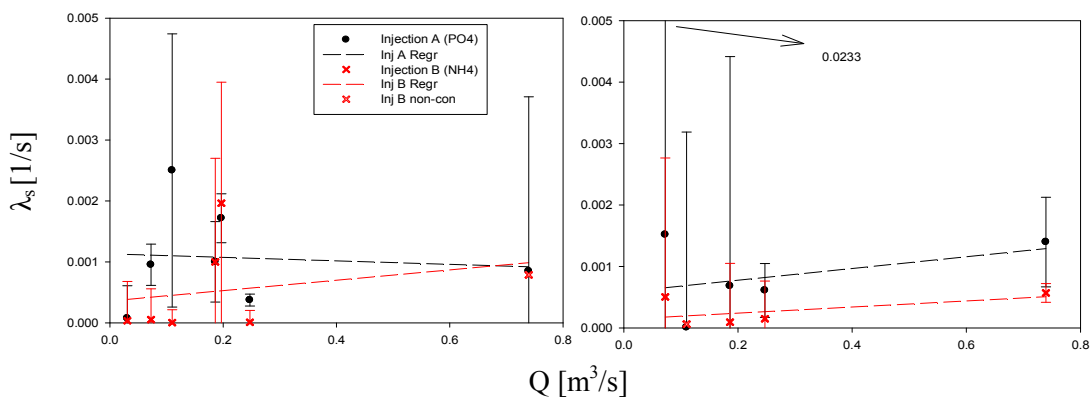


Figure 3-12 Linear regression between Decay coefficient in storage zone ( $\lambda_s$ ) and Discharge ( $Q$ ) with 95% confidence limits, left is Reach 1, right is Reach 2 at I8 Inlet

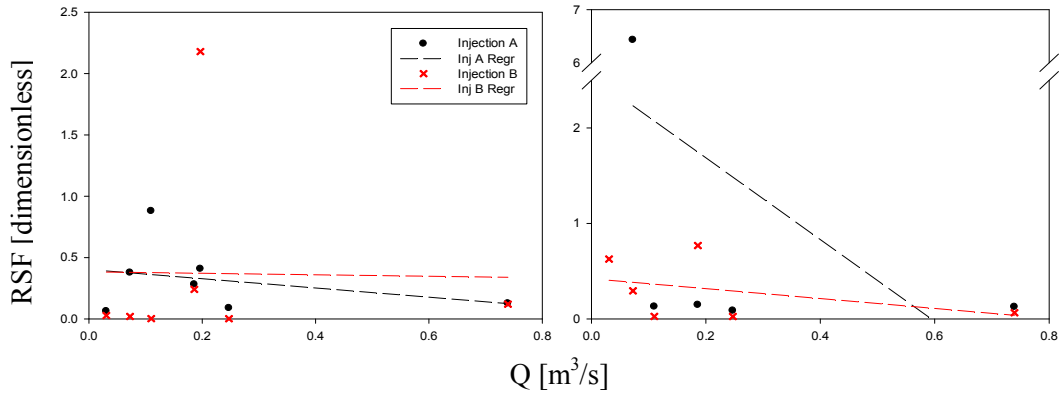


Figure 3-13 Linear regression between RSF and Discharge (Q), left is Reach 1, right is Reach 2 at I8 Inlet

### 3.2.2 I8Outlet

In the figure 3-14, dispersion coefficients display strong positive correlation with discharge in reach 1 ( $p=0.001$  Reach 1 Injection A and  $p=0.0069$  Reach 1 Injection B), and negative correlation in reach 2 (no significant trends). The main stream cross sectional area also has positive correlation with discharge at reach 1 and 2 as similar with the result of I8 Inlet. To be specific, only main stream area in reach 1 displays significant trends (Figure 3-15,  $p=0.002$  Reach 1 injection A and  $p=0.03$  Reach 1 injection B), however, in the case of injection A in reach 2, the regression has a p-value close to 0.1 ( $p=0.134$  Reach 2 Injection A).

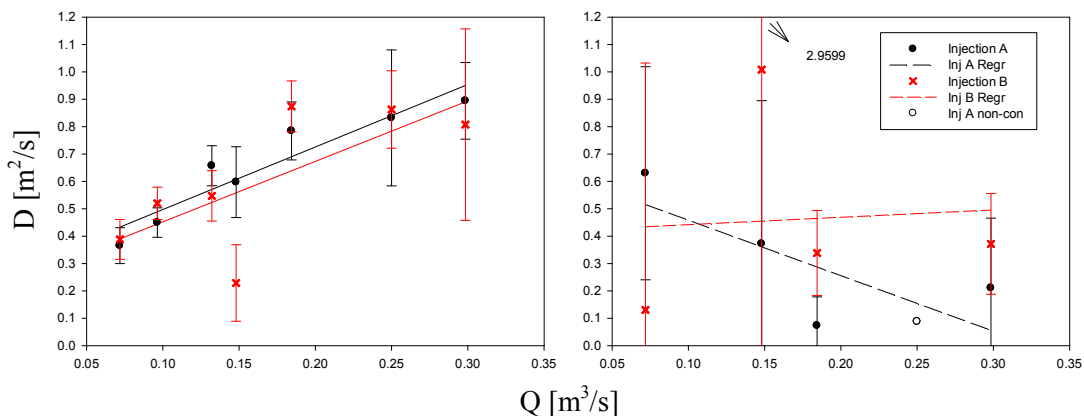


Figure 3-14 Linear regression between Dispersion coefficient (D) and Discharge (Q) with 95% confidence limits, left is Reach 1, right is Reach 2 at I8 outlet

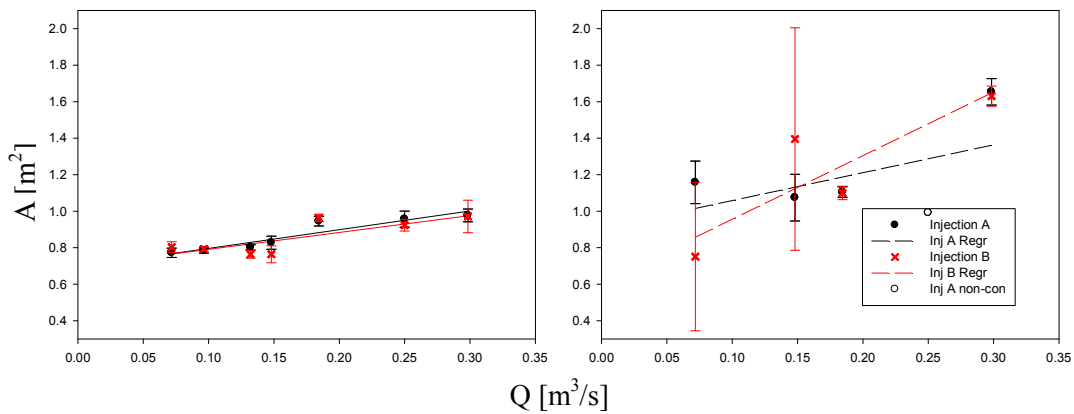


Figure 3-15 Linear regression between Main stream area (A) and Discharge (Q) with 95% confidence limits, left is Reach 1, right is Reach 2 at I8 outlet

Two transient storage parameters- storage zone cross sectional area and exchange coefficient –were also related to discharge to determine whether there was a hydraulic control on transient storage. The storage zone cross sectional area is not correlated with discharge in either reach (Figure 3-16). The exchange flux coefficient displays strong positive correlation with discharge ( $p=0.015$  Reach 1 Injection A,  $p=0.033$  Reach 1 Injection B and  $p=0.0049$  Reach 2 Injection A; Figure 3-16). The transient storage zone area as a proportion of stream cross sectional area is also not correlated with discharge (Figure 3-17).

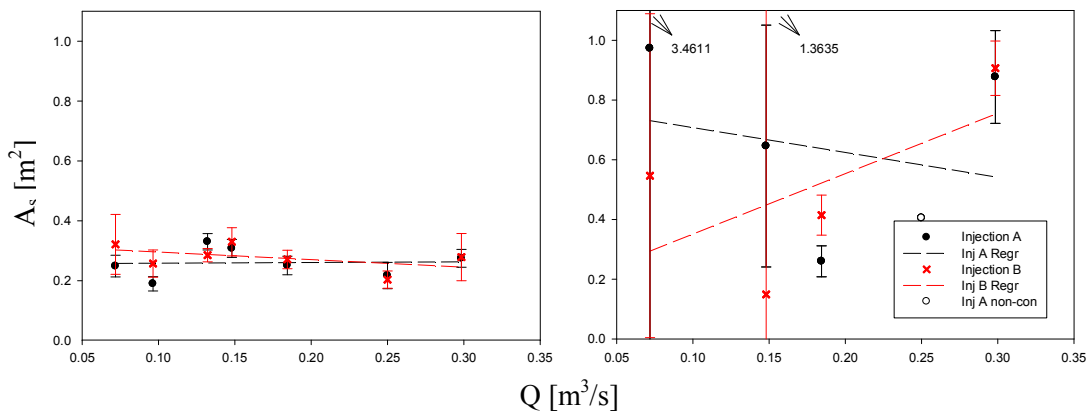


Figure 3-16 Linear regression between Storage zone stream area ( $A_s$ ) and Discharge (Q) with 95% confidence limits, left is Reach 1, right is Reach 2 at I8 outlet

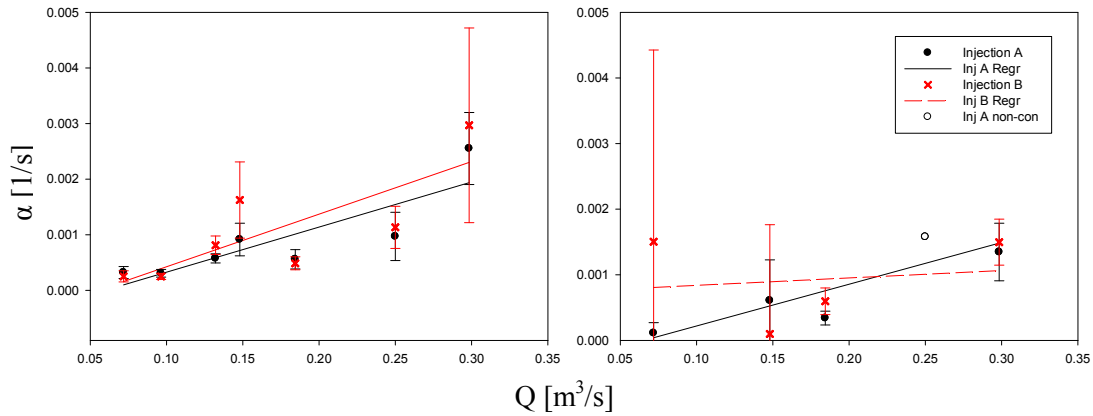


Figure 3-17 Linear regression between Exchange coefficient ( $\alpha$ ) and Discharge ( $Q$ ) with 95% confidence limits, left is Reach 1, right is Reach 2 at I8 outlet

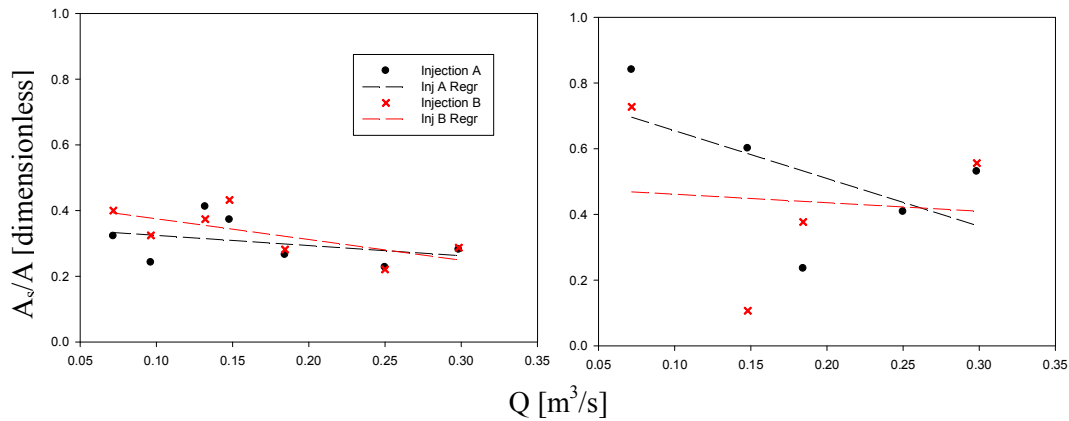


Figure 3-18 Linear regression between  $A_s/A$  and Discharge ( $Q$ ) with 95% confidence limits, left is Reach 1, right is Reach 2 at I8 outlet

The turnover lengths have similar result as I8Inlet. They have negative correlation with no significant trends (Figure 3-19). The storage exchange fluxes display distinct positive correlation with discharge in reach 1 and 2 except injection B in reach 2 ( $p=0.012$  Reach 1 Injection A and  $p=0.002$  Reach 1 Injection B and  $p=0.023$  Reach 2 Injection A; Figure 3-20). Average residence time in storage has different results in I8 outlet than I8 inlet (Figure 3-21). This metric has a significant negative relationship with discharge in reach 1 ( $p=0.001$  Reach 1 Injection A,  $p=0.023$  Reach 1 Injection B). Thus, average residence time in the storage zone is strongly related to discharge in I8 inlet. It is worth noting that I8 outlet flow regime was lower than I8 inlet.

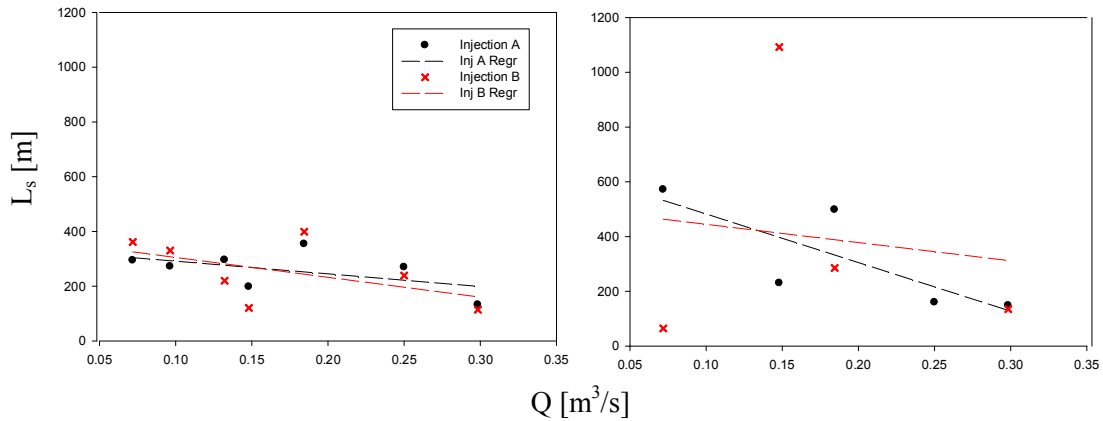


Figure 3-19 Linear regression between Turn over length ( $L_s$ ) and Discharge ( $Q$ ) with 95% confidence limits, left is Reach 1, right is Reach 2 at I8 outlet

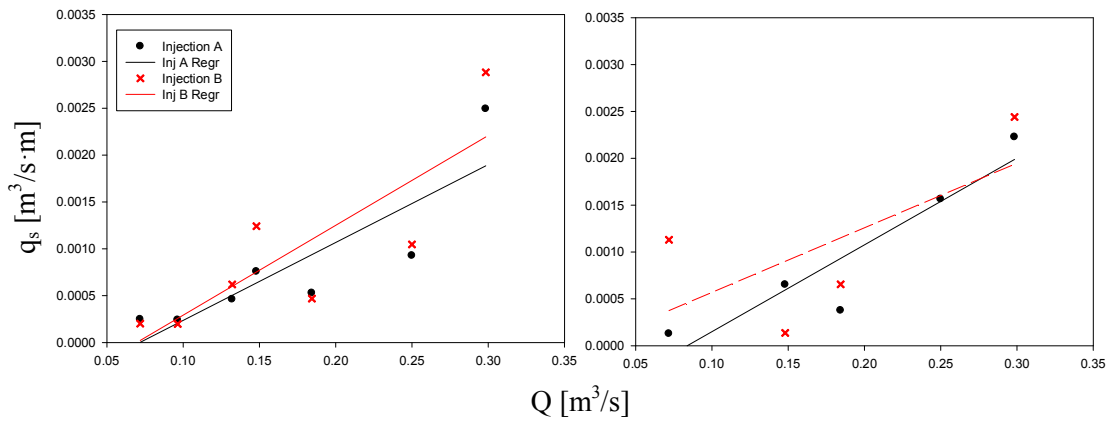


Figure 3-20 Linear regression between Storage exchange flux ( $q_s$ ) and Discharge ( $Q$ ) with 95% confidence limits, left is Reach 1, right is Reach 2 at I8 outlet

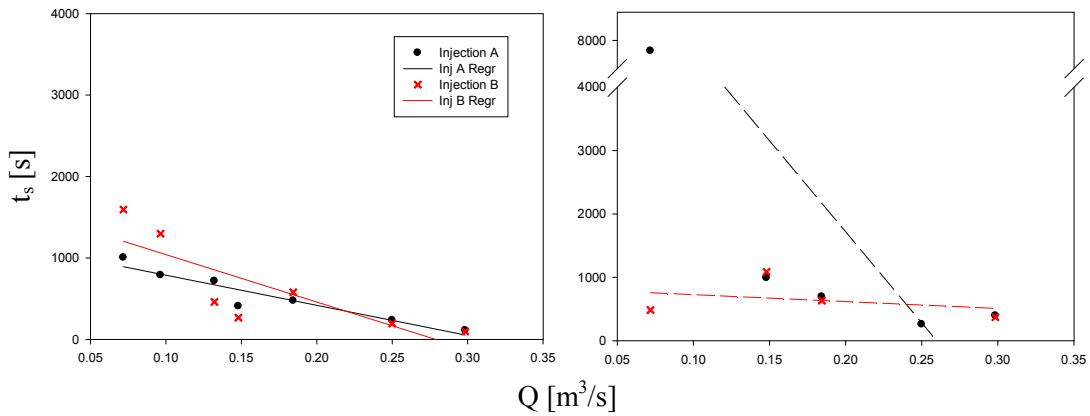


Figure 3-21 Linear regression between Average residence time in storage zone ( $t_s$ ) and Discharge ( $Q$ ) with 95% confidence limits, left is Reach 1, right is Reach 2 at I8 outlet

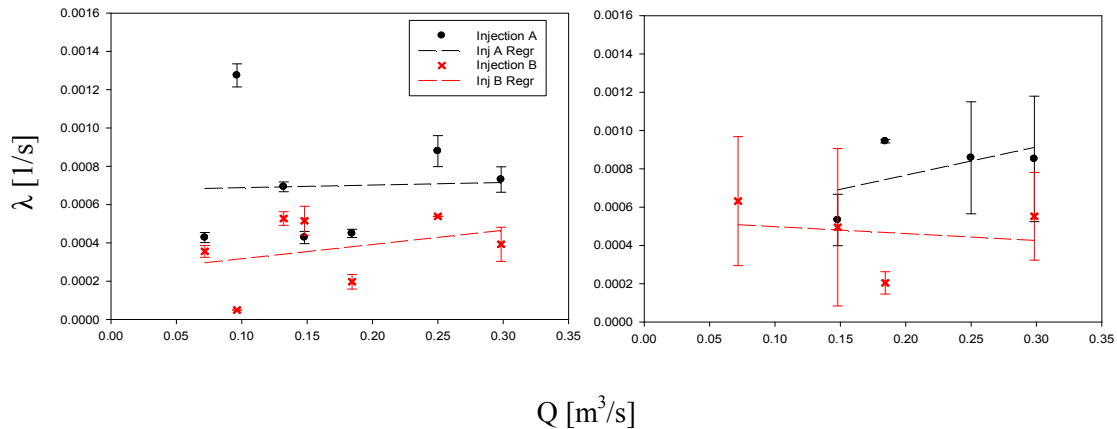


Figure 3-22 Linear regression between Decay coefficient in main channel ( $\lambda$ ) and Discharge (Q) with 95% confidence limits, left is Reach 1, right is Reach 2 at I8 outlet

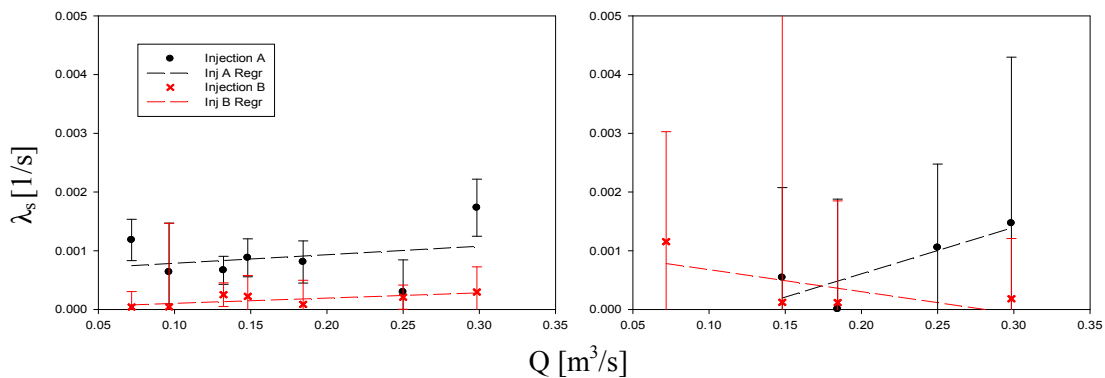


Figure 3-23 Linear regression between Decay coefficient storage zone ( $\lambda_s$ ) and Discharge (Q) with 95% confidence limits, left is Reach 1, right is Reach 2 at I8 outlet

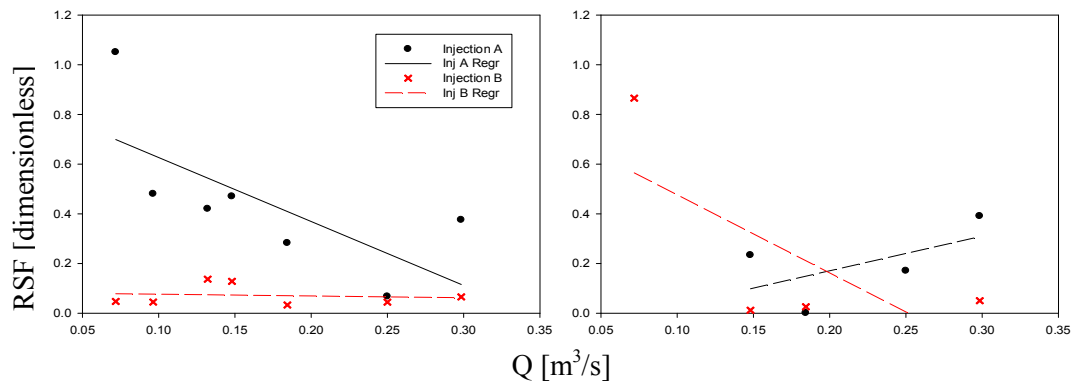


Fig 3-24 Linear regression between RSF and Discharge (Q) with 95% confidence limits, left is Reach 1, right is Reach 2 at I8 outlet

The parameters related to nutrient uptake – 1<sup>st</sup> order decay coefficient in main channel and storage zone - are not correlated to with discharge (Figure 3-22 and 3-23). The RSF metric displays only a significant relationship to discharge in reach1 (Figure. 3-24 p=0.001 Reach 1 Injection A). However, when we consider the former result and equation of

this metric (equation 2-11), it is hard to suggest that discharge does not controls nutrient uptake.

### 3.3 Date and Thaw Depth

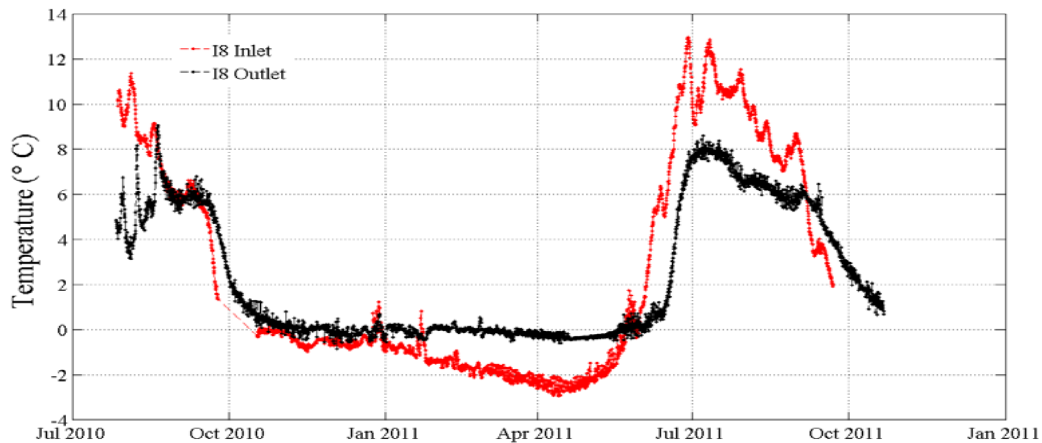


Figure 3-25 Time series of temperatures at 1m depth beneath stream bed on I8 Inlet and I8 Outlet Source: “Solute transport dynamics in alaskan arctic tundra streams” by Wlostoski N. Adam. (2012) Master’s thesis, Pennsylvania State University

In both I8 inlet and outlet streams, streambed temperature monitoring stations have been deployed for several years. Both reach 1m depth. The temperature time series from two thaw seasons is provided to demonstrate the thaw process in both stream channels (Figure 3-25). Temperature beneath I8 Inlet declines more rapidly than I8Inlet during September 2010 and October 2011 and I8 Inlet has higher temperature than I8 outlet in the thaw season. From this data, it is implied that the subsurface thaw season is between mid June and early October in this region.

#### 3.3.1 I8Inlet

Although field studies were conducted in 2010 and 2011, thaw seasons were fairly similar (no anomalous weather). Because of this, we can evaluate, as if all data were collected

in the same year for linear regression analysis. We hypothesized if thaw depth affects solute transport, parameter values would change in a particular direction (increasing and decreasing) as a function of date. Dispersion coefficient has no distinct relationship with date (Figure 3-26). Main stream cross-sectional area has relatively high value in the thaw season (Figure 3-27). However it is continuous to be a high value in late Sep. This is indicated that both transport parameters are more correlated with discharge than thaw bulb condition.

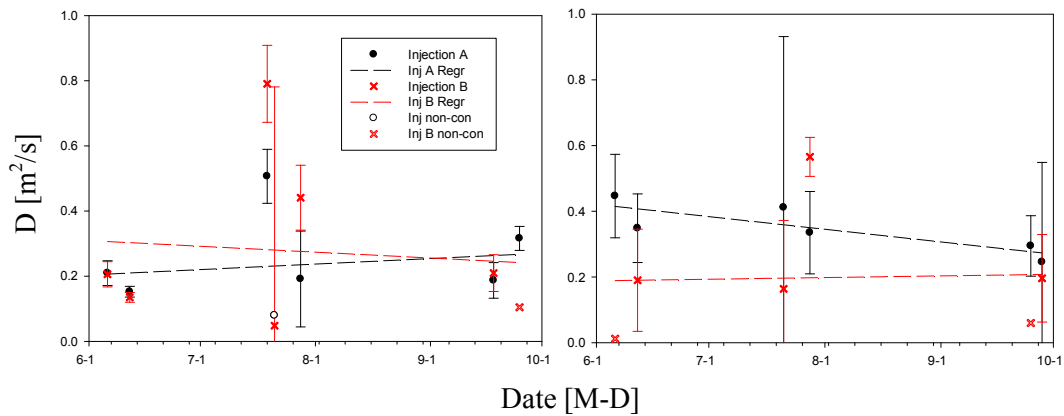


Figure 3-26 Linear regression between Dispersion coefficient (D) and Date with 95% confidence limits, left is Reach 1, right is Reach 2 at I8 Inlet

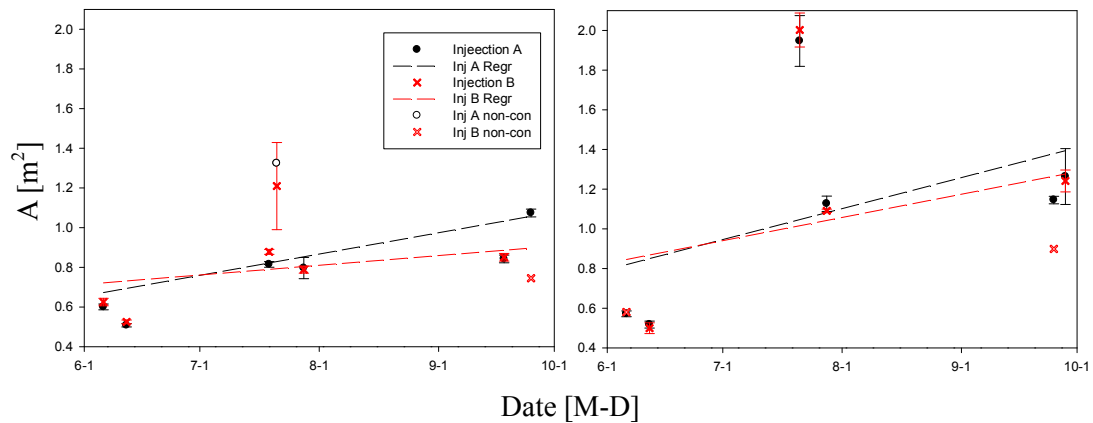


Figure 3-27 Linear regression between Main stream area (A) and Date with 95% confidence limits, left is Reach 1, right is Reach 2 at I8 Inlet

The two parameters related to transient storage - storage zone cross-sectional area and exchange coefficient - also do not have distinct relationships with date (Figure 3-28 and 3-29). This supports previous study results indicated that transient storage of tracer solute did not increase with increasing thaw depths [Zarnetske et al., 2008].

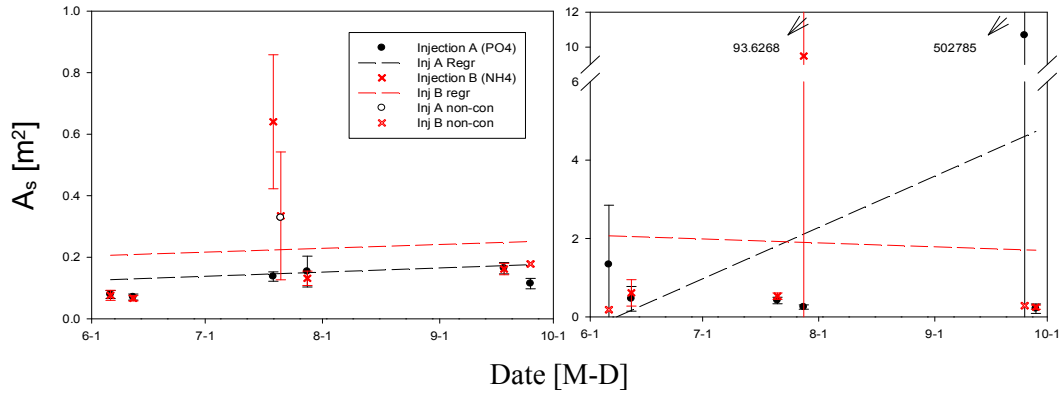


Figure 3-28 Linear regression between Storage zone area ( $A_s$ ) and Date with 95% confidence limits, left is Reach 1, right is Reach 2 at I8 Inlet

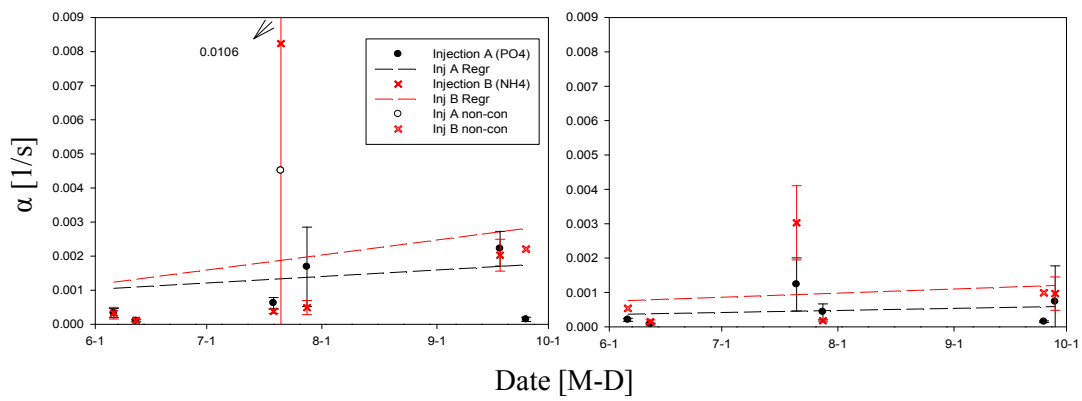


Figure 3-29 Linear regression between Exchange coefficient ( $\alpha$ ) and Date with 95% confidence limits, left is Reach 1, right is Reach 2 at I8 Inlet

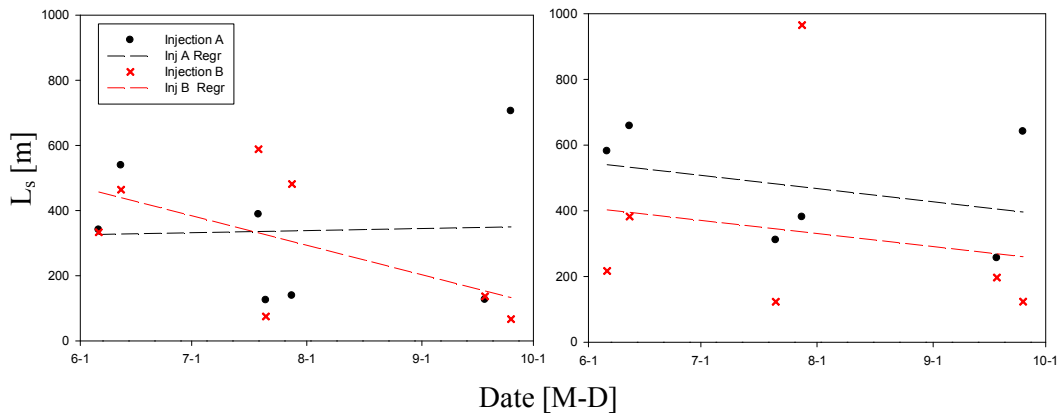


Figure 3-30 Linear regression between Turn over length ( $L_s$ ) and Date with 95% confidence limits, left is Reach 1, right is Reach 2 at I8 Inlet

Turnover length has no relationship with date (Fig 3-29). The average residence time in storage zone and storage exchange flux have relatively high values in the mid summer (Figure 3-30 and 3-31). However, they do not show similar trends with time series of temperatures at 1m depth beneath stream and relationship with date. This suggests that active

layer condition in this period does not affect solute transport.

To determine whether active layer condition affects the fate of  $\text{NH}_4$  and  $\text{PO}_4$ , 1<sup>st</sup> order decay coefficients in two conceptual area and metric RSF are related to date. Although 1<sup>st</sup> order decay coefficients have relative high values in the thaw season; they do not display correlation with date and similar trends with temperature at 1m beneath streambed. (Figure 3-33, 3-34 and 3-35). In the figure 3-34, there is a significant correlation with date for reach 2 ( $p=0.048$  Reach 2 Injection A). However, we hypothesized this may be more greatly affected by stream temperatures condition.

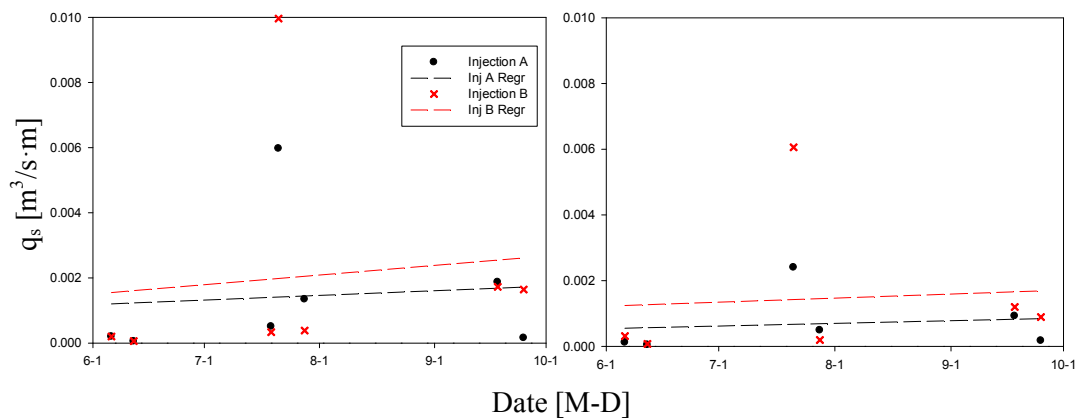


Figure 3-31 Linear Regression between Storage exchange flux ( $q_s$ ) and Date with 95% confidence limits, left is Reach 1, right is Reach 2 at I8 Inlet

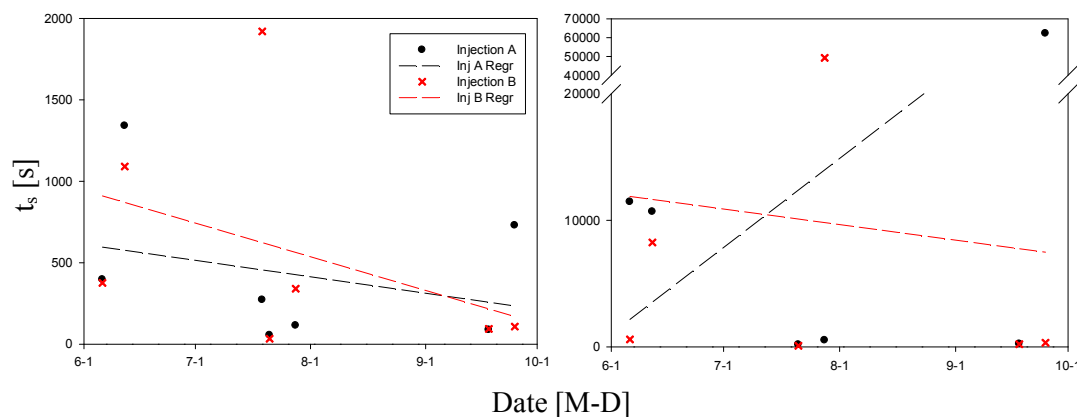


Figure 3-32 Linear regression between Average residence time in storage zone ( $t_s$ ) and Date with 95% confidence limits, left is Reach 1, right is Reach 2 at I8 Inlet

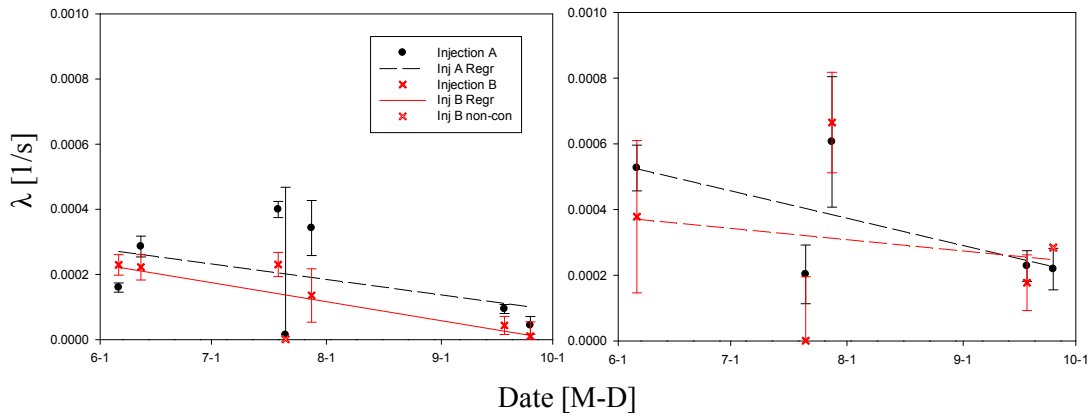


Figure 3-33 Linear regression between Decay coefficient in main channel ( $\lambda$ ) and Date with 95% confidence limits, left is Reach 1, right is Reach 2 at I8 Inlet

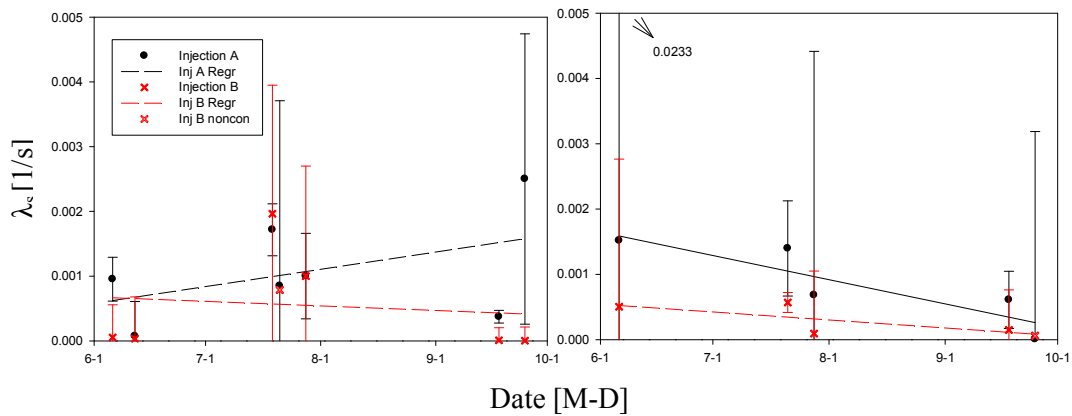


Figure 3-34 Linear regression between Decay coefficient in storage zone ( $\lambda_s$ ) and Date with 95% confidence limits, left is Reach 1, right is Reach 2 at I8 Inlet

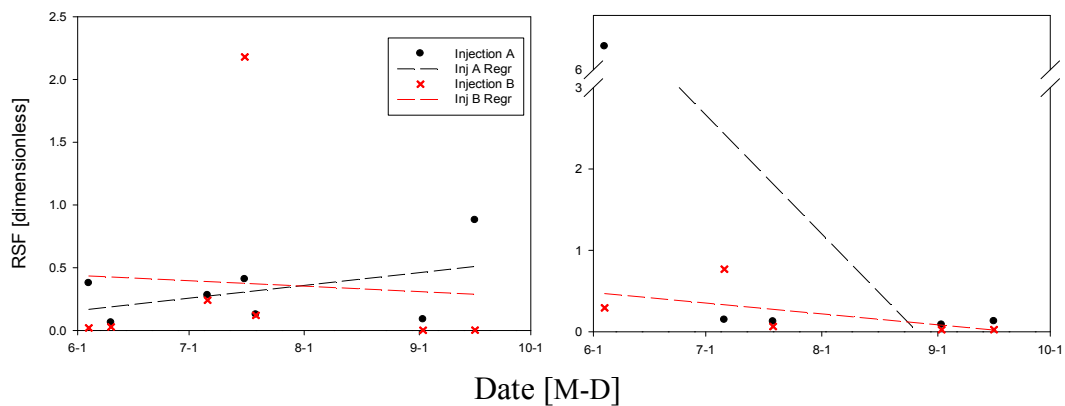


Figure 3-35 Linear regression between RSF and Date with 95% confidence limits, left is Reach 1, right is Reach 2 at I8 Inlet

### 3.3.2 I8 outlet

In the figure 3-36, the dispersion coefficient is not correlated with date. The main stream cross-sectional areas have relatively high values in middle of thaw season and

indicate a positive correlation with date. However, these parameters do not have significant trends (Figure 3-37). These results support the idea that transport parameters have stronger relationships with hydraulic characteristics than active layer condition (Section 3.3.1).

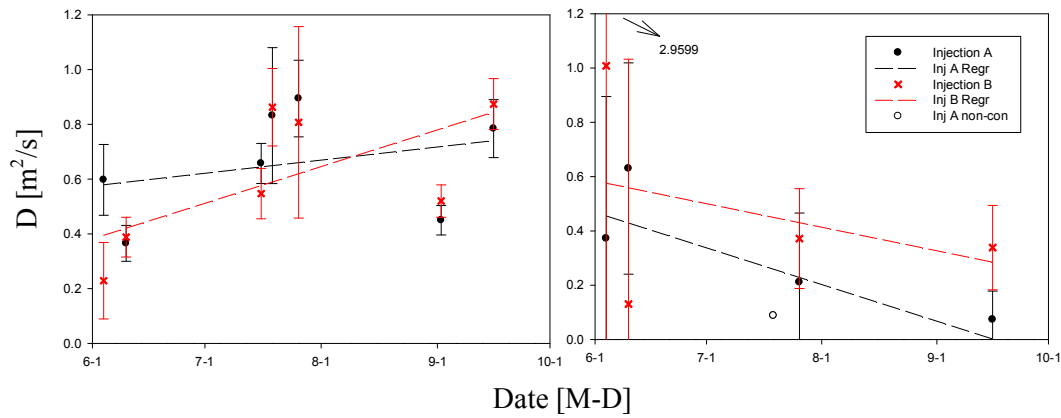


Figure 3-36 Linear regression between Dispersion coefficient (D) and Date with 95% confidence limits, left is Reach 1, right is Reach 2 at I8 Outlet

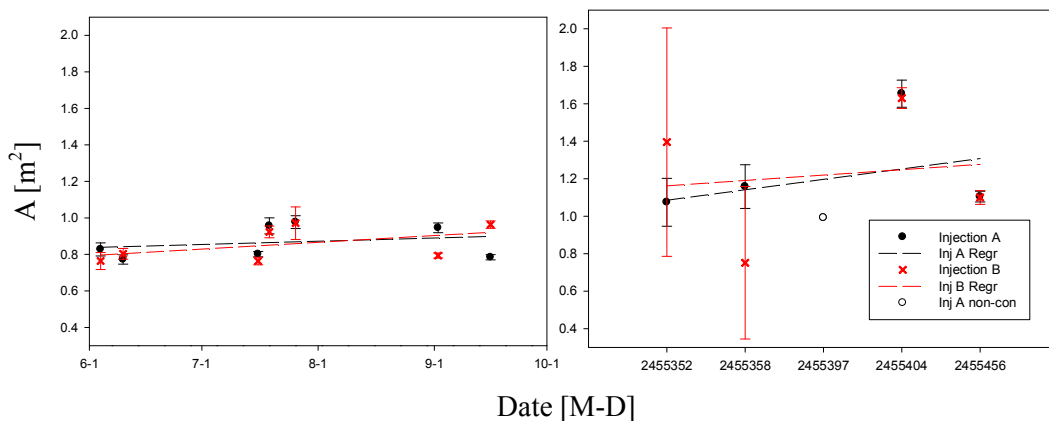


Figure 3-37 Linear regression between Main stream area (A) and Date with 95% confidence limits, left is Reach 1, right is Reach 2 at I8 Outlet

The transient storage parameters - storage zone cross sectional areas and exchange coefficients – are related to date to determine whether active layer condition controls transient storage. They do not display any relationship with date (Figure 3-38 and 3-39). These results strongly indicate that transient storage of tracer solute was not directly controlled by increasing thaw depths. In both streams (I8 Inlet and Outlet), none of the transient storage parameters display correlation with date. This suggests that there are other factors which affect transient storage more strongly than thaw bulb condition.

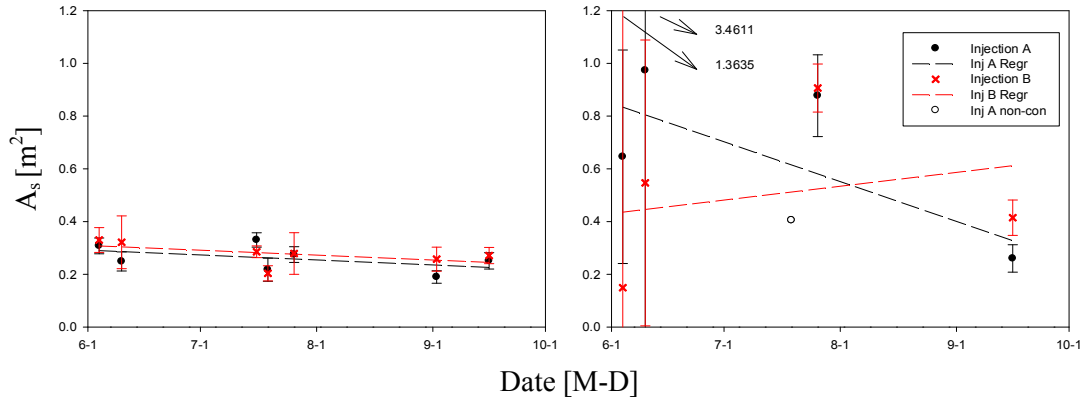


Figure 3-38 Linear regression between Storage zone area ( $A_s$ ) and Date with 95% confidence limits, left is Reach 1, line is Reach 2 at I8 Outlet

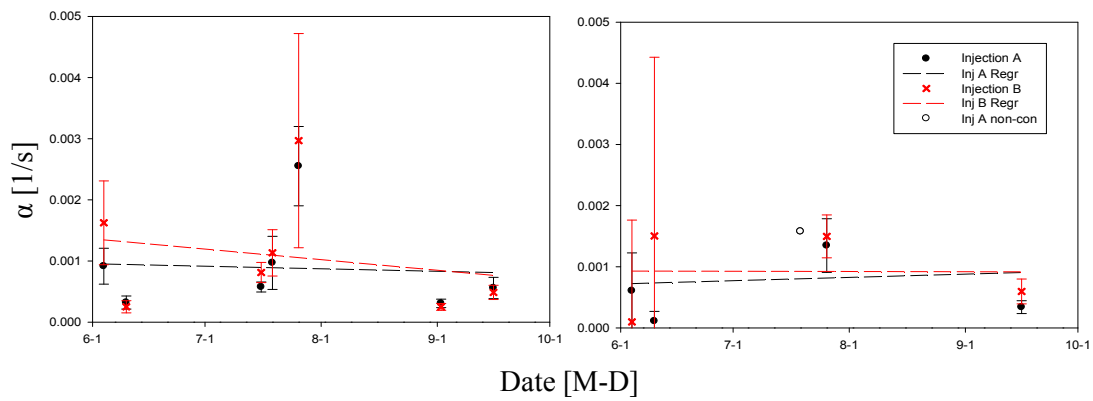


Figure 3-39 Linear regression between Exchange coefficient ( $\alpha$ ) and Date with 95% confidence limits, left is Reach 1, right is Reach 2 at I8 Outlet

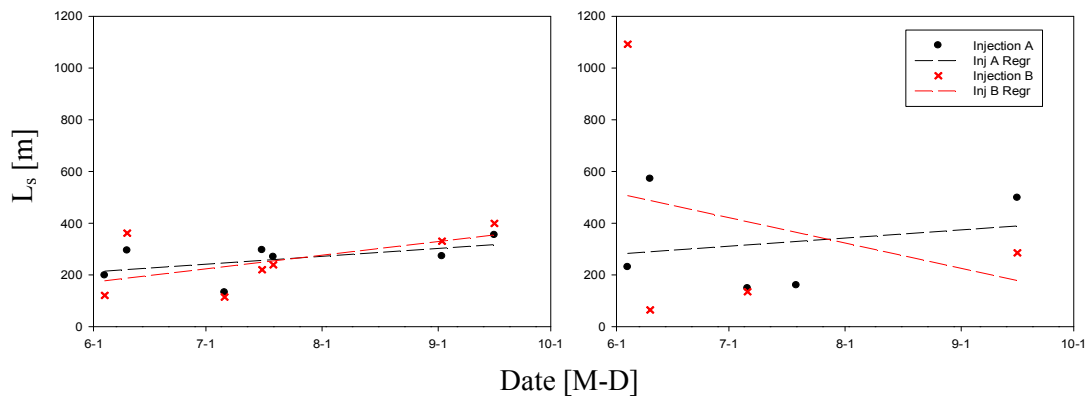


Fig 3-40 Linear regression between Turn over length ( $L_s$ ) and Date with 95% confidence limits, left is Reach 1, right is Reach 2 at I8 Outlet

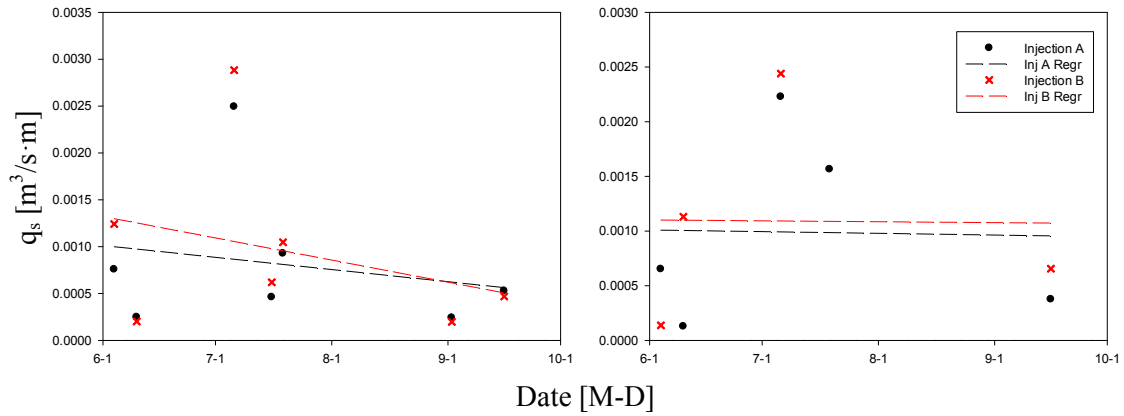


Figure 3-41 Linear regression between Storage exchange flux ( $q_s$ ) and Date with 95% confidence limits, left is Reach 1, right is Reach 2 at I8 Outlet

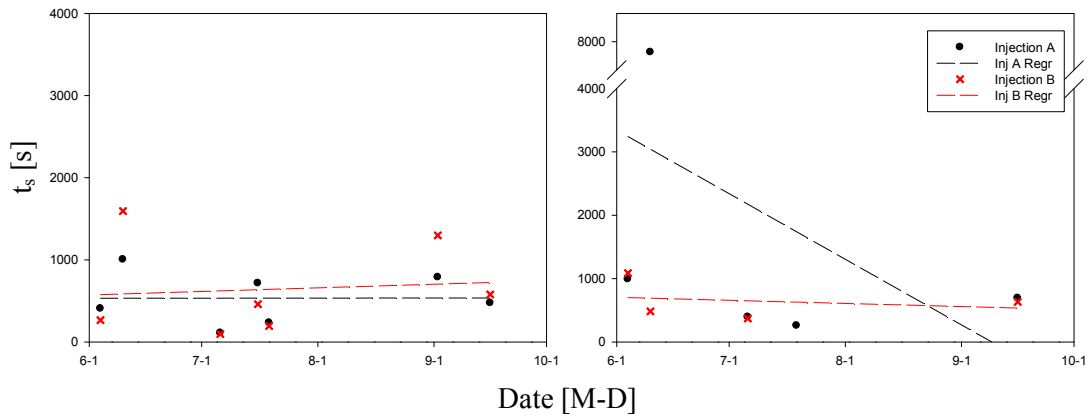


Figure 3-42 Linear Regression between Average residence time in storage zone ( $t_s$ ) and Date, with 95% confidence limits left is Reach 1, right is Reach 2 at I8 Outlet

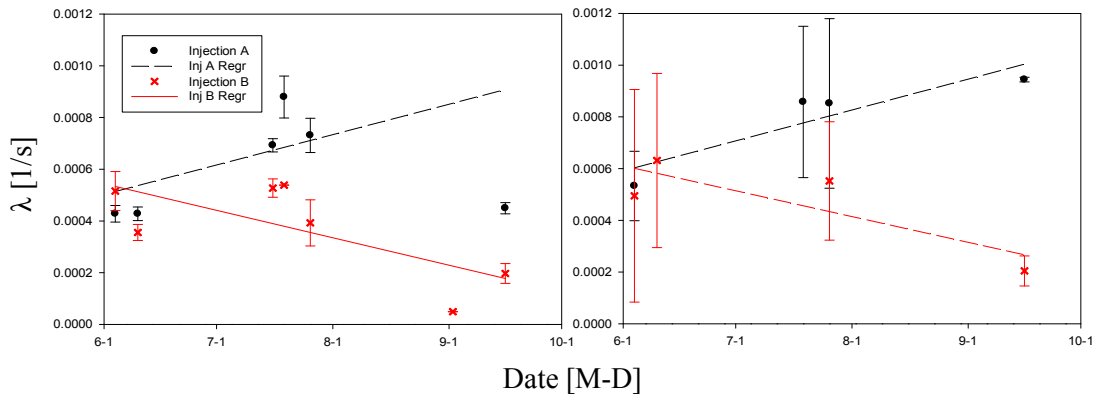


Figure 3-43 Linear regression between Decay coefficient in main channel ( $\lambda$ ) and Date with 95% confidence limits, left is Reach 1, right is Reach 2 at I8 Outlet

When we consider three metrics (turnover length, storage exchange flux and average residence time in storage zone) related to transport and transient storage, they display no

correlation with date (Figure 3-40, 3-41 and 3-42). In the case of storage exchange flux, there is relatively high value in middle of summer and a similar trend with temperature at 1m beneath streambed (Reach 2 Injection B). However, this is not enough evidence for supporting active layer conditions controls on transient storage.

In the figure 3-43, best fit 1<sup>st</sup> order decay coefficients display similar trends with temperature at 1m beneath streambed and have significant correlation to date ( $p=0.0072$  Reach1 Injection B). However, in the case of reach 2, there is no correlation with date. In addition, 1<sup>st</sup> order decay coefficient in storage zone and the RSF metric are also not correlated with date (Figure 3-44 and 3-45). These results also do not enough for support active layer condition controls on nutrient uptake dynamics.

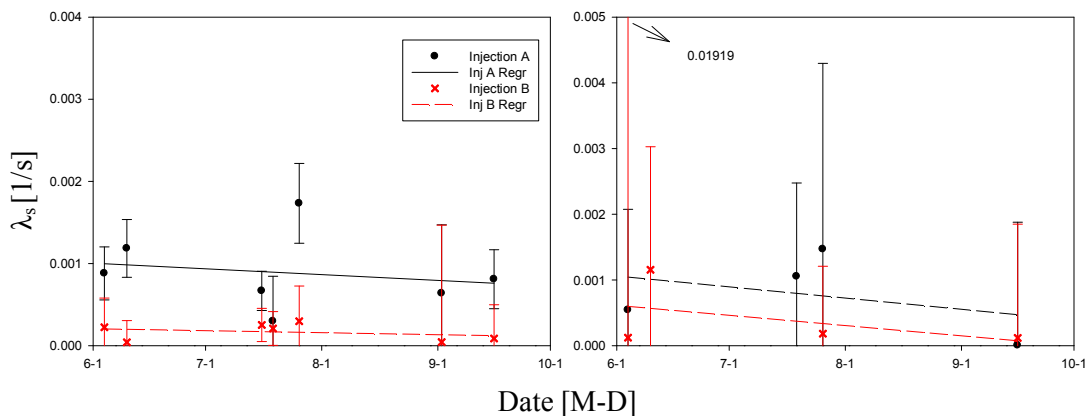


Figure 3-44 Linear regression between Decay coefficient in storage zone ( $\lambda_s$ ) and Date with 95% confidence limits, left is Reach 1, right is Reach 2 at I8 Outlet

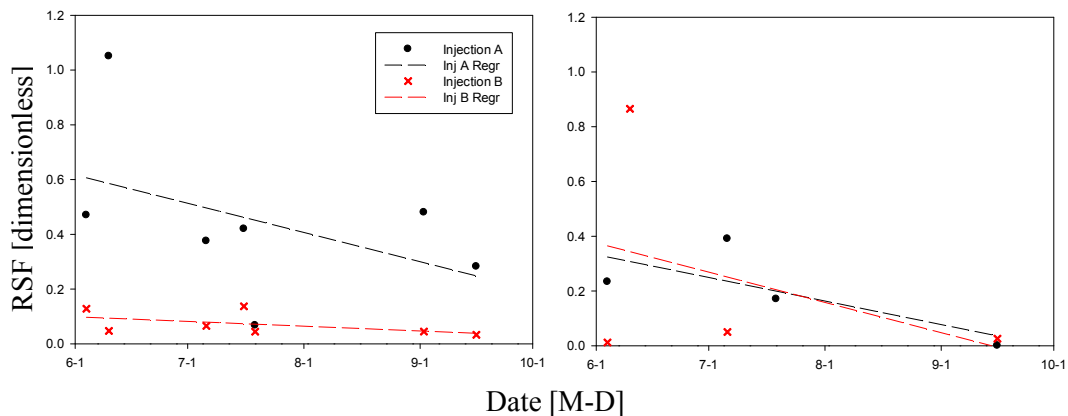


Figure 3-45 Linear regression between RSF and date, left is Reach 1, right is Reach 2 at I8 Outlet

### 3.4 The Ratio non-conservative to conservative masses and Mass loss

To determine whether there is a dependence of the ratio conservative (Cl) masses to non-conservative (PO<sub>4</sub> and NH<sub>4</sub>) masses as a function of parameters and metrics related to transient storage mechanisms (A, A<sub>s</sub>, α, q<sub>s</sub>, L<sub>s</sub> and t<sub>s</sub>), linear regressions were conducted between them. Specific values of the ratio of nutrient to tracer masses are provided in appendix 4. The ratios decrease from reach 1 and reach 2 and this change between reach 1 and 2 are provided in the Table 4-2. Masses used in the ratio of nutrient to tracer masses were calculated under the main channel BTCs. This means the change of ratio is related to mass loss downstream. The analysis between ratio and parameter related to transient storage parameter can assess the effect of mass loss on transient storage of non-conservative solute.

Stream and Date	SIM Mass	OBS Mass	SIM/INJ	OBS/INJ	SIM Mass	OBS Mass	SIM/INJ	OBS/INJ	
	Ratio of PO <sub>4</sub> _P : Cl				Ratio of NH <sub>4</sub> _N : Cl				
I8 IN (R1-R2)	20100721	0.0001	0.0014	0.0110	0.1516	0.0004	-0.0007	0.0514	-0.0847
	20100728	0.0014	0.0016	0.2328	0.2721	0.0012	0.0018	0.2295	0.3410
	20100918	0.0030	0.0034	0.1904	0.2162	0.0010	0.0017	0.1477	0.2454
	20100925	0.0023	0.0020	0.1424	0.1264	0.0022	0.0024	0.3200	0.3521
	20110606	0.0266	0.0343	0.3025	0.3912	0.0073	0.0040	0.3539	0.1951
	20100719	0.0021	0.0040	0.1504	0.2851	0.0079	0.0082	0.4538	0.4735
I8 Out (R1-R2)	20100726	0.0014	0.0017	0.1831	0.2198	0.0012	0.0014	0.1820	0.2187
	20100916	0.0029	0.0017	0.1888	0.1103	0.0007	0.0015	0.0957	0.2205
	20110604	0.0024	0.0023	0.1528	0.1460	0.0015	-0.0001	0.1699	-0.0085
	20110610					0.0019	0.0018	0.2409	0.2298

Table 4-2 The ratio change between reach 1 and reach 2

#### 3.4.1 I8Inlet

There is no significant correlation between main channel cross-sectional area and the ratio conservative masses to non-conservative masses (Figure 3-46). In addition, storage zone cross-sectional area and exchange coefficient also do not demonstrate a relationship with the ratio. (Figure 3-47 and 3-48). However, the main stream cross-sectional area and exchange

coefficient increased when the ratio increased.

Three metrics ( $L_s, q_s$  and  $t_s$ ) display some correlation with the ratio of nutrient to tracer masses. The turnover length has significant negative relationship with the ratio in reach 1 for  $PO_4$  ( $p=0.055$ ) and reach 2 for  $NH_4$  (Figure 3-49,  $p=0.014$ ). Storage exchange fluxes do not display distinct correlation with the ratio of nutrient to tracer masses. However, they show that when ratio increased storage exchange flux also increased (Figure 3-50). Average residence time in the storage zone has positive significant negative correlation with the ratio of nutrient to tracer masses in reach 1 for  $PO_4$  (Figure 3-51,  $p=0.034$ ).

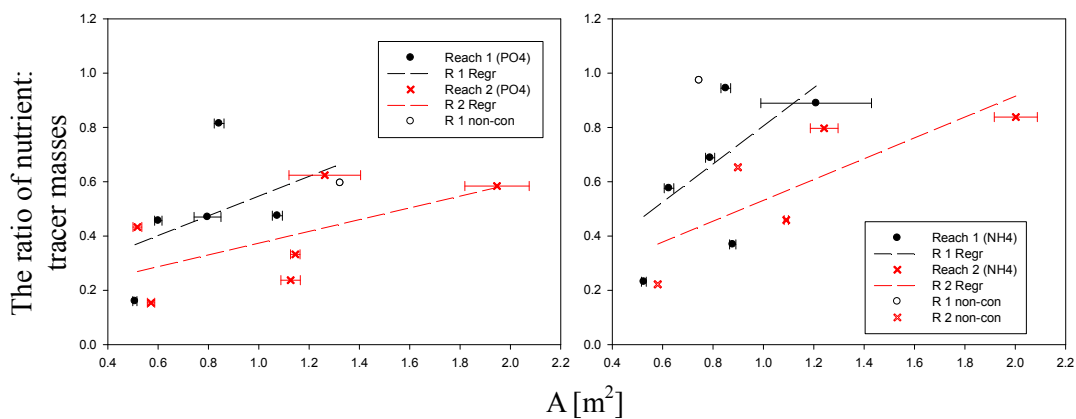


Figure 3-46 Linear regression between Ratio of nutrient: tracer masses and Main channel area (A) with 95% confidence limits, left is Injection A, right is Injection B at I8 Inlet

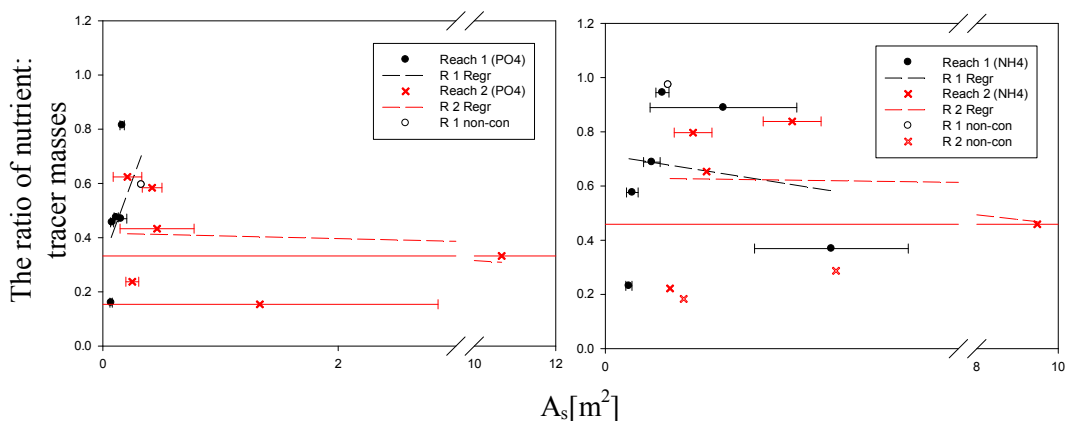


Figure 3-47 Linear regression between Ratio of nutrient: tracer masses and Storage zone area ( $A_s$ ) with 95% confidence limits, left is Injection A, right is Injection B at I8 Inlet

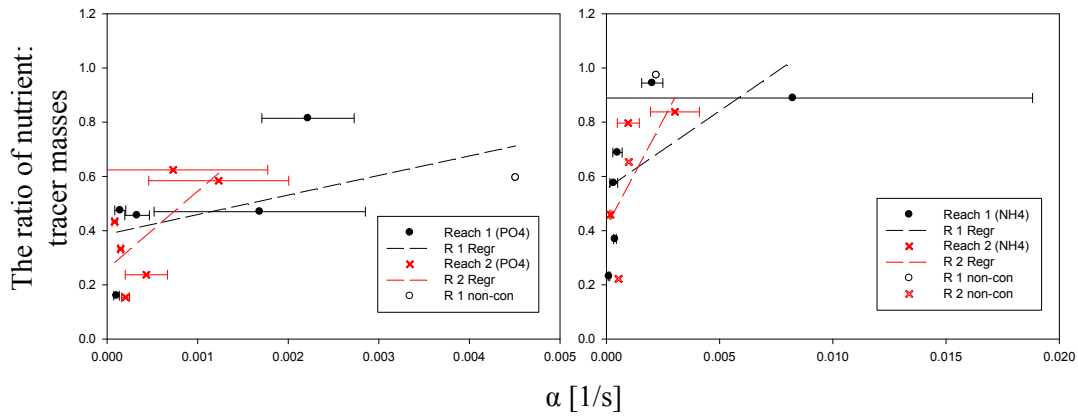


Figure 3-48 Linear Regression between ratio of nutrient: tracer masses and Exchange coefficient ( $\alpha$ ) with 95% confidence limits, left is Injection A, right is Injection B at I8 Inlet

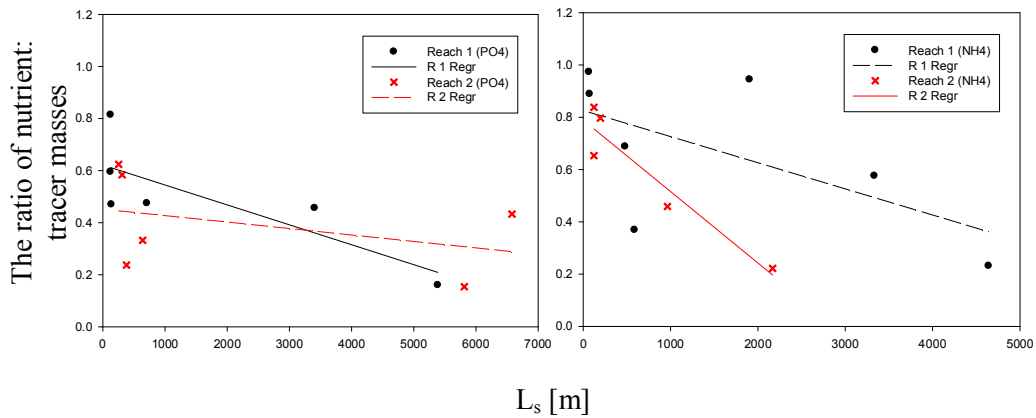


Figure 3-49 Linear regression between Ratio of nutrient: tracer masses and Turn over length ( $L_s$ ) with 95% confidence limits, left is Injection A, right is Injection B at I8 Inlet

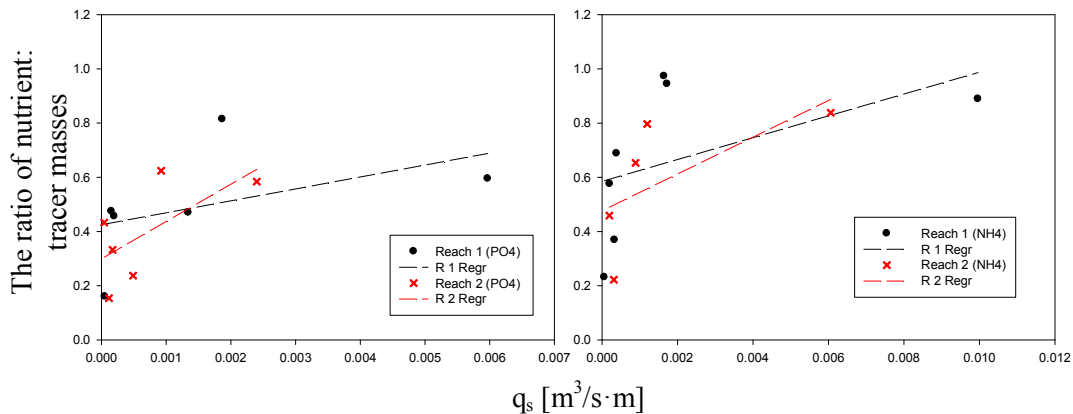


Figure 3-50 Linear regression between Ratio of nutrient: tracer masses and Storage exchange flux ( $q_s$ ) with 95% confidence limits, left is Injection A, right is Injection B at I8 Inlet

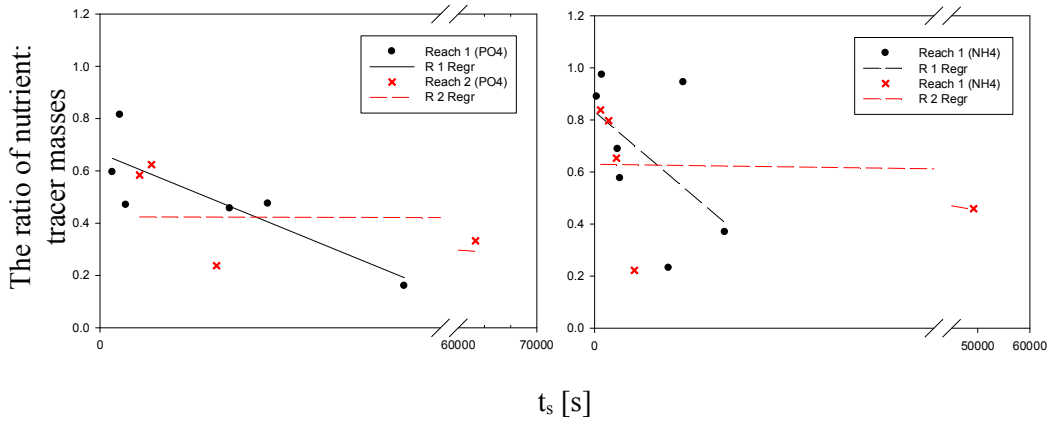


Figure 3-51 Linear regression between Ratio of nutrient: tracer masses and Average residence time in storage zone ( $t_s$ ) with 95% confidence limits, left is Injection A, right is Injection B at I8 Inlet

### 3.4.2 I8 Outlet

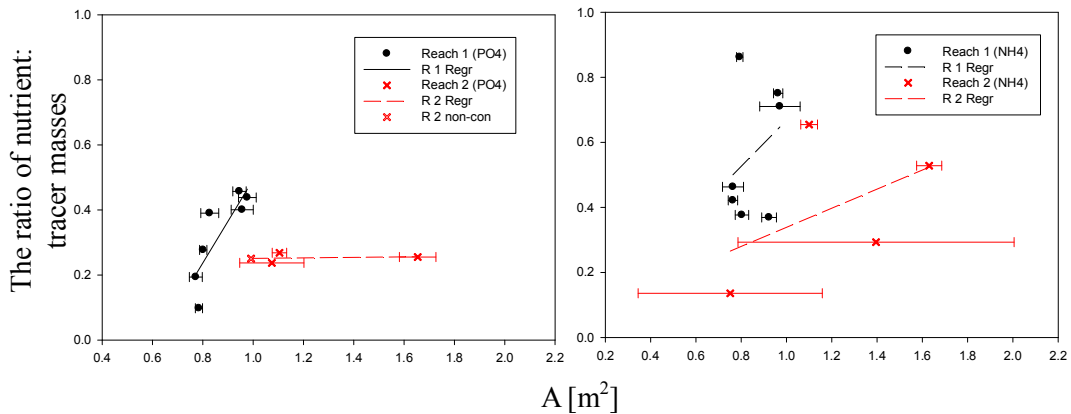


Figure 3-52 Linear regression between Ratio of nutrient: tracer masses and Main channel area (A) with 95% confidence limits, left is Injection A, right is Injection B at I8 Outlet

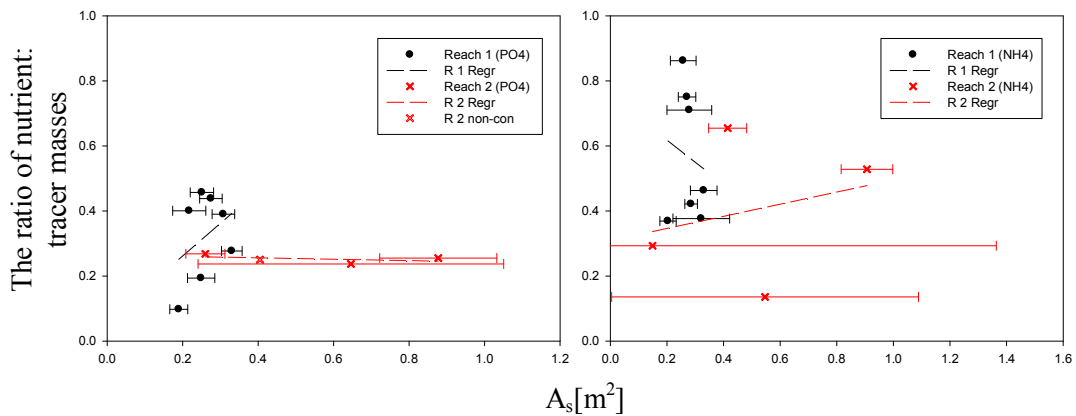


Figure 3-53 Linear regression between Ratio of nutrient: tracer masses and Storage zone area ( $A_s$ ) with 95% confidence limits, left is Injection A, right is Injection B at I8 Outlet

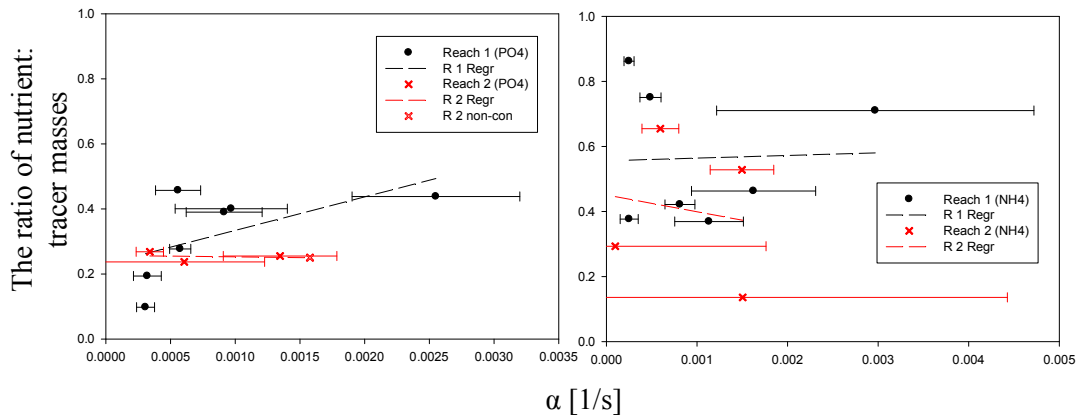


Figure 3-54 Linear regression between Ratio of nutrient: tracer masses and Exchange coefficient ( $\alpha$ ) with 95% confidence limits, left is Injection A, right is Injection B at I8 Outlet

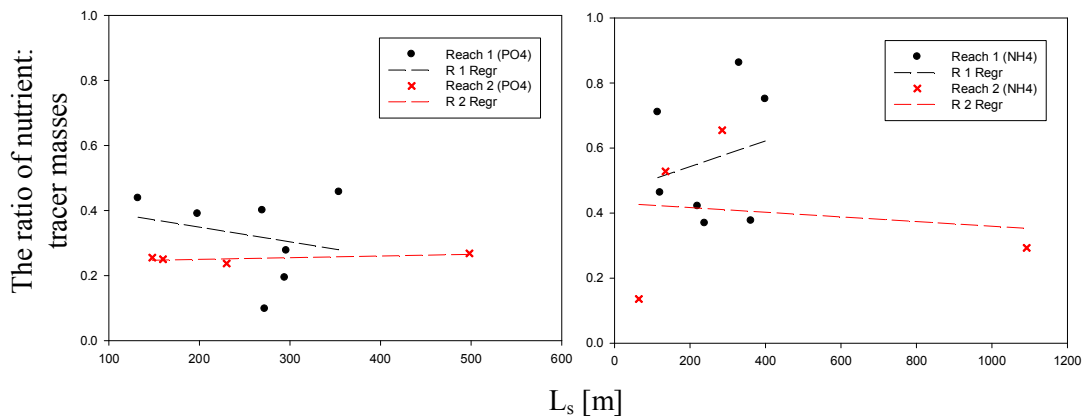


Figure 3-55 Linear regression between Ratio of nutrient: tracer masses and Turn over length ( $L_s$ ) with 95% confidence limits, left is Injection A, right is Injection B at I8 Outlet

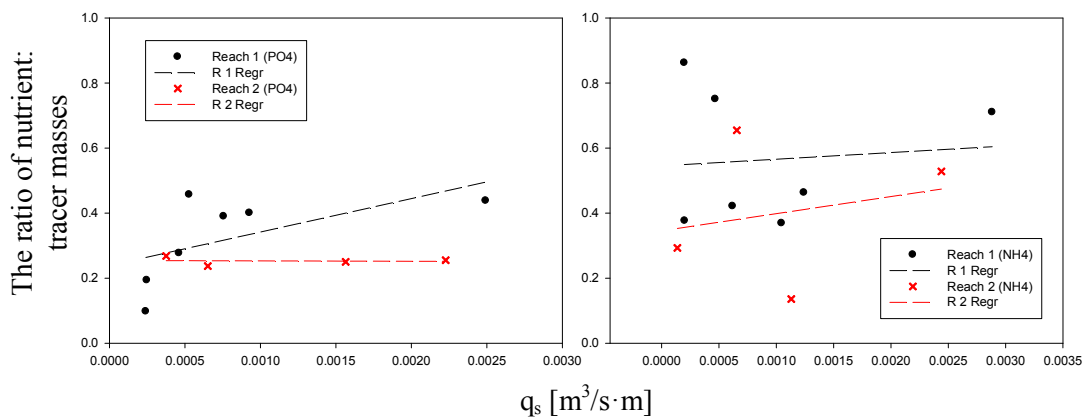


Figure 3-56 Linear regression between Ratio of nutrient: tracer masses and Storage exchange flux ( $q_s$ ) with 95% confidence limits, left is Injection A, right is Injection B at I8 Outlet

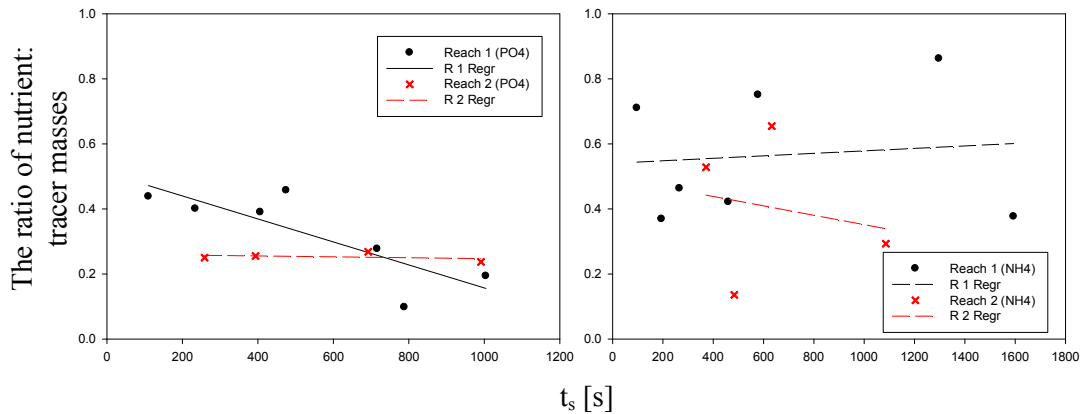


Figure 3-57 Linear regression between Ratio of nutrient: tracer masses and Average residence time in storage zone ( $t_s$ ) with 95% confidence limits, left is Injection A, right is Injection B at I8 Outlet

In the I8 Outlet, parameters related to transient storage ( $A$ ,  $A_s$  and  $\alpha$ ) do not show relationship with the ratio of nutrient to tracer masses (Figure 3-52, 3-53 and 3-54). These results are same as those of I8 Inlet.

Three metrics related to transient storage also do not display distinct correlation with the ratio of nutrient to tracer masses. Only average residence time in storage zone has significant negative relationship with the ratio in reach 1 for NH<sub>4</sub> (Figure. 3-57,  $p=0.022$ ). In the I8 Outlet, the metrics do not have similar trends which display in the I8-Inlet.

### 3.5 Stream Water Temperature as a Potential Control on the fate of PO<sub>4</sub> and NH<sub>4</sub>

#### 3.5.1 I8 Inlet

To determine whether average stream water temperature may influence solute transport dynamics, dispersion coefficient and main channel cross sectional area are related to stream water temperature. Dispersion coefficient displays positive correlation to stream water temperature with no significant trends (Figure 3-58). Main channel cross sectional area shows negative correlation to stream water temperature with no significant trends (Figure 3-59). This suggests that stream water temperature does not control on dispersion and advection mechanisms.

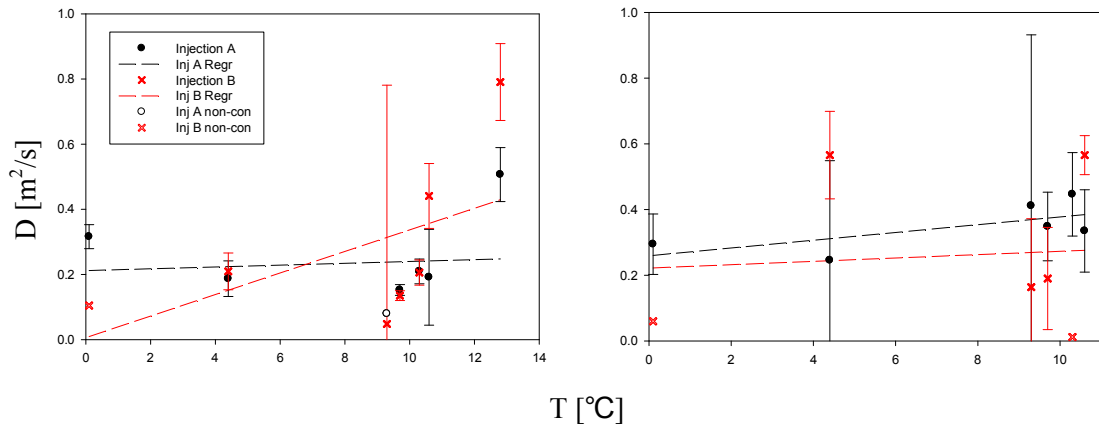


Figure 3-58 Linear regression between Dispersion coefficient (D) and Temperature (°C) with 95% confidence limits, left is Reach 1, right is Reach 2 at I8 Inlet

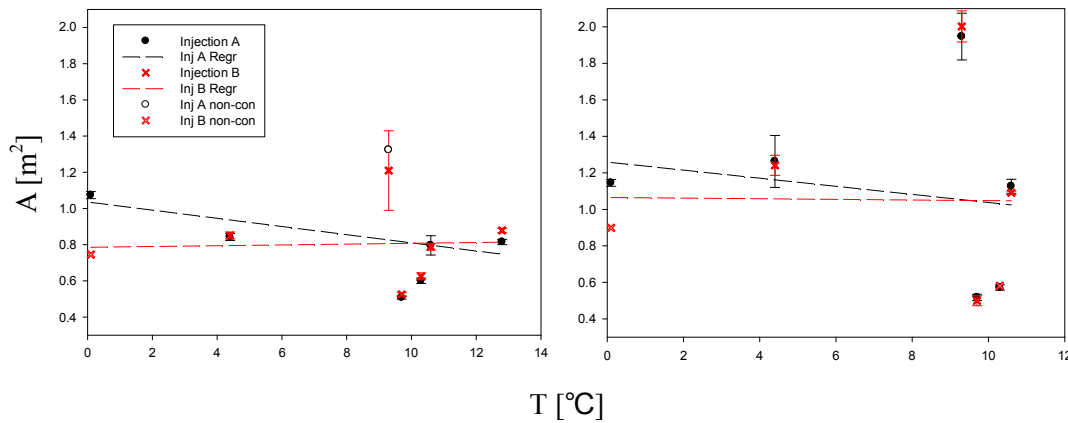


Figure 3-59 Linear regression between Main Stream Area (A) and Temperature (°C) with 95% confidence limits, left is Reach 1, right is Reach 2 at I8 Inlet

Two parameters related to transient storage – storage zone cross sectional area and exchange coefficient – are tested to determine influence of stream water temperature on transient storage mechanism. One potential reason for the influence of stream water temperature on exchange is that the dynamic viscosity of water is dependent on temperature. Similar to the transport metrics, there are no distinct relationships between estimated parameters and stream water temperature (Figure 3-60 and 3-61).

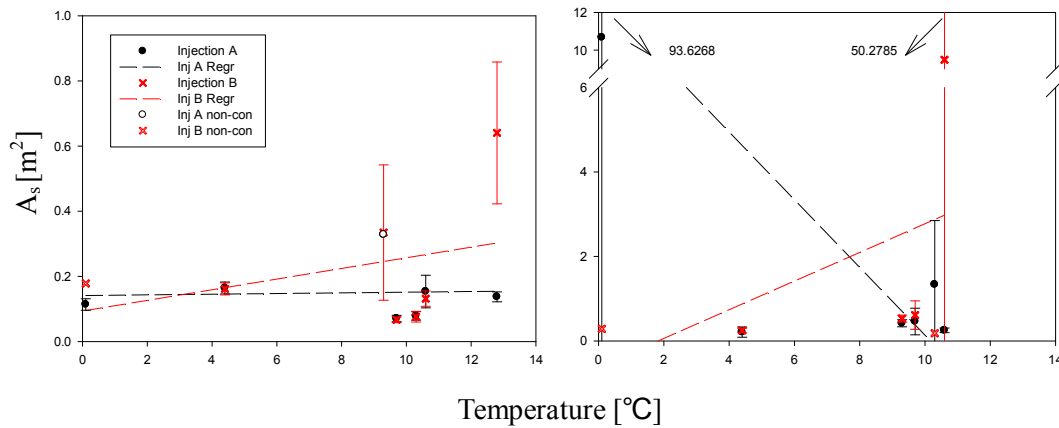


Figure 3-60 Linear regression between Storage zone area ( $A_s$ ) and Temperature ( $^{\circ}\text{C}$ ) with 95% confidence limits, left is Reach 1, right is Reach 2 at I8 Inlet

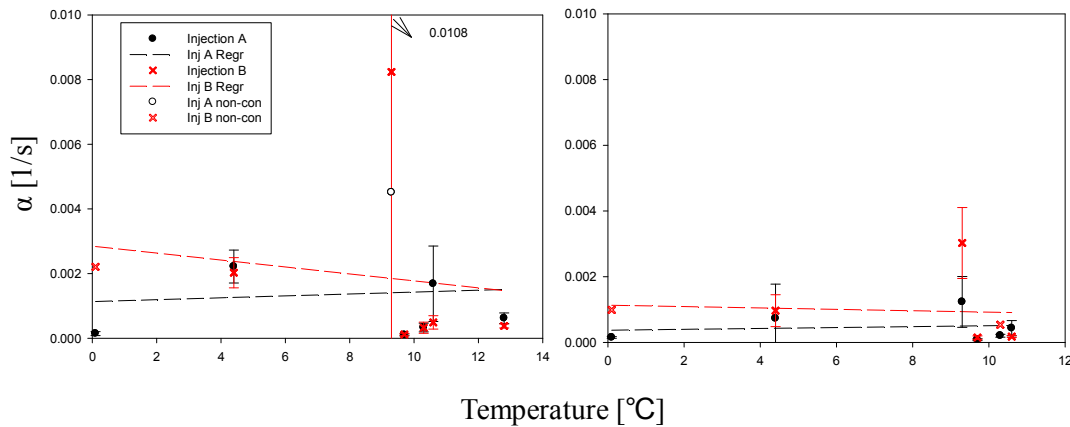


Figure 3-61 Linear Regression between Exchange Coefficient ( $\alpha$ ) and Temperature ( $^{\circ}\text{C}$ ) with 95% confidence limits, left is Reach 1, right is Reach 2 at I8 Inlet

Estimated turnover length is significantly correlated to stream water temperature in reach 1 (Figure 3-62,  $p=0.042$  Reach 1 Injection B), but no other injection set is correlated with stream water temperature. In addition, storage exchange flux and average residence time in storage zone also display no correlation with average stream water temperature (Figure 3-63).

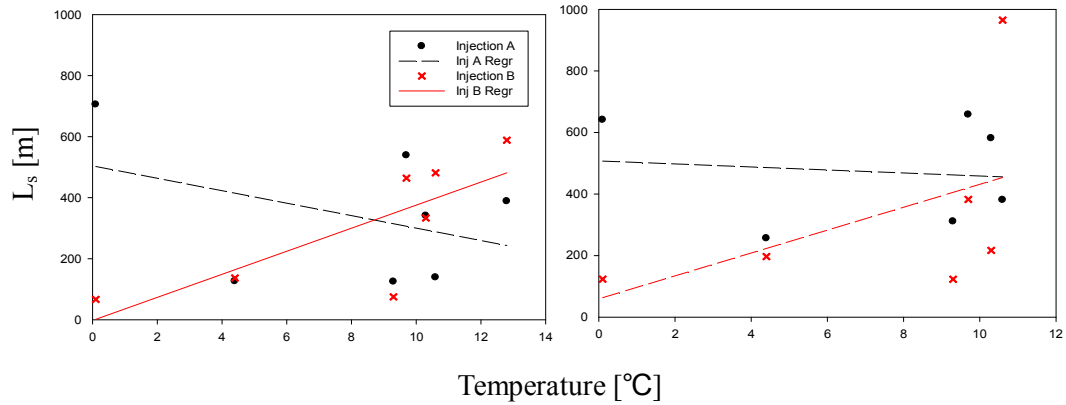


Figure 3-62 Linear regression between Turn over length ( $L_s$ ) and Temperature ( $^{\circ}\text{C}$ ), left is Reach 1, right is Reach 2 at I8 Inlet

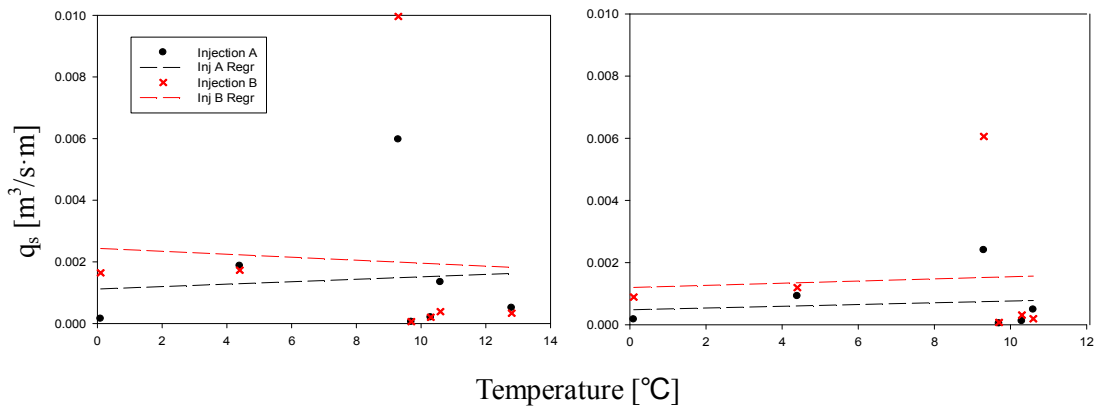


Figure 3-63 Linear regression between Storage exchange flux ( $q_s$ ) and Temperature ( $^{\circ}\text{C}$ ), left is Reach 1, right is Reach 2 at I8 Inlet

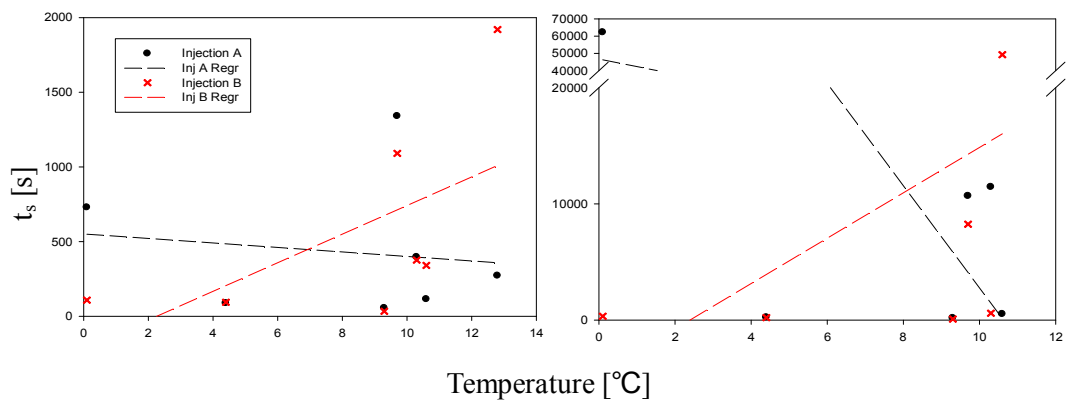


Figure 3-64 Linear regression between Average residence time in storage zone ( $t_s$ ) and Temperature ( $^{\circ}\text{C}$ ), left is Reach 1, right is Reach 2 at I8 Inlet

The 1<sup>st</sup> order decay coefficient in main channel cross sectional area display positive correlation with average stream water temperature in reach 1 for both  $\text{NH}_4$  and  $\text{PO}_4$  (Figure 3-65,  $p=0.086$  Reach1 Injection A,  $p=0.064$  Reach 1 Injection B). This parameter values do not

have significant trends in reach 2. However, they also display positive correlation. The 1<sup>st</sup> order decay coefficient for PO<sub>4</sub> in storage zone has distinct relationship with stream water temperature in reach2 (Figure 3-66, p=0.089 Reach 2 Injection A). This parameter has negative correlation with water temperature in reach 1 for PO<sub>4</sub>, this suggests that when stream water temperature increases, uptake of PO<sub>4</sub> also increase. The RSF metric does not have any relationship with stream water temperature for either nutrient (Figure 3-67). This is likely because the metric is a function of uptake and transient storage, which may not be related. Similar to the previous result between transient storage parameters and stream water temperature, we conclude that stream water temperature only affects nutrient uptake, and does not have a significant impact on transport exchange processes. In addition, the estimated parameter values are different between both injections (PO<sub>4</sub> and NH<sub>4</sub>).

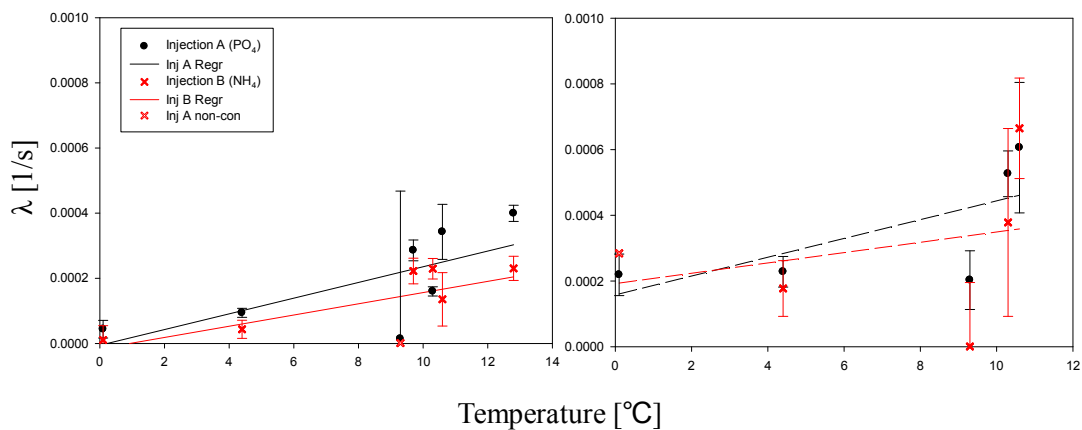


Figure 3-65 Linear Regression between Decay coefficient in main channel ( $\lambda$ ) and Temperature ( $^{\circ}\text{C}$ ) with 95% confidence limits, left is Reach 1, right is Reach 2 at 18 Inlet

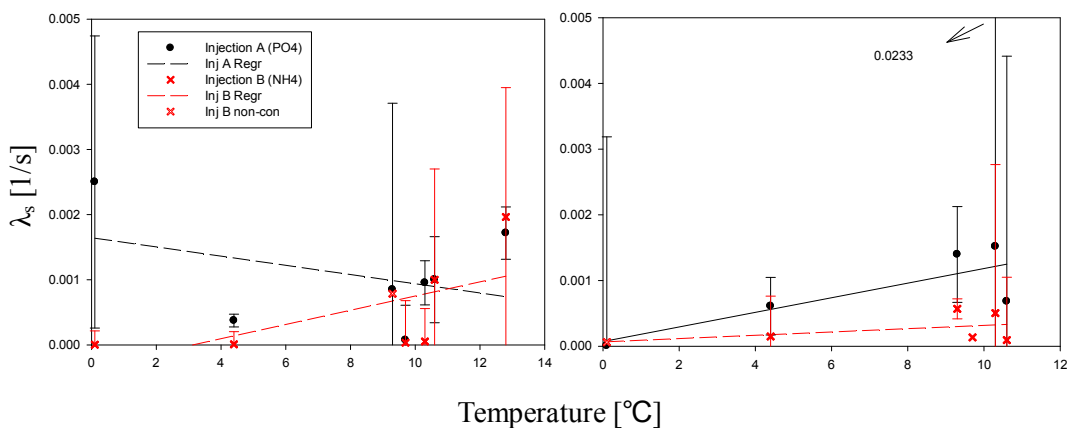


Figure 3-66 Linear Regression between Decay coefficient in storage zone ( $\lambda_s$ ) and Temperature ( $^{\circ}\text{C}$ ) with 95% confidence limits, left is Reach 1, right is Reach 2 at I8 Inlet

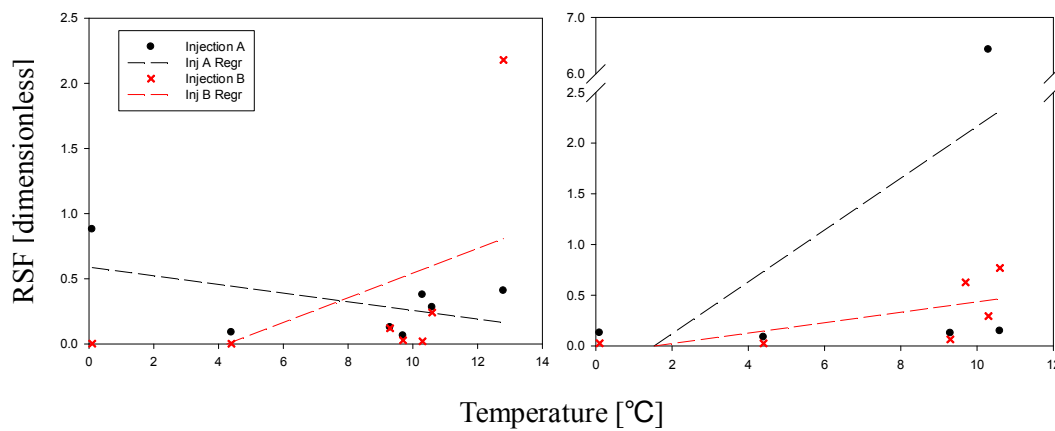


Figure 3-67 Linear regression between RSF and Temperature ( $^{\circ}\text{C}$ ), left is Reach 1, right is Reach 2 at I8 Inlet

### 3.5.2 I8 Outlet

Similar to I8 Inlet, dispersion coefficients and main channel cross sectional areas simulated in I8 Outlet are not correlated with stream water temperature (Figure 3-68 and 3-69). These results are similar to those in I8 Inlet, stream water temperature does not have relationship with advection and dispersion mechanisms (Section 3.3.1) and these transport parameters only have strong relationships with hydraulic characteristics (Section 3.2.1).

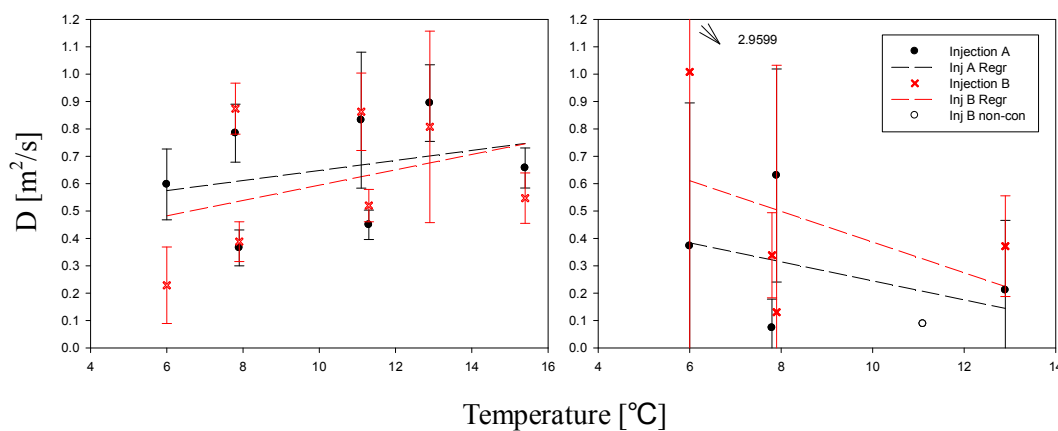


Figure 3-68 Linear Regression between Dispersion coefficient ( $D$ ) and Temperature ( $^{\circ}\text{C}$ ) with 95% confidence limits, left is Reach 1, right is Reach 2 at I8 Outlet

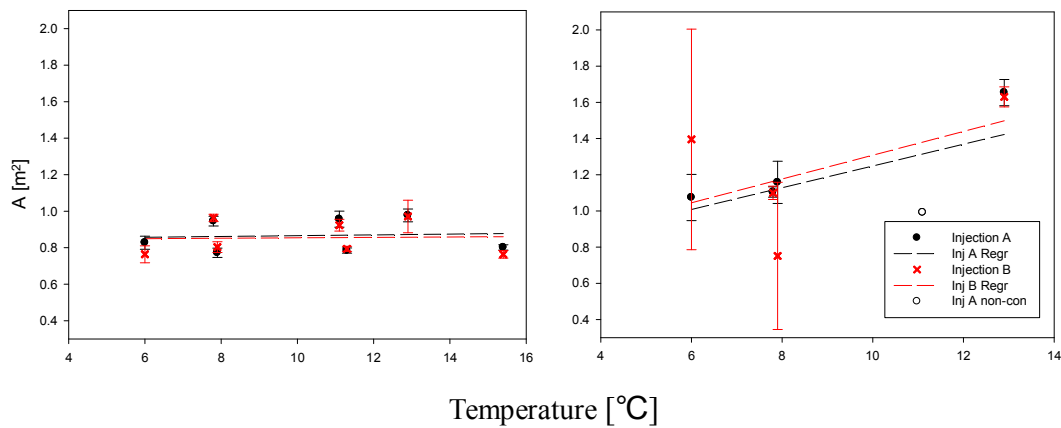


Figure 3-69 Linear regression between Main Stream Area (A) and Temperature ( $^{\circ}\text{C}$ ) with 95% confidence limits, left is Reach 1, right is Reach 2 at I8 Outlet

The transient storage parameters – storage zone cross sectional area and exchange coefficient- have slightly different relationships, compared to I8Inlet. Storage zone cross sectional area displays a positive correlation with stream water temperature in reach 2 (Figure 3-70,  $p=0.038$  Reach 2 Injection B), however uncertainties in these parameters are great. Exchange coefficients display same trends that increasing trends when stream water temperature increase in both streams (Figure 3-71). However, these results do not have significant trends. Because of these reasons, this is not enough to suggest that stream water temperature controls transient storage dynamics.

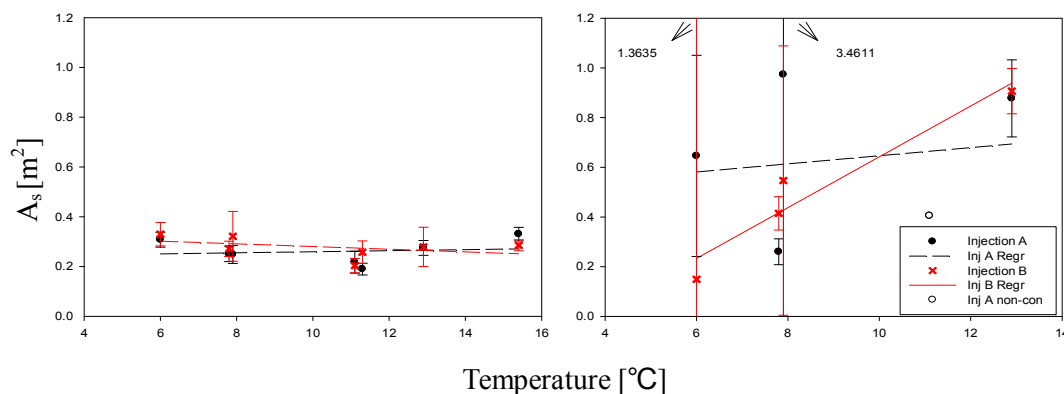


Figure 3-70 Linear regression between Storage zone area ( $A_s$ ) and Temperature ( $^{\circ}\text{C}$ ) with 95% confidence limits, left is Reach 1, right is Reach 2 at I8 Outlet

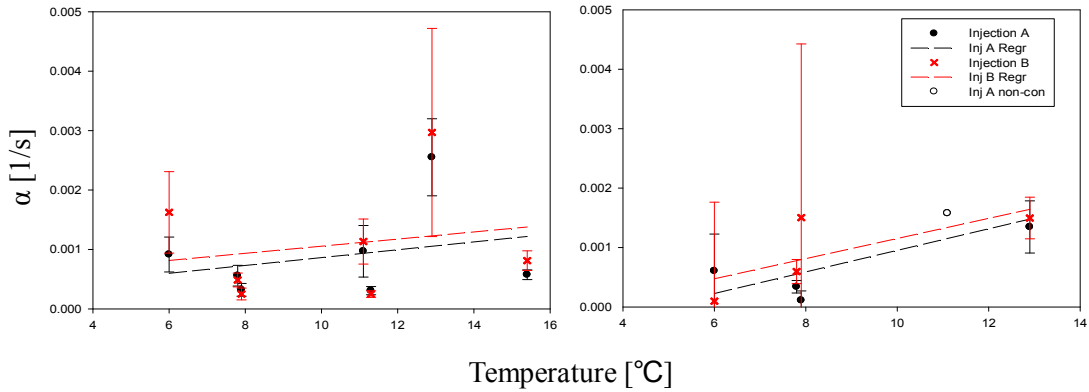


Figure 3-71 Linear regression between Exchange coefficient ( $\alpha$ ) and Temperature ( $^{\circ}\text{C}$ ) with 95% confidence limits, left is Reach 1, right is Reach 2 at I8 Outlet

Turnover length is not correlated with stream water temperature, similar to I8 Inlet (Figure 3-72). However, storage exchange flux displays significant correlation with water temperature in reach 2 (Figure 3-73,  $p=0.044$  Reach 2 Injection A and  $p=0.002$  Reach 2 Injection B). The average residence time in storage zone also does not have correlation with stream water temperature (Figure 3-74). These results support the idea that stream water temperature does not control transport or transient storage dynamics.

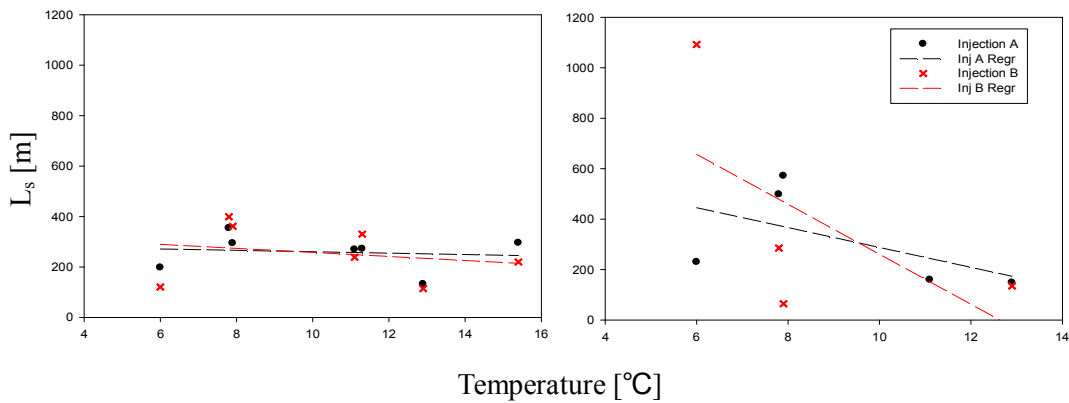


Figure 3-72 Linear regression between Turn over length ( $L_s$ ) and Temperature ( $^{\circ}\text{C}$ ), left is Reach 1, right is Reach 2 at I8 Outlet

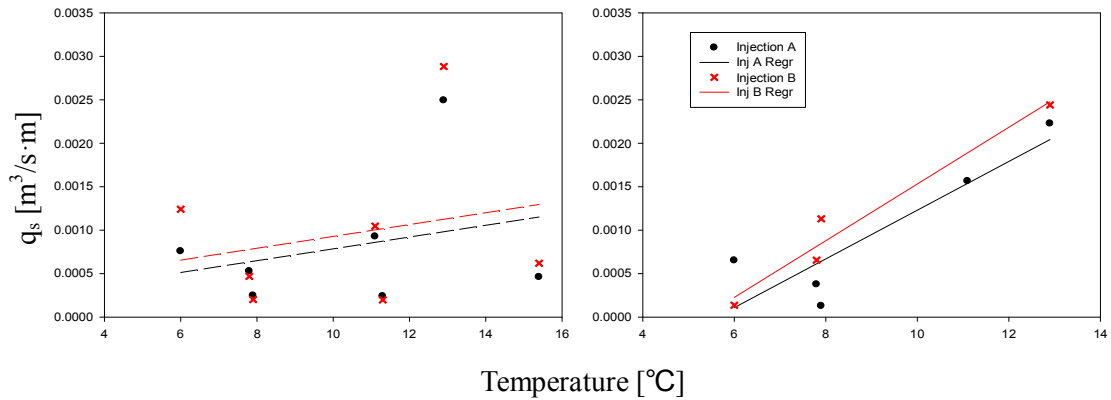


Figure 3-73 Linear regression between Storage exchange flux ( $q_s$ ) and Temperature ( $^{\circ}\text{C}$ ), left is Reach 1, right is Reach 2 at I8 Outlet

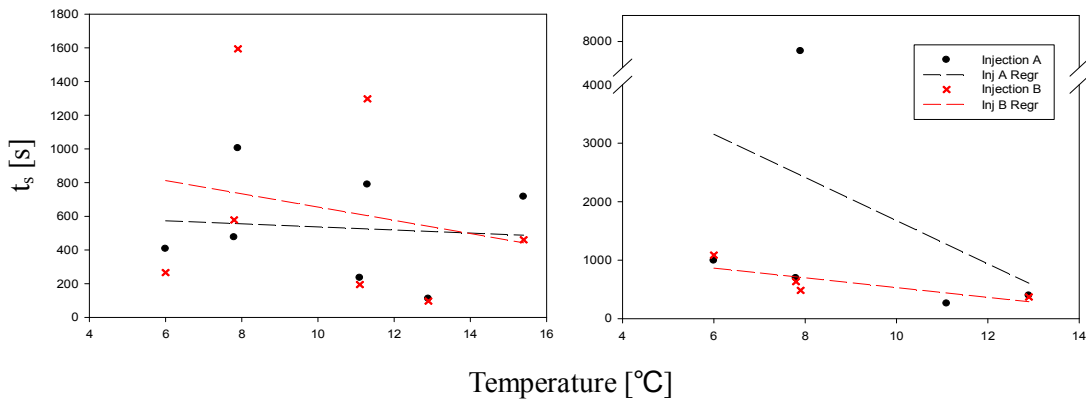


Figure 3-74 Linear regression between Average residence time in storage zone ( $t_s$ ) and Temperature ( $^{\circ}\text{C}$ ), left is Reach 1, right is Reach 2 at I8 Outlet

The 1<sup>st</sup> order decay coefficients in the main channel and storage zone were related to stream temperature to determine whether temperature controls nutrient uptake. These nutrient uptake rates are not significantly correlated with stream water temperature, which is different from the results of I8 Inlet (Figure 3-75 and 3-76). These results suggest that there are other factors which affect nutrient uptake rates in I8 Outlet. Additionally, there are differences between estimated parameter values from both injections ( $\text{PO}_4$  and  $\text{NH}_4$ ), similar to I8 Inlet.

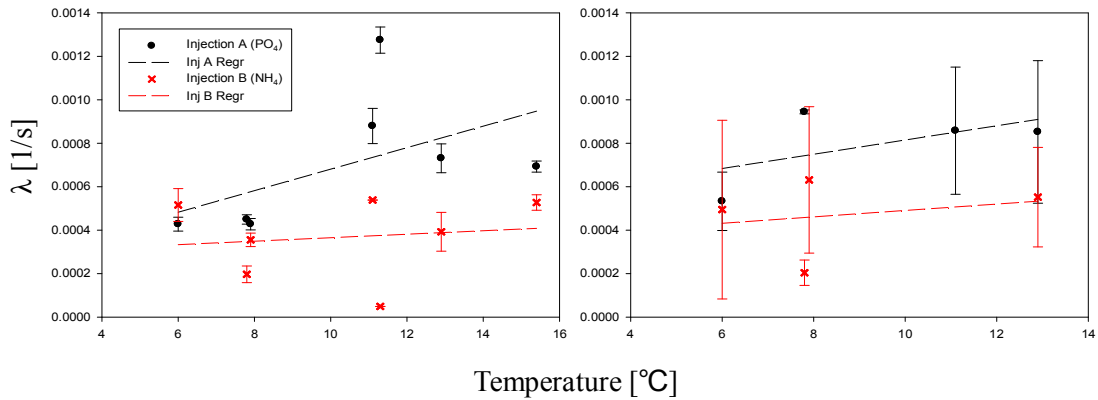


Figure 3-75 Linear regression between Decay coefficient in main channel ( $\lambda$ ) and Temperature (°C) with 95% confidence limits, left is Reach 1, right is Reach 2 at I8 Outlet

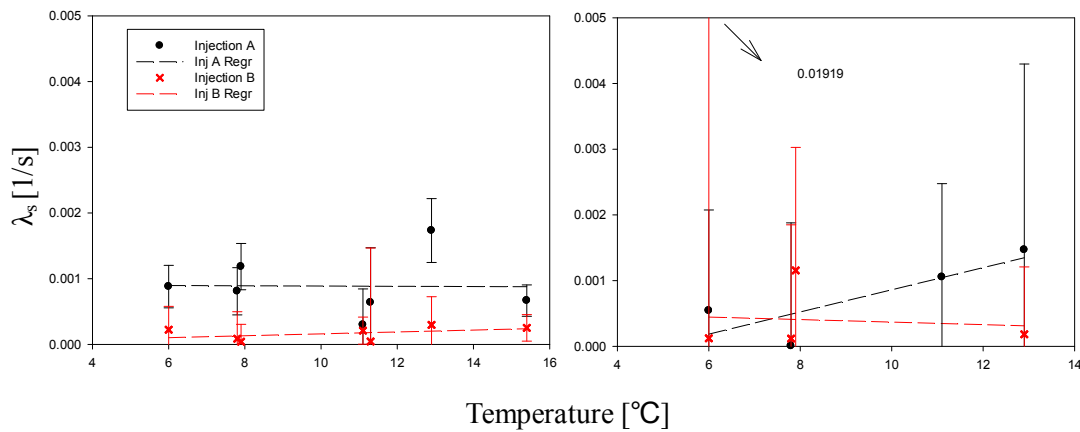


Figure 3-76 Linear regression between Decay coefficient in storage zone ( $\lambda_s$ ) and Temperature (°C) with 95% confidence limits, left is Reach 1, right is Reach 2 at I8 Outlet

The RSF metric is also not correlated with stream water temperature, similar to the result of I8 Inlet (Figure 3-77). This result supports the previous suggestion that, in addition to transport and transient storage dynamics, stream water temperature does not control nutrient uptake in I8 Outlet.

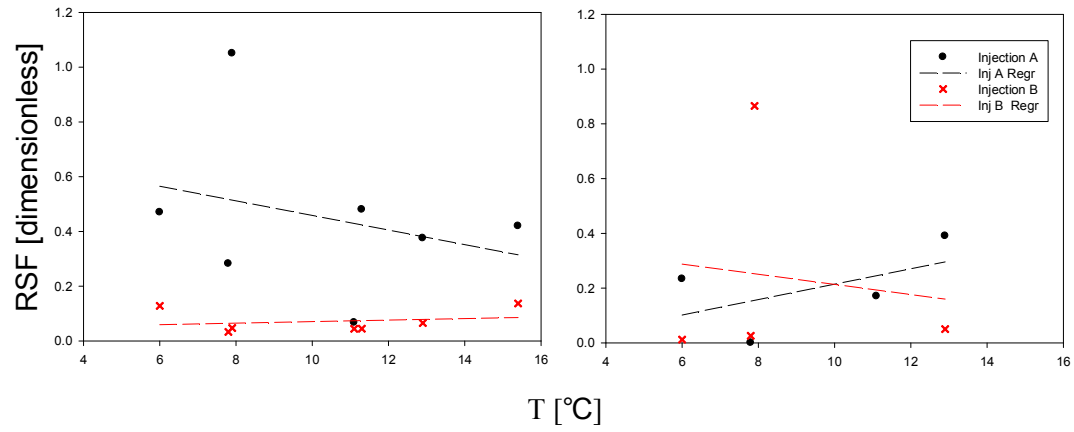


Fig 3-77 Linear regression between RSF and Temperature (°C), left is Reach 1, right is Reach 2 at I8 Outlet

## 4 Discussion

### 4.1 OTIS-P and uncertainty

The parameters estimated from simulations are not always reliable for various reasons such as measurement errors, structure of model errors and errors from nonlinear least squares parameter methods. For reliability of these simulations, coefficients of determination between observed data and simulated data are provided in appendix. Almost all of these values are greater than 0.9, indicating excellent simulation fits to observed data. However, we should consider about uncertainty during the analysis.

Many of the estimated parameters for reach 1 have lower uncertainty than those for reach 2. This is likely due to the difference in the number of observations in the two reaches and model structure. Frequently, the number of observations at reach 2 is less than in reach 1 (Appendix 7-3). The simulations of reach 1 and 2 were conducted at the same time. As mentioned, initial value of parameters are required to run the simulations. It is possible that these initial parameter values for reach 1 have an effect on estimation of parameters for reach 2.

Stream	Date(MM/DD)	Inj A (Cl)		Inj B (Cl)		Inj A (PO <sub>4</sub> )		Inj B (NH <sub>4</sub> )	
		R 1	R 2	R 1	R 2	R 1	R 2	R 1	R 2
I8IN	06/06	19	13	22	11	19	12	17	9
	06/12	25	12	24	11	26	13	23	10
	07/19	34		32		34		34	
	07/21	11	20	11	22	11	21	11	21
	07/28	12	22	13	21	12	21	13	21
	09/16	26	13	22	12	23	15	22	12
	09/25	23	24	23	12	23	12	23	11
I8OUT	06/04	22	11	17	11	23	11	18	10
	06/10	20	12	21	11	19		18	11
	07/16	34		31		34		31	
	07/19	34		32		34		34	
	07/26	27	12	24	11	26	13	23	10
	09/02	33		31		24		20	
	09/16	25	14	23	12	25	13	23	12

Table 4-1 the number of observation

In OTIS-P, all model parameters were estimated by linear regression optimization, these include a random error term within 95% confidence limits. These confidence intervals provide opportunity to consider the uncertainty of each estimated parameter. This is an important benefit of OTIS-P [Scott et al., 2003]. Estimates of parameter simulation uncertainty are valuable for assessing confidence in optimized parameter values. In the case of four metrics ( $q_s$ ,  $t_s$ ,  $L_s$  and RSF), since the metrics are acquired from equations which consisted of estimated parameters, the metrics have greater uncertainty than these for estimated parameters.

#### **4.2 Relationship between each parameter and control variable**

One dimensional solute transport with inflow and storage model (OTIS) includes transport (dispersion and advection), transient storage and chemical reaction mechanisms. Linear regressions between estimated parameters related to mechanisms and control variables were conducted to determine which variables may control which mechanisms (e.g. Q influence on transient storage processes). In addition, considering uncertainty was useful for identifying potential controls. This analysis has helped to identify relationships between mechanisms and controls in these streams.

Discharge is used as a parameter related to channel hydraulics and has some correlation with estimated parameters. Mainstream cross sectional area, exchange coefficient ( $A$ , and  $\alpha$ ) were found to be correlated to discharge in the both streams. In addition, dispersion coefficients ( $D$ ) displayed correlation with discharge in I8 outlet reach 1. In I8 Inlet reach 2, dispersion coefficient increased when discharge increased. Analyzing four metrics ( $A_s/A$ ,  $L_s$ ,  $q_s$ , and  $t_s$ ) is useful for interpreting the solute transport dynamics and quantified values are provided in table 4-2. Uncertainty of linear regression analysis and the calculation of metrics should be considered (eq. 2-7, 2-8 and 2-9). Ratios of storage zone

cross sectional areas to the main channel cross sectional area ( $A_s/A$ ) do not have relationship with discharge. However, this metric increase as stream discharge decreases in all reaches except I8inlet in reach1. Turn over length did not display significant correlation to three control variables due to the uncertainty of estimated parameter which used in the equation ( $\alpha$ ). Velocity is also influenced by many control variables. However, this metric was found to decrease when discharge increased in every stream. Storage exchange fluxes show distinct positive relation with discharge in both reaches of I8 Inlet and reach 1 in I8 outlet. Although average residence time in storage zone was not correlated with temperature and date in reach 2 of I8outlet, this metric has significant relationship with discharge. Additionally, this metric decreased when discharge decreased in every study stream. These results indicate that discharge is an important on transport and an inconsistent control on transient storage. These support suggestions from various previous studies regarding hydraulic control on transient storage [Legrand, Marcq, & Laudelout, 1985; D' Angelo et al., 1993; Wondzell & Swanson, 1996]. In addition, discharge does not exhibit correlation with parameters related to nutrient uptake. This means that discharge does not affect nutrient uptake, directly.

Average stream water temperature also exhibited a distinct relationship with nutrient uptake parameters ( $\lambda$ ,  $\lambda_s$ ). The 1<sup>st</sup> order decay in main channel has a positive relationship in I8 Inlet reach 1 and the 1<sup>st</sup> order decay in storage zone is significantly positively correlated with stream water temperature in I8 Inlet reach 2. Even though they have smaller p-value than 0.1, they have similar positive trends. Other previous studies also suggested that stream temperature has an influence on the uptake of  $PO_4$  and  $NH_4$ . Stream water temperature affects changes in microbial densities and activities and these have an effect on nutrient retention [Butturini & Sabater, 1998; D' Angelo et al., 1991]. The RSF metric related to nutrient uptake is not correlated with stream water temperature.

The ratio of nutrient to tracer masses do not display significant relationships with the

parameters related to transient storage. However metrics related to transient storage have some correlation with the ratio of nutrient to tracer masses. This suggests that the mass loss in main channel is affected by transient storage. In addition, the change of ratio of  $\text{PO}_4$  and  $\text{NH}_4$  are quite different.

Although, in this study, we found some direct relationships between estimated parameters and controls, there is another valuable result. Five parameters/metrics ( $D$ ,  $A$ ,  $\alpha$ ,  $q_s$  and  $t_s$ ) showed correlation with discharge. Hence, we show discharge has strong control transport and transient storage. However, other parameters related to these mechanisms ( $A_s$  and  $L_s$ ) did not display correlation with discharge. In addition, there are not any estimated parameters which have significant relationship with date which is a surrogate for thaw depth. However, these results do not mean thaw bulb is not a control on solute transport dynamics. Moreover, uptake rates of  $\text{PO}_4$  are generally higher than those for  $\text{NH}_4$  in the all reaches and these results could not be explained with stream temperature. In conclusion, other control variables should be adopted to predict solute transport dynamics without experiment.

### **4.3 Other control variables effects on solute transport dynamics**

The transient storage model representation of solute transport dynamics could not be elucidated with only discharge, date (thaw depth) and temperature. Although, the results from this study did not display significant relationship, channel hydraulics, active layer conditions and temperature should have some influence on transport, transient storage and nutrient uptake. In addition, a number of studies provided other factors which we did not consider affecting solute transport dynamics.

Apart from these three variables, stream morphology has been found to control solute transport dynamics. Morphology characteristics of streams play an important role in dominant solute transport processes (advection and dispersion) and transient storage [Leopold

& Maddock, 1953; Kasahara & Wondzell, 2003]. Additionally, this factor also has been shown to influence on transient storage in hyporheic zone. Harvey and Wagner [2000] suggested that various morphologic factors operate on transient storage in hyporheic zone such as channel slope, width, sinuosity and catchment. Packman and Salehin [2003] suggested that sediment characteristics such as porous bed and bed permeability also influence hyporheic exchange. Moreover, elevation of channel stage and water table and perturbations in the discharge affect transient storage [D' Angelo et al., 1993; Harvey & Bencala, 1993]. Degree of channel complexity and presence of secondary channels or channel splits also influences hyporheic exchange [Kasahara & Wondzell, 2003; Gooseff et al., 2007].

In the case of nutrient uptake, there are other control variables besides temperature. However, none were measured in concert with the solute injections. Many studies suggested nutrient cycling in the stream influences non-conservative solute transport dynamics [Mulholland et al., 1997; Hall et al., 2002]. Oxidation/reduction processes occurring in stream and availability of organic matter to be mineralized affect nutrient transformation and demand [Holmes et al., 1996]. Kim [1991] and Mulholland [1994] suggested the benthic biota is also controls on nutrient uptake. In addition, the degree of water exchange can be also correlated to nutrient demand [Berhanrdt et al., 2005; Mullholland et al., 2008]. Nutrient dynamics related to benthic microbial communities also control nutrient uptake of non-conservative solute [Mulholland et al., 1994; Mcknight et al., 2004]. Considering these additional controls may explain differences values of estimated parameters between  $PO_4$  and  $NH_4$ . Since  $PO_4$  and  $NH_4$  have different characteristics, they have different effects from biological communities and have different metabolic rates. Additionally, n-cycling such as nitrification and denitrification processes ma have influences on the uptake of  $NH_4$ . Mc Knight et al. [2004] also suggested benthic algal mats does not control uptake of  $NH_4$ . The

differences between the changes of ratios of  $\text{PO}_4$  to Cl masses and the changes of ratios of  $\text{NH}_4$  to Cl masses also indicate other controls.

## 5 Conclusion

The purpose of this study is to investigate relationship between three mechanisms of solute transport and fate (transport, transient storage and nutrient uptake) and control variables (discharge, date, mass loss and stream water temperature). These findings enhance our assists understanding of solute transport dynamics in arctic streams and effect of solute transport on ecosystem. The OTIS-P is used to estimate transport and transient storage parameters ( $D$ ,  $A$ ,  $A_s$ ,  $\alpha$ ) with conservative solute and nutrient uptake parameters ( $\lambda$  and  $\lambda_s$ ) with non-conservative solute. Solutes were injected with slug injection method. Additionally, five metrics ( $q_s$ ,  $t_s$ ,  $L_s$ , RSF and  $A_s/A$ ) were calculated to help understanding solute transport dynamics with estimated parameters.

During thaw season, arctic tundra streams are not significantly different from streams in temperate streams. However, a distinct difference in arctic streams is the thaw bulb which creates opportunity for hyporheic exchange during the thaw season. Transport and transient storage mechanisms are positively correlated with discharge, suggesting strong hydraulic controls on conservative processes. Although thaw depth is related to date, we did not observe date to control solute transport directly. However, thaw below a stream channel is still important control due to hyporheic exchange. Morphology characteristics (e.g. channel slope, width, sinuosity, etc) have also been shown to be important controls, affecting these mechanisms. In case of reactive solute transport dynamics, stream water temperature has a positive relationship with fate of non-conservative solutes. However, fate of non-conservative solutes is different for  $\text{NH}_4$  and  $\text{PO}_4$ . This is expected because they have different nutrient demand, cycling, and metabolic rates. In addition, difference between the ratio change of  $\text{PH}_4$  to Cl masses and the ratio change of  $\text{NH}_4$  to Cl masses can explain when we consider these controls. Additionally, biological communities and their change through time also affect nutrient uptake through time.

## Reference

- Bencala, K. E. (1983). Simulation of solute transport in a mountain pool-and-riffle stream with a kinetic mass transfer model for sorption. *Water Resources Research*, 19(3), 732-738.
- Bencala, K. E., Duff, J. H., Harvey, J. W., Jackman, A. P., & Triska, F. J. (1993). Modelling within the stream-catchment continuum. *Modelling change in environmental systems*, 163-187.
- Bernhardt, E. S., Likens, G. E., Hall, R. O., Buso, D. C., Fisher, S. G., Burton, T. M., ... & Lowe, W. H. (2005). Can't see the forest for the stream? In-stream processing and terrestrial nitrogen exports. *Bioscience*, 55(3), 219-230.
- Bradford, J. H., McNamara, J. P., Bowden, W., & Gooseff, M. N. (2003, December). Imaging depth-of-thaw beneath Arctic streams using ground-penetrating radar. In *AGU Fall Meeting Abstracts* (Vol. 1, p. 0818).
- Brosten, T. R., Bradford, J. H., McNamara, J. P., Gooseff, M. N., Zarnetske, J. P., Bowden, W. B., & Johnston, M. E. (2009). Estimating 3D variation in active-layer thickness beneath arctic streams using ground-penetrating radar. *Journal of Hydrology*, 373(3), 479-486.
- Brosten, T. R., Bradford, J. H., McNamara, J. P., Zarnetske, J. P., Gooseff, M. N., & Bowden, W. B. (2006). Profiles of temporal thaw depths beneath two arctic stream types using ground-penetrating radar. *Permafrost and Periglacial Processes*, 17(4), 341-355.
- Butturini, A., & Sabater, F. (1998). Ammonium and phosphate retention in a Mediterranean stream: hydrological versus temperature control. *Canadian Journal of Fisheries and Aquatic Sciences*, 55(8), 1938-1945.
- D'angelo, D. J., Webster, J. R., & Benfield, E. F. (1991). Mechanisms of stream phosphorus

- retention: an experimental study. *Journal of the North American Benthological Society*, 225-237.
- D'Angelo, D. J., Webster, J. R., Gregory, S. V., & Meyer, J. L. (1993). Transient storage in Appalachian and Cascade mountain streams as related to hydraulic characteristics. *Journal of the North American Benthological Society*, 223-235.
- Edwardson, K. J., Bowden, W. B., Dahm, C., & Morrice, J. (2003). The hydraulic characteristics and geochemistry of hyporheic and parafluvial zones in Arctic tundra streams, north slope, Alaska. *Advances in Water Resources*, 26(9), 907-923.
- Gooseff MN, McKnight DM, Runkel RL, Duff JH (2004). Denitrification and hydrologic transient storage in a glacial meltwater stream, McMurdo Dry Valleys, Antarctica. *Limnol Oceanogr* 49:1884–95
- Gooseff, M. N., & McGlynn, B. L. (2005). A stream tracer technique employing ionic tracers and specific conductance data applied to the Maimai catchment, New Zealand. *Hydrological processes*, 19(13), 2491-2506.
- Gooseff, M. N., Bencala, K. E., Scott, D. T., Runkel, R. L., & McKnight, D. M. (2005). Sensitivity analysis of conservative and reactive stream transient storage models applied to field data from multiple-reach experiments. *Advances in water resources*, 28(5), 479-492.
- Gooseff, M. N., Hall, R. O., & Tank, J. L. (2007). Relating transient storage to channel complexity in streams of varying land use in Jackson Hole, Wyoming. *Water Resources Research*, 43(1).
- Gooseff, M. N., McKnight, D. M., Runkel, R. L., & Duff, J. H. (2004). Denitrification and hydrologic transient storage in a glacial meltwater stream, McMurdo Dry Valleys, Antarctica. *Limnology and Oceanography*, 49(5), 1884-1895.
- Hall, R. O., Bernhardt, E. S., & Likens, G. E. (2002). Relating nutrient uptake with transient

- storage in forested mountain streams. *Limnology and Oceanography*, 47(1), 255-265.
- Hall, R. O., Bernhardt, E. S., & Likens, G. E. (2002). Relating nutrient uptake with transient storage in forested mountain streams. *Limnology and Oceanography*, 47(1), 255-265.
- Harvey, J. W., & Wagner, B. J. (2000). Quantifying hydrologic interactions between streams and their subsurface hyporheic zones. *Streams and ground waters*, 344.
- Harvey, J. W., Wagner, B. J., & Bencala, K. E. (1996). Evaluating the reliability of the stream tracer approach to characterize stream-subsurface water exchange. *Water Resources Research*, 32(8), 2441-2451.
- Holmes, R. M., Jones Jr, J. B., Fisher, S. G., & Grimm, N. B. (1996). Denitrification in a nitrogen-limited stream ecosystem. *Biogeochemistry*, 33(2), 125-146.
- Kane, D. L., Hinzman, L. D., Benson, C. S., & Everett, K. R. (1989). Hydrology of Imnavait Creek, an arctic watershed. *Ecography*, 12(3), 262-269.
- Kasahara, T., & Wondzell, S. M. (2003). Geomorphic controls on hyporheic exchange flow in mountain streams. *Water Resources Research*, 39(1), SBH-3.
- Kim, B. K., Jackman, A. P., & Triska, F. J. (1992). Modeling biotic uptake by periphyton and transient hyporheic storage of nitrate in a natural stream. *Water resources research*, 28(10), 2743-2752.
- Legrand-Marcq, C., & Laudelout, H. (1985). Longitudinal dispersion in a forest stream. *Journal of Hydrology*, 78(3), 317-324.
- Leopold, L. B., & Maddock, T. (1953). The hydraulic geometry of stream channels and some physiographic implications.
- McKnight DM, Runkel RL, Duff JH, Tate CM, Moorhead D (2004). Inorganic nitrogen and phosphorous dynamics of Antarctic glacial meltwater streams as controlled by hyporheic exchange and benthic autotrophic communities. *J N Am Benthol Soc* 23(2):171-88.

- McNamara, J. P., Kane, D. L., & Hinzman, L. D. (1997). Hydrograph separations in an Arctic watershed using mixing model and graphical techniques. *Water Resources Research*, 33(7), 1707-1719.
- McNamara, J. P., Kane, D. L., & Hinzman, L. D. (1998). An analysis of streamflow hydrology in the Kuparuk River Basin, Arctic Alaska: a nested watershed approach. *Journal of Hydrology*, 206(1), 39-57.
- Mulholland, P. J., Helton, A. M., Poole, G. C., Hall, R. O., Hamilton, S. K., Peterson, B. J., ... & Thomas, S. M. (2008). Stream denitrification across biomes and its response to anthropogenic nitrate loading. *Nature*, 452(7184), 202-205.
- Mulholland, P. J., Marzolf, E. R., Webster, J. R., Hart, D. R., & Hendricks, S. P. (1997). Evidence that hyporheic zones increase heterotrophic metabolism and phosphorus uptake in forest streams. *Limnology and Oceanography*, 42(3), 443-451.
- Mulholland, P. J., Steinman, A. D., Marzolf, E. R., Hart, D. R., & DeAngelis, D. L. (1994). Effect of periphyton biomass on hydraulic characteristics and nutrient cycling in streams. *Oecologia*, 98(1), 40-47.
- Osterkamp, T. E., & Romanovsky, V. E. (1999). Evidence for warming and thawing of discontinuous permafrost in Alaska. *Permafrost and Periglacial Processes*, 10(1), 17-37.
- Packman, A. I., & Salehin, M. (2003). Relative roles of stream flow and sedimentary conditions in controlling hyporheic exchange. In *The Interactions between Sediments and Water* (pp. 291-297). Springer Netherlands.
- Payn, R. A., Gooseff, M. N., McGlynn, B. L., Bencala, K. E., & Wondzell, S. M. (2009). Channel water balance and exchange with subsurface flow along a mountain headwater stream in Montana, United States. *Water Resources Research*, 45(11).
- Runkel, R. L. (1991). Runkel, R. L., & Broshears, R. E. (1991). One-dimensional transport

with inflow and storage (OTIS): A solute transport model for small streams.

CADSWES, Center for Advanced Decision Support for Water and Environmental Systems, Department of Civil Engineering, University of Colorado.

Runkel, R. L. (1998). One dimensional transport with inflow and storage (OTIS): a solute transport model for streams and rivers. US Geological Survey Water-Resources Investigation Report 98-4018. US Geological Survey, Denver, Colorado.

(Available from: <http://co.water.usgs.gov/otis>)

Runkel, R. L. (2002). A new metric for determining the importance of transient storage. *Journal of the North American Benthological Society*, 21(4), 529-543.

Runkel, R. L., & S. C. (1993). An efficient numerical solution of the transient storage equations for solute transport in small streams. *Water Resources Research*, 29(1), 211-215.

Scott, D. T., Gooseff, M. N., Bencala, K. E., & Runkel, R. L. (2003). Automated calibration of a stream solute transport model: implications for interpretation of biogeochemical parameters. *Journal of the North American Benthological Society*, 22(4), 492-510.

Sturm, M., Douglas, T., Racine, C., & Liston, G. E. (2005). Changing snow and shrub conditions affect albedo with global implications. *Journal of Geophysical Research: Biogeosciences (2005–2012)*, 110(G1).

Thackston, E. L., & Schnelle, K. B. (1970). Predicting effects of dead zones on stream mixing. *Journal of the Sanitary Engineering Division*, 96(2), 319-331.

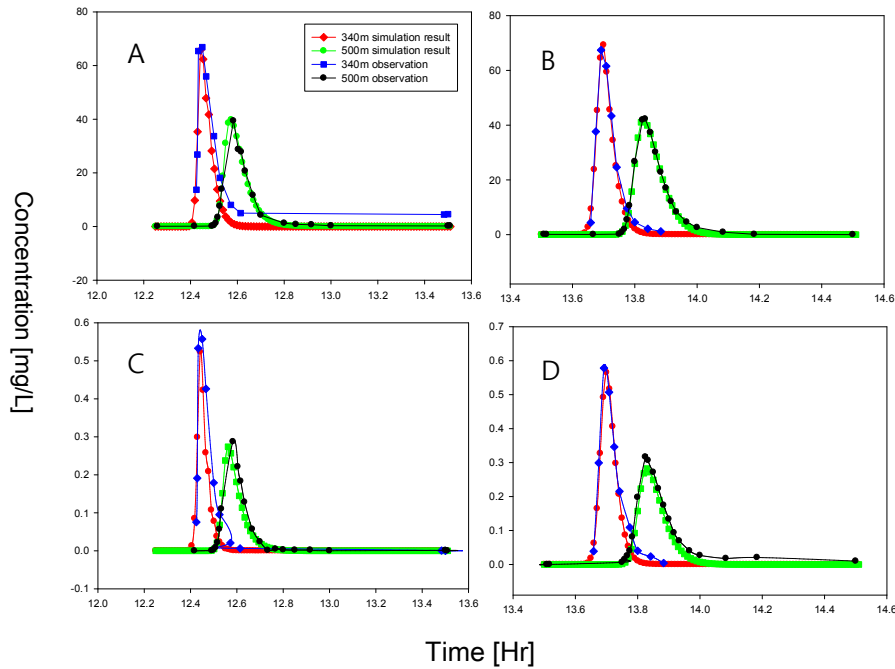
Wlostoski N. Adam. (2012). *Solute transport dynamics in alaskan arctic tundra streams*. Unpublished master's thesis, Pennsylvania State University.

Wondzell, S. M., & Swanson, F. J. (1996). Seasonal and storm dynamics of the hyporheic zone of a 4th-order mountain stream. II: Nitrogen cycling. *Journal of the North American Benthological Society*, 20-34.

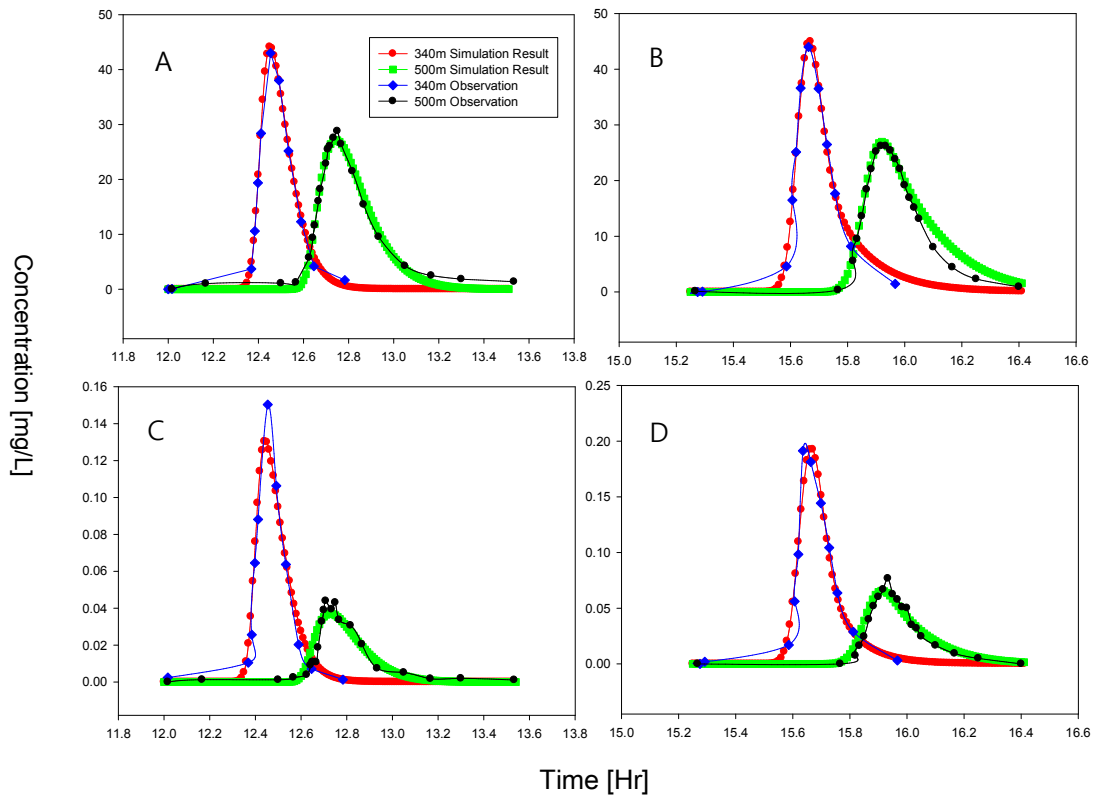
Zarnetske, J. P., Gooseff, M. N., Brosten, T. R., Bradford, J. H., McNamara, J. P., & Bowden, W. B. (2007). Transient storage as a function of geomorphology, discharge, and permafrost active layer conditions in Arctic tundra streams. *Water Resources Research*, 43(7).

**Appendix 1 Break through Curves [BTCs] and Optimized Parameter Value  
- 18IN/2010/07/21 [STREAM/YYYY/MM/DD]**

A                      Cl from injection A                      B                      Cl from injection B  
C                      PO<sub>4</sub> from Injection A                      D                      NH<sub>4</sub> from injection B

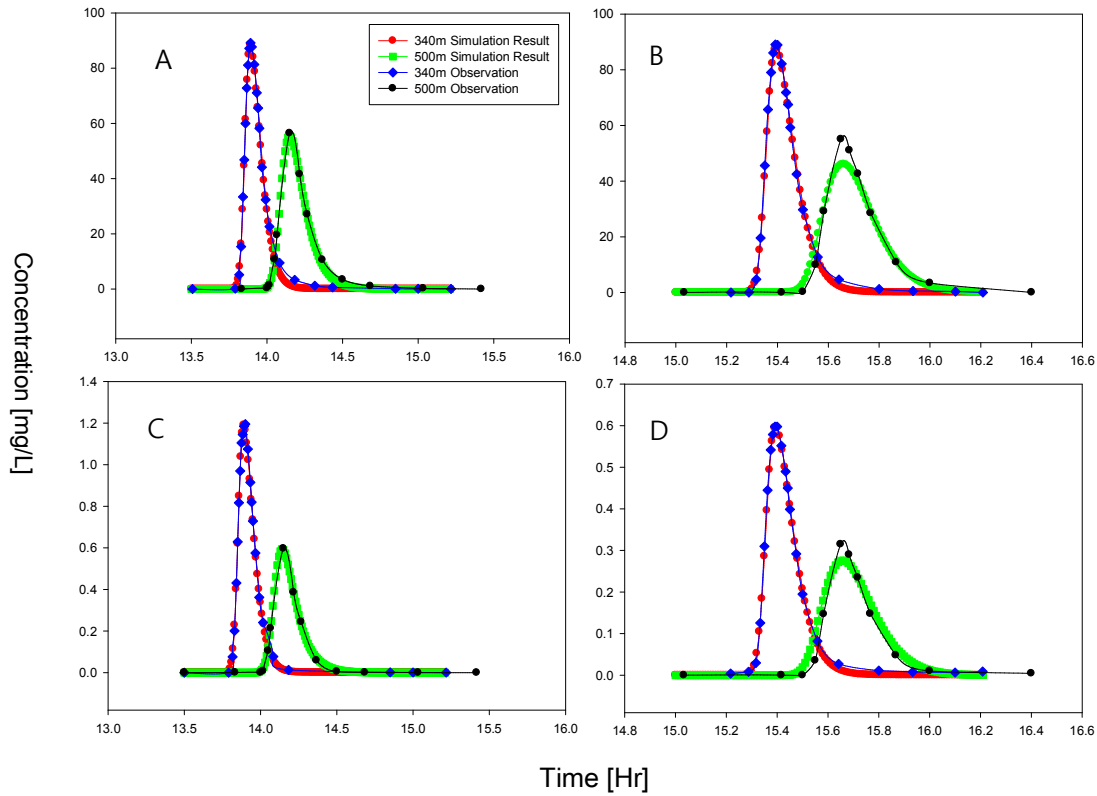


	Reach 1	Reach 2
Parameters	Injection A	Injection A
D (m <sup>2</sup> /s)	7.95 x 10 <sup>-2</sup>	4.11 x 10 <sup>-1</sup> (0-9.3 x 10 <sup>-1</sup> )
A (m <sup>2</sup> )	1.323	1.947 (1.81-2.07)
A <sub>s</sub> (m <sup>2</sup> )	3.28 x 10 <sup>-1</sup>	4.186 x 10 <sup>-1</sup> (3.34-5.02 x 10 <sup>-1</sup> )
α (1/s)	4.511 x 10 <sup>-3</sup>	1.232 x 10 <sup>-3</sup> (0.46-2.01 x 10 <sup>-3</sup> )
λ (1/s)	1.436 x 10 <sup>-5</sup> (0-4.68 x 10 <sup>-4</sup> )	2.027 x 10 <sup>-4</sup> (1.13-2.92 x 10 <sup>-5</sup> )
λ <sub>s</sub> (1/s)	8.487 x 10 <sup>-4</sup> (0-3.71 x 10 <sup>-3</sup> )	1.397 x 10 <sup>-4</sup> (0.67-2.13 x 10 <sup>-3</sup> )
	Reach 1	Reach 2
Parameters	Injection B	Injection B
D (m <sup>2</sup> /s)	4.81 x 10 <sup>-2</sup> (0-7.8 x 10 <sup>-1</sup> )	1.64 x 10 <sup>-1</sup> (0-3.7 x 10 <sup>-1</sup> )
A (m <sup>2</sup> )	1.2095 (0.98-1.43)	2.002 (1.91-2.087)
A <sub>s</sub> (m <sup>2</sup> )	3.347 x 10 <sup>-1</sup> (1.27-5.42 x 10 <sup>-1</sup> )	5.29 x 10 <sup>-1</sup> (4.47-6.11 x 10 <sup>-1</sup> )
α (1/s)	8.236 x 10 <sup>-3</sup> (0-18.8 x 10 <sup>-3</sup> )	3.026 x 10 <sup>-3</sup> (1.95-4.11 x 10 <sup>-3</sup> )
λ (1/s)	1.306 x 10 <sup>-6</sup>	7.605 x 10 <sup>-7</sup> (0-1.96 x 10 <sup>-4</sup> )
λ <sub>s</sub> (1/s)	7.873 x 10 <sup>-4</sup>	5.69 x 10 <sup>-4</sup> (4.17-7.21 x 10 <sup>-3</sup> )
Discharge [m <sup>3</sup> /s]	Lateral Inflow Reach1 [m <sup>3</sup> /s·m]	Lateral outflow Reach 2 [m <sup>3</sup> /s·m]
0.6969	0.000310	0.00031495



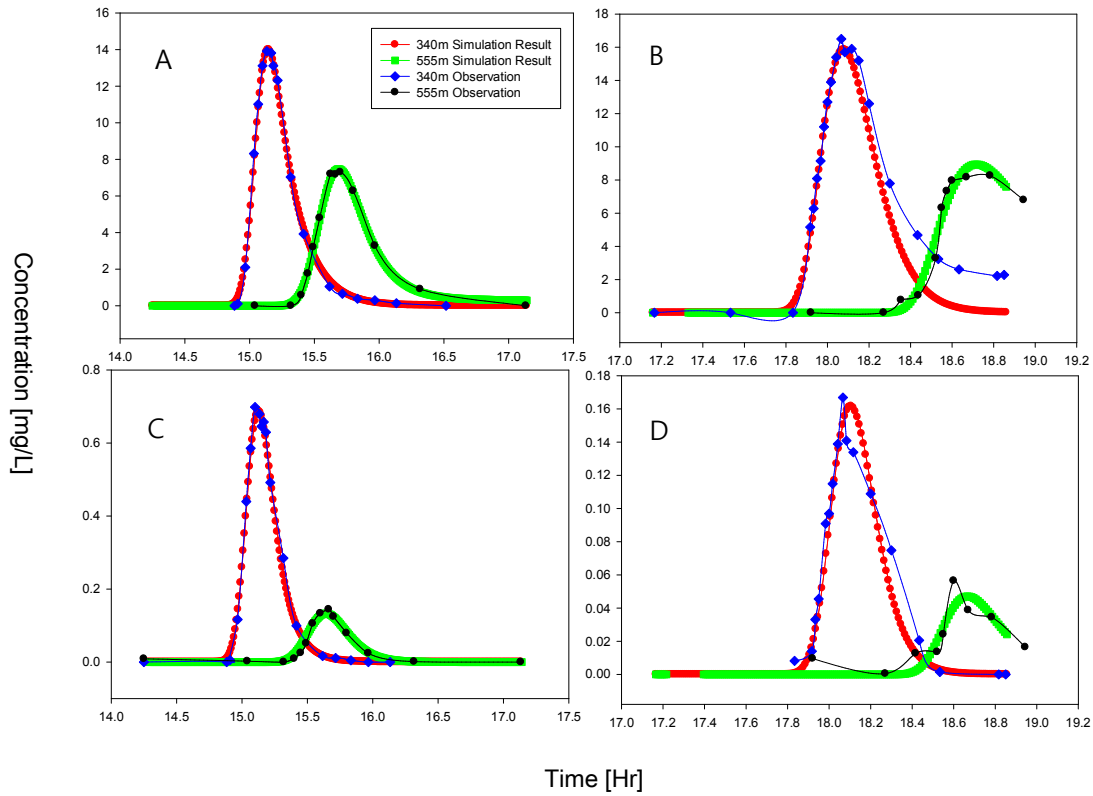
	Reach 1	Reach 2
Parameters	Injection A	Injection A
D (m <sup>2</sup> /s)	1.915 x 10 <sup>-1</sup> (0.445-3.38 x 10 <sup>-1</sup> )	3.34 x 10 <sup>-1</sup> (2.09-4.6 x 10 <sup>-1</sup> )
A (m <sup>2</sup> )	7.96 x 10 <sup>-1</sup> (7.43-8.49 x 10 <sup>-1</sup> )	1.126 (1.08-1.165)
A <sub>s</sub> (m <sup>2</sup> )	1.535 x 10 <sup>-1</sup> (1.03-2.04 x 10 <sup>-1</sup> )	2.506 x 10 <sup>-1</sup> (1.96-3.05 x 10 <sup>-1</sup> )
α (1/s)	1.685 x 10 <sup>-3</sup> (0.52-2.85 x 10 <sup>-3</sup> )	4.33 x 10 <sup>-4</sup> (2.01-6.66 x 10 <sup>-4</sup> )
λ (1/s)	3.426 x 10 <sup>-4</sup> (2.58-4.27 x 10 <sup>-4</sup> )	6.06 x 10 <sup>-4</sup> (4.07-8.05 x 10 <sup>-4</sup> )
λ <sub>s</sub> (1/s)	1.001 x 10 <sup>-3</sup> (0.341-1.66 x 10 <sup>-3</sup> )	6.82 x 10 <sup>-4</sup> (0-44.1 x 10 <sup>-4</sup> )
	Reach 1	Reach 2
Parameters	Injection B	Injection B
D (m <sup>2</sup> /s)	4.41 x 10 <sup>-1</sup> (3.41-5.4 x 10 <sup>-1</sup> )	5.656 x 10 <sup>-1</sup> (5.06-6.25 x 10 <sup>-1</sup> )
A (m <sup>2</sup> )	7.88 x 10 <sup>-1</sup> (7.7-8.06 x 10 <sup>-1</sup> )	1.091 (1.082-1.099)
A <sub>s</sub> (m <sup>2</sup> )	1.32 x 10 <sup>-1</sup> (1.08-1.55 x 10 <sup>-1</sup> )	9.48 (0-93.6)
α (1/s)	4.9 x 10 <sup>-4</sup> (2.82-6.98 x 10 <sup>-4</sup> )	1.767 x 10 <sup>-4</sup> (1.48-2.05 x 10 <sup>-4</sup> )
λ (1/s)	1.355 x 10 <sup>-4</sup> (0.54-2.17 x 10 <sup>-4</sup> )	6.65 x 10 <sup>-4</sup> (5.12-8.18 x 10 <sup>-4</sup> )
λ <sub>s</sub> (1/s)	1.005 x 10 <sup>-3</sup> (0-2.7 x 10 <sup>-3</sup> )	9.412 x 10 <sup>-5</sup> (0-1.05 x 10 <sup>-3</sup> )
Discharge [m <sup>3</sup> /s]	Lateral Inflow Reach1 [m <sup>3</sup> /s·m]	Lateral outflow Reach 2 [m <sup>3</sup> /s·m]
0.186	0	0

- I8IN/2010/09/18 [STREAM/YYYY/MM/DD]

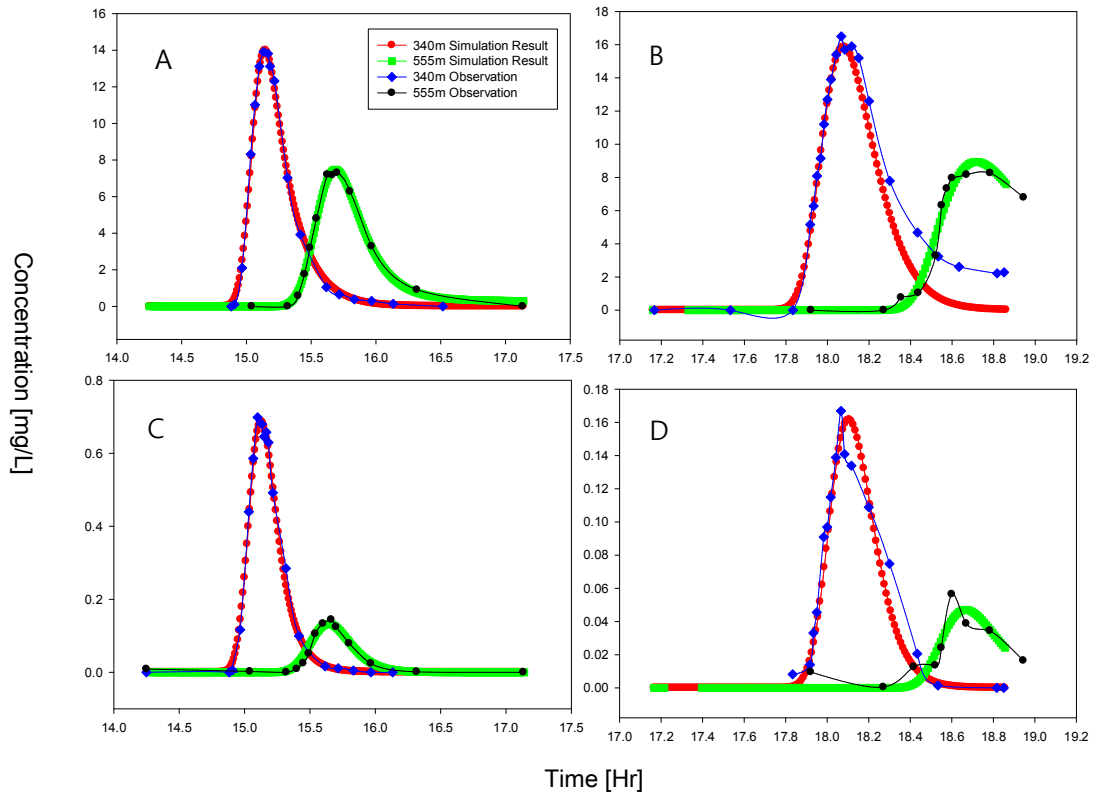


	Reach 1	Reach 2
Parameters	Injection A	Injection A
D (m <sup>2</sup> /s)	1.87 x 10 <sup>-1</sup> (1.32-2.42 x 10 <sup>-1</sup> )	2.45 x 10 <sup>-1</sup> (0-5.48 x 10 <sup>-1</sup> )
A (m <sup>2</sup> )	8.42 x 10 <sup>-1</sup> (8.23-8.62 x 10 <sup>-1</sup> )	1.26 (1.12-1.404)
A <sub>s</sub> (m <sup>2</sup> )	1.64 x 10 <sup>-1</sup> (1.46-1.83 x 10 <sup>-1</sup> )	2.09 x 10 <sup>-1</sup> (0.88-3.31 x 10 <sup>-1</sup> )
α (1/s)	2.22 x 10 <sup>-3</sup> (1.71-2.73 x 10 <sup>-1</sup> )	7.3 x 10 <sup>-4</sup> (0-17.3 x 10 <sup>-4</sup> )
λ (1/s)	9.42 x 10 <sup>-5</sup> (8.04-10.8 x 10 <sup>-5</sup> )	2.28 x 10 <sup>-1</sup> (1.82-2.75 x 10 <sup>-1</sup> )
λ <sub>s</sub> (1/s)	3.73 x 10 <sup>-4</sup> (2.76-4.71 x 10 <sup>-4</sup> )	6.09 x 10 <sup>-4</sup> (1.72-10.5 x 10 <sup>-4</sup> )
	Reach 1	Reach 2
Parameters	Injection B	Injection B
D (m <sup>2</sup> /s)	2.095 x 10 <sup>-1</sup> (1.53-2.66 x 10 <sup>-1</sup> )	1.96 x 10 <sup>-1</sup> (0.63-3.3 x 10 <sup>-1</sup> )
A (m <sup>2</sup> )	8.51 x 10 <sup>-1</sup> (8.31-8.69 x 10 <sup>-1</sup> )	1.24 (1.18-1.29)
A <sub>s</sub> (m <sup>2</sup> )	1.62 x 10 <sup>-1</sup> (1.43-1.8 x 10 <sup>-1</sup> )	2.48 x 10 <sup>-1</sup> (1.95-3.02 x 10 <sup>-1</sup> )
α (1/s)	2.03 x 10 <sup>-3</sup> (1.56-2.49 x 10 <sup>-3</sup> )	9.66 x 10 <sup>-4</sup> (4.82-14.5 x 10 <sup>-4</sup> )
λ (1/s)	4.35 x 10 <sup>-5</sup> (1.58-7.14 x 10 <sup>-5</sup> )	1.773 x 10 <sup>-4</sup> (0.925-2.62 x 10 <sup>-4</sup> )
λ <sub>s</sub> (1/s)	8.89 x 10 <sup>-6</sup> (0-2.03 x 10 <sup>-4</sup> )	1.48 x 10 <sup>-4</sup> (0-7.62 x 10 <sup>-4</sup> )
Discharge [m <sup>3</sup> /s]	Lateral Inflow Reach1 [m <sup>3</sup> /s·m]	Lateral Inflow Reach 2 [m <sup>3</sup> /s·m]
0.227913	1.535 E-05	8.78 E-05

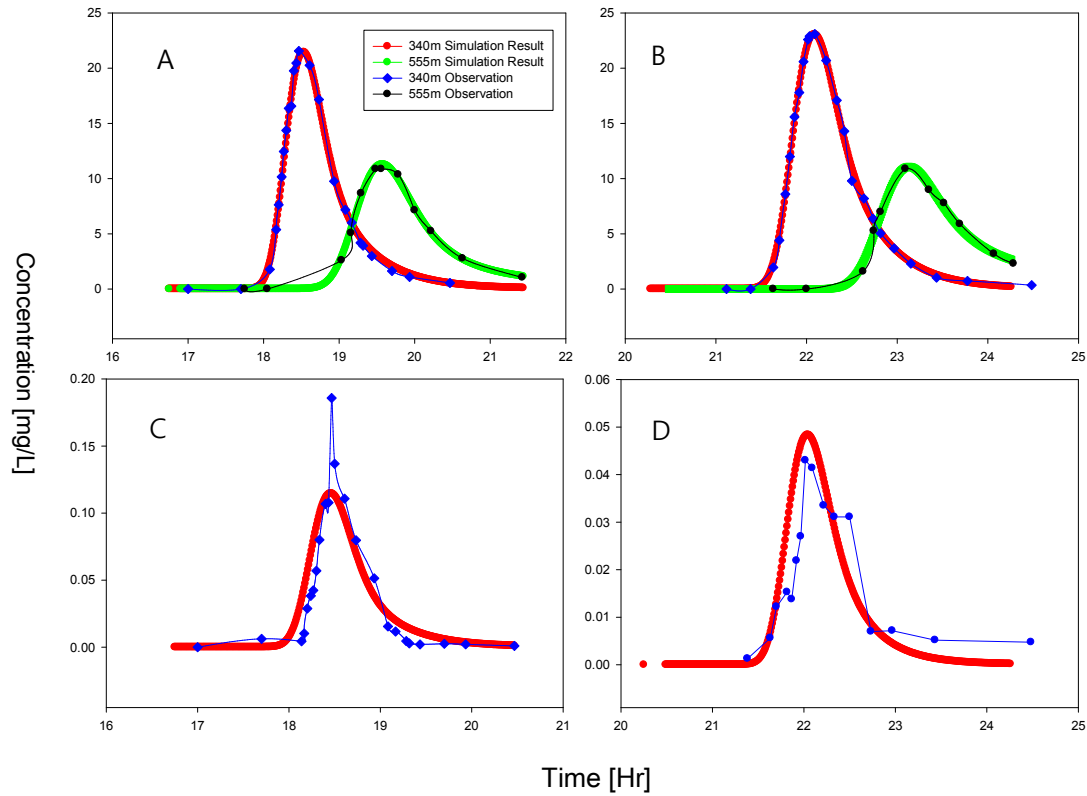
- I8IN/2010/09/25 [STREAM/YYYY/MM/DD]



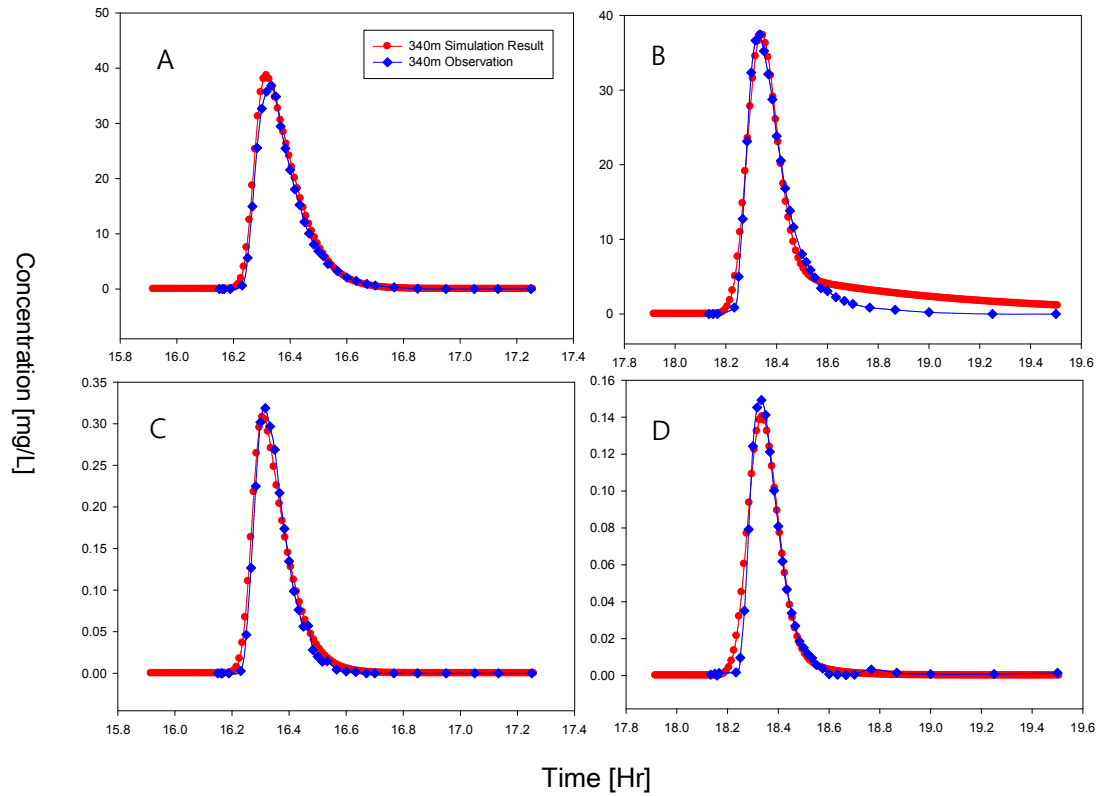
	Reach 1	Reach 2
Parameters	Injection A	Injection A
D (m <sup>2</sup> /s)	3.16 x 10 <sup>-1</sup> (2.79-3.53 x 10 <sup>-1</sup> )	2.945 x 10 <sup>-1</sup> (2.025-3.53 x 10 <sup>-1</sup> )
A (m <sup>2</sup> )	1.074 (1.05-1.09)	1.14 (1.126-1.164)
A <sub>s</sub> (m <sup>2</sup> )	1.137 x 10 <sup>-1</sup> (0.96-1.31 x 10 <sup>-1</sup> )	10.67 (0-50.28)
α (1/s)	1.45 x 10 <sup>-4</sup> (1.25-1.75 x 10 <sup>-4</sup> )	1.49 x 10 <sup>-4</sup> (1.25-1.75 x 10 <sup>-4</sup> )
λ (1/s)	4.38 x 10 <sup>-5</sup> (1.67-7.1 x 10 <sup>-5</sup> )	2.18 x 10 <sup>-4</sup> (1.56-2.82 x 10 <sup>-4</sup> )
λ <sub>s</sub> (1/s)	2.51 x 10 <sup>-3</sup> (0.259-4.74 x 10 <sup>-3</sup> )	4.38 x 10 <sup>-6</sup> (0-3.19 x 10 <sup>-3</sup> )
	Reach 1	Reach 2
Parameters	Injection B	Injection B
D (m <sup>2</sup> /s)	1.044 x 10 <sup>-1</sup>	5.991 x 10 <sup>-2</sup>
A (m <sup>2</sup> )	7.451 x 10 <sup>-1</sup>	8.986 x 10 <sup>-1</sup>
A <sub>s</sub> (m <sup>2</sup> )	1.78 x 10 <sup>-1</sup>	2.87 x 10 <sup>-1</sup>
α (1/s)	2.21 x 10 <sup>-3</sup>	9.9 x 10 <sup>-4</sup>
λ (1/s)	1.07 x 10 <sup>-5</sup> (0-5.47 x 10 <sup>-5</sup> )	2.84 x 10 <sup>-4</sup>
λ <sub>s</sub> (1/s)	3.9 x 10 <sup>-6</sup> (0-2.15 x 10 <sup>-4</sup> )	6.16 x 10 <sup>-5</sup>
Discharge [m <sup>3</sup> /s]	Lateral Inflow Reach1 [m <sup>3</sup> /s·m]	Lateral Inflow Reach 2 [m <sup>3</sup> /s·m]
0.11	0	0



	Reach 1	Reach 2
Parameters	Injection A	Injection A
D (m <sup>2</sup> /s)	2.09 x 10 <sup>-1</sup> (1.715-2.47 x 10 <sup>-1</sup> )	4.46 x 10 <sup>-5</sup> (3.19-5.73 x 10 <sup>-5</sup> )
A (m <sup>2</sup> )	6.00 x 10 <sup>-1</sup> (5.86-6.15 x 10 <sup>-1</sup> )	5.71 x 10 <sup>-1</sup> (5.57-5.86 x 10 <sup>-5</sup> )
A <sub>s</sub> (m <sup>2</sup> )	7.88 x 10 <sup>-2</sup> (6.58-9.19 x 10 <sup>-2</sup> )	1.334 (0-2.845)
α (1/s)	3.31 x 10 <sup>-4</sup> (1.96-4.67 x 10 <sup>-4</sup> )	2.04 x 10 <sup>-4</sup> (1.6-2.48 x 10 <sup>-4</sup> )
λ (1/s)	1.60 x 10 <sup>-4</sup> (1.46-1.74 x 10 <sup>-4</sup> )	5.26 x 10 <sup>-4</sup> (4.57-5.96 x 10 <sup>-4</sup> )
λ <sub>s</sub> (1/s)	9.53 x 10 <sup>-4</sup> (0.129-6.14 x 10 <sup>-4</sup> )	1.52 x 10 <sup>-3</sup> (0-2.34 x 10 <sup>-2</sup> )
	Reach 1	Reach 2
Parameters	Injection B	Injection B
D (m <sup>2</sup> /s)	2.059 x 10 <sup>-1</sup> (1.67-2.44 x 10 <sup>-1</sup> )	1.2 x 10 <sup>-2</sup>
A (m <sup>2</sup> )	6.25 x 10 <sup>-1</sup> (6.06-6.44 x 10 <sup>-1</sup> )	5.81 x 10 <sup>-1</sup>
A <sub>s</sub> (m <sup>2</sup> )	7.64 x 10 <sup>-2</sup> (6.00-9.28 x 10 <sup>-2</sup> )	1.83 x 10 <sup>-1</sup>
α (1/s)	3.25 x 10 <sup>-4</sup> (1.53-4.97 x 10 <sup>-4</sup> )	5.38 x 10 <sup>-4</sup>
λ (1/s)	2.29 x 10 <sup>-4</sup> (1.98-2.61 x 10 <sup>-4</sup> )	3.78 x 10 <sup>-4</sup> (0.925-6.1 x 10 <sup>-4</sup> )
λ <sub>s</sub> (1/s)	5.32 x 10 <sup>-5</sup> (0-5.58 x 10 <sup>-4</sup> )	5.049 x 10 <sup>-4</sup> (0-2.76 x 10 <sup>-3</sup> )
Discharge [m <sup>3</sup> /s]	Lateral Inflow Reach1 [m <sup>3</sup> /s·m]	Lateral Inflow Reach 2 [m <sup>3</sup> /s·m]
0.06263	1.8614 E-05	4.5256 E-05

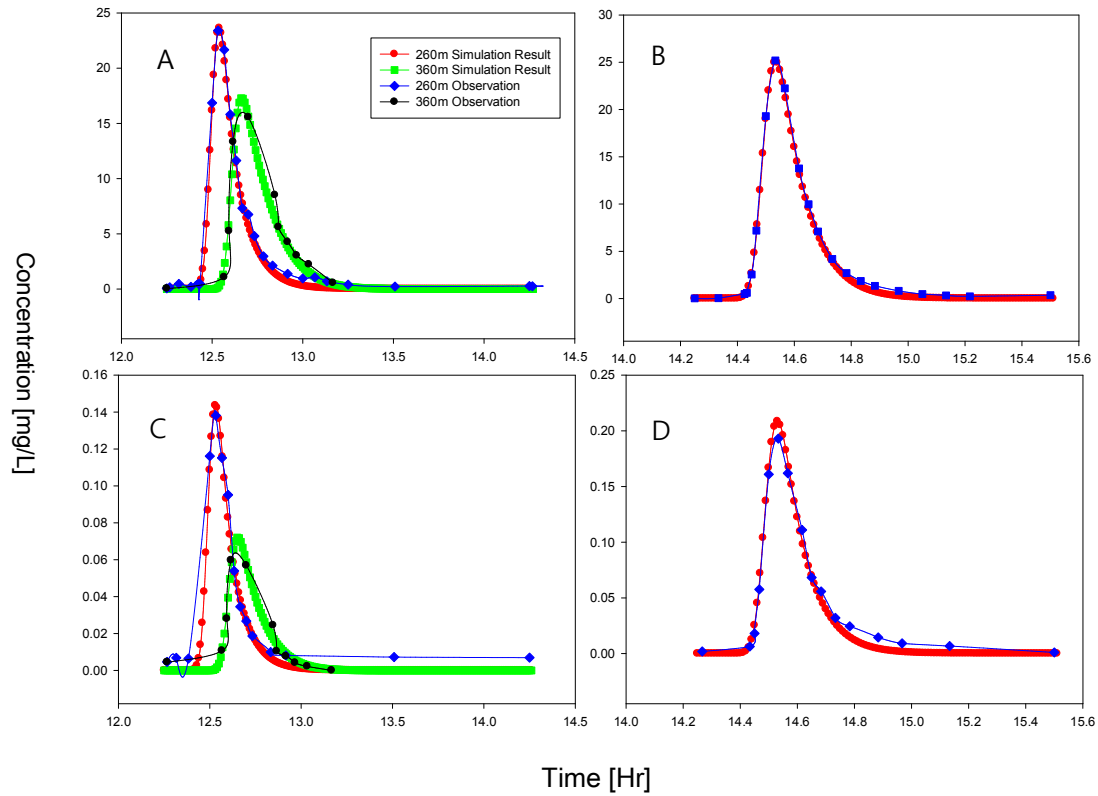


	Reach 1	Reach 2
Parameters	Injection A	Injection A
D (m <sup>2</sup> /s)	1.52 x 10 <sup>-1</sup> (1.36-1.69 x 10 <sup>-1</sup> )	3.48 x 10 <sup>-1</sup> (2.44-4.53 x 10 <sup>-1</sup> )
A (m <sup>2</sup> )	5.07 x 10 <sup>-1</sup> (4.99-5.15 x 10 <sup>-1</sup> )	5.17 x 10 <sup>-1</sup> (5.00-5.35 x 10 <sup>-1</sup> )
A <sub>s</sub> (m <sup>2</sup> )	7.07 x 10 <sup>-2</sup> (6.09-8.05 x 10 <sup>-2</sup> )	4.61 x 10 <sup>-1</sup> (1.46-7.75 x 10 <sup>-1</sup> )
α (1/s)	1.04 x 10 <sup>-4</sup> (0.73-1.34 x 10 <sup>-4</sup> )	8.34 x 10 <sup>-5</sup> (5.56-10.11 x 10 <sup>-5</sup> )
λ (1/s)	2.86 x 10 <sup>-4</sup> (2.54-3.18 x 10 <sup>-4</sup> )	
λ <sub>s</sub> (1/s)	7.45 x 10 <sup>-5</sup> (0-6.09 x 10 <sup>-4</sup> )	
Parameters	Injection B	Injection B
D (m <sup>2</sup> /s)	1.35 x 10 <sup>-1</sup> (1.19-1.50 x 10 <sup>-1</sup> )	1.90 x 10 <sup>-1</sup> (0.35-3.46 x 10 <sup>-1</sup> )
A (m <sup>2</sup> )	5.25 x 10 <sup>-1</sup> (5.15-5.35 x 10 <sup>-1</sup> )	4.99 x 10 <sup>-1</sup> (4.72-5.26 x 10 <sup>-1</sup> )
A <sub>s</sub> (m <sup>2</sup> )	6.68 x 10 <sup>-2</sup> (5.8-7.56 x 10 <sup>-2</sup> )	6.12 x 10 <sup>-1</sup> (2.75-9.5 x 10 <sup>-1</sup> )
α (1/s)	1.16 x 10 <sup>-4</sup> (0.79-1.54 x 10 <sup>-4</sup> )	1.48 x 10 <sup>-4</sup> (0.978-2.0 x 10 <sup>-4</sup> )
λ (1/s)	2.22 x 10 <sup>-4</sup> (1.83-2.62 x 10 <sup>-4</sup> )	
λ <sub>s</sub> (1/s)	3.52 x 10 <sup>-5</sup> (0-6.8 x 10 <sup>-4</sup> )	
Discharge [m <sup>3</sup> /s]	Lateral Inflow Reach1 [m <sup>3</sup> /s·m]	Lateral Inflow Reach 2 [m <sup>3</sup> /s·m]
0.02663	3.73661 E-06	1.31782 E-05

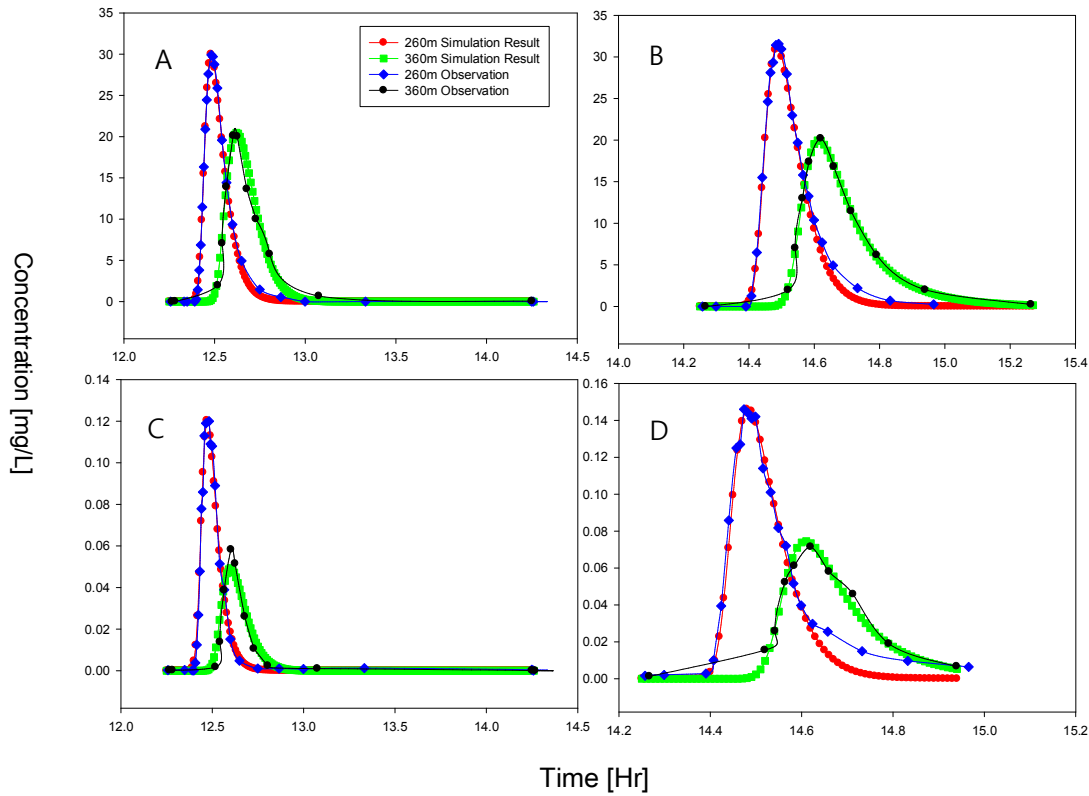


	Reach 1	Reach 2
Parameters	Injection A	Injection A
D (m <sup>2</sup> /s)	5.06 x 10 <sup>-1</sup> (4.24-5.89 x 10 <sup>-1</sup> )	
A (m <sup>2</sup> )	8.15 x 10 <sup>-1</sup> (8.00-8.3 x 10 <sup>-1</sup> )	
A <sub>s</sub> (m <sup>2</sup> )	1.37 x 10 <sup>-1</sup> (1.22-1.53 x 10 <sup>-1</sup> )	
α (1/s)	6.20 x 10 <sup>-4</sup> (4.56-7.85 x 10 <sup>-4</sup> )	
λ (1/s)	4.00 x 10 <sup>-4</sup> (3.75-4.24 x 10 <sup>-4</sup> )	
λ <sub>s</sub> (1/s)	1.716 x 10 <sup>-3</sup> (1.32-2.12 x 10 <sup>-1</sup> )	
Parameters	Reach 1	Reach 2
	Injection B	Injection B
D (m <sup>2</sup> /s)	7.91 x 10 <sup>-1</sup> (6.72-9.08 x 10 <sup>-1</sup> )	
A (m <sup>2</sup> )	8.79 x 10 <sup>-1</sup> (8.65-8.91 x 10 <sup>-1</sup> )	
A <sub>s</sub> (m <sup>2</sup> )	6.40 x 10 <sup>-1</sup> (4.22-8.6 x 10 <sup>-1</sup> )	
α (1/s)	3.79 x 10 <sup>-4</sup> (3.19-4.41 x 10 <sup>-4</sup> )	
λ (1/s)	2.305 x 10 <sup>-4</sup> (1.98-2.68 x 10 <sup>-4</sup> )	
λ <sub>s</sub> (1/s)	1.96 x 10 <sup>-3</sup> (3.95-1.69 x 10 <sup>-3</sup> )	
Discharge [m <sup>3</sup> /s]	Lateral Outflow Reach 1 [m <sup>3</sup> /s·m]	Lateral Inflow Reach 2 [m <sup>3</sup> /s·m]
0.198	1.54938 E-05	1.60193 E-05

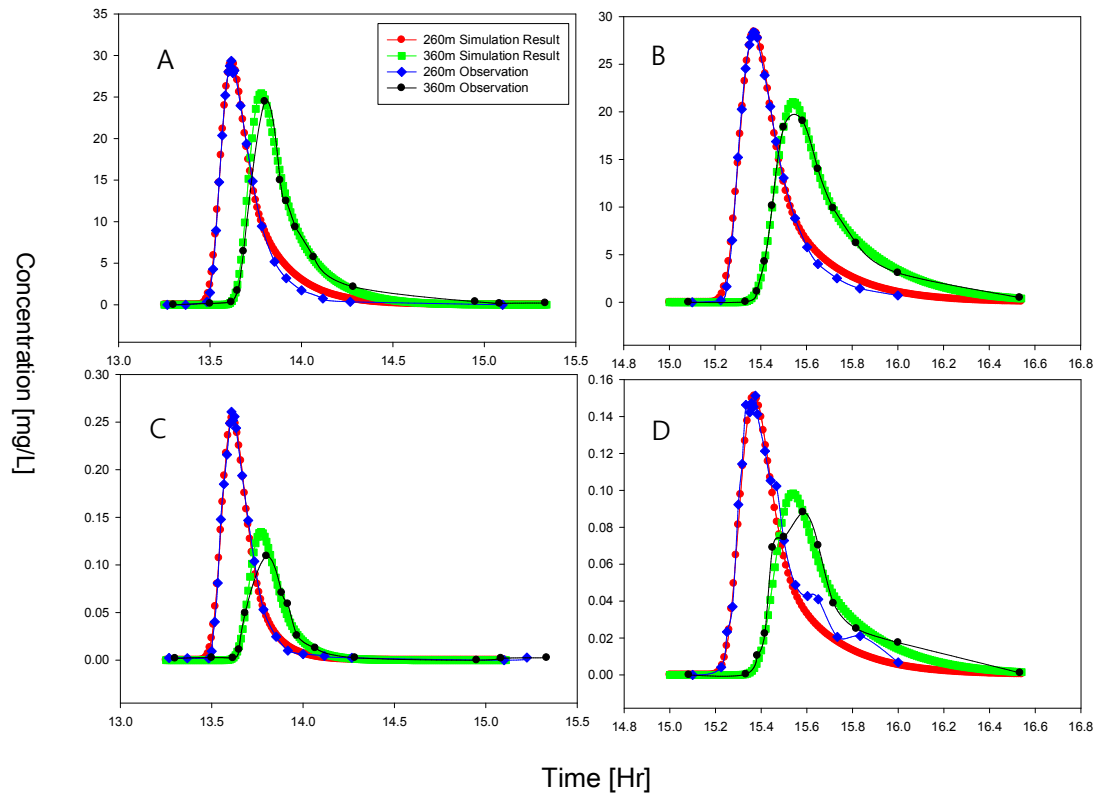
- I8OUT/2010/07/19 [STREAM/YYYY/MM/DD]



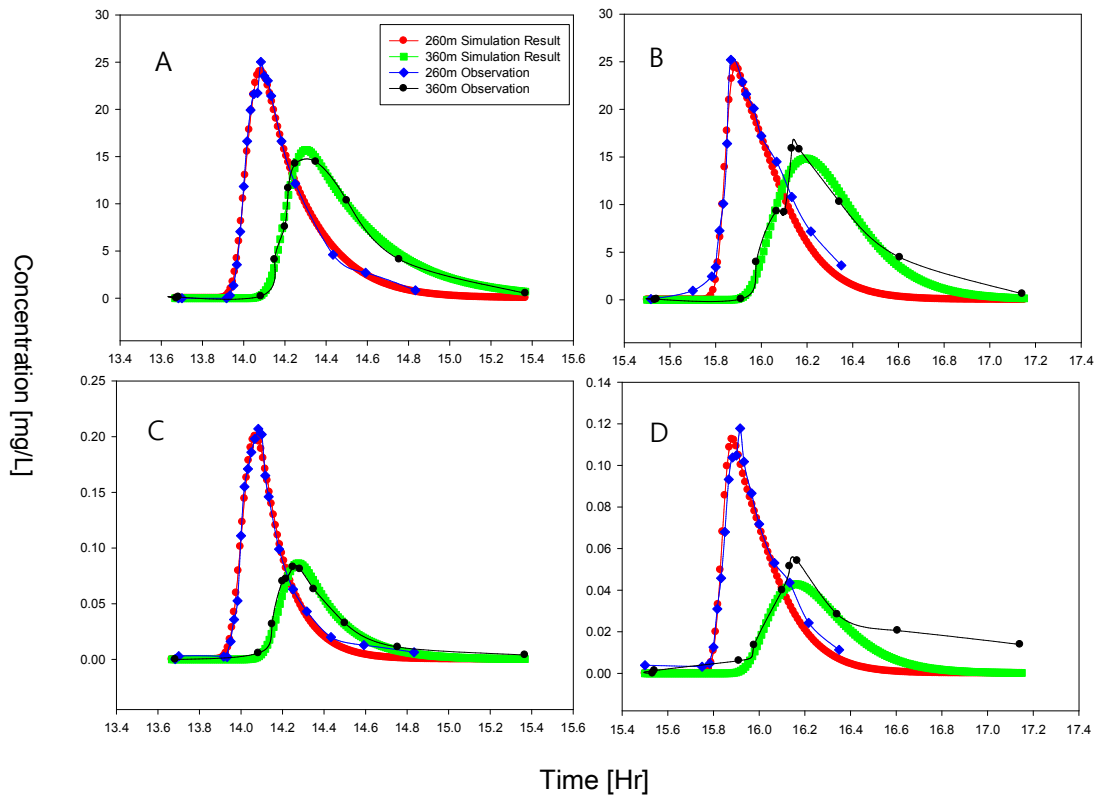
	Reach 1	Reach 2
Parameters	Injection A	Injection A
D (m <sup>2</sup> /s)	8.32 x 10 <sup>-1</sup> (5.84-10.8 x 10 <sup>-1</sup> )	8.78 x 10 <sup>-1</sup>
A (m <sup>2</sup> )	9.56 x 10 <sup>-1</sup> (9.12-10.0 x 10 <sup>-1</sup> )	9.92 x 10 <sup>-1</sup>
A <sub>s</sub> (m <sup>2</sup> )	2.17 x 10 <sup>-1</sup> (1.7-2.61 x 10 <sup>-1</sup> )	4.05x 10 <sup>-1</sup>
α (1/s)	9.69 x 10 <sup>-4</sup> (5.36-14.0 x 10 <sup>-4</sup> )	1.57 x 10 <sup>-3</sup>
λ (1/s)	8.79 x 10 <sup>-4</sup> (7.98-9.6 x 10 <sup>-4</sup> )	8.58 x 10 <sup>-4</sup> (5.65-11.5 x 10 <sup>-4</sup> )
λ <sub>s</sub> (1/s)	2.97 x 10 <sup>-4</sup> (0-8.45 x 10 <sup>-4</sup> )	1.05 x 10 <sup>-3</sup> (0-2.48 x 10 <sup>-3</sup> )
	Reach 1	Reach 2
Parameters	Injection B	Injection B
D (m <sup>2</sup> /s)	8.62 x 10 <sup>-1</sup> (7.21-10.0 x 10 <sup>-1</sup> )	
A (m <sup>2</sup> )	9.23 x 10 <sup>-1</sup> (8.91-9.55 x 10 <sup>-1</sup> )	
A <sub>s</sub> (m <sup>2</sup> )	2.04 x 10 <sup>-1</sup> (1.75-2.33 x 10 <sup>-1</sup> )	
α (1/s)	1.13 x 10 <sup>-3</sup> (0.755-1.51 x 10 <sup>-3</sup> )	
λ (1/s)	5.385 x 10 <sup>-1</sup> (5.38-5.39 x 10 <sup>-4</sup> )	
λ <sub>s</sub> (1/s)	2.09 x 10 <sup>-4</sup> (0.04-4.15 x 10 <sup>-4</sup> )	
Discharge [m <sup>3</sup> /s]	Lateral Inflow Reach 1 [m <sup>3</sup> /s·m]	Lateral Inflow Reach 2 [m <sup>3</sup> /s·m]
0.25	0	0



	Reach 1	Reach 2
Parameters	Injection A	Injection A
D (m <sup>2</sup> /s)	8.94 x 10 <sup>-1</sup> (0.75-10.3 x 10 <sup>-1</sup> )	2.11 x 10 <sup>-1</sup> (0-4.66 x 10 <sup>-1</sup> )
A (m <sup>2</sup> )	9.77 x 10 <sup>-1</sup> (9.42-10.1 x 10 <sup>-1</sup> )	1.65 (1.58-1.72)
A <sub>s</sub> (m <sup>2</sup> )	2.74 x 10 <sup>-1</sup> (2.45-3.05 x 10 <sup>-1</sup> )	8.77 x 10 <sup>-1</sup> (7.22-10.3 x 10 <sup>-1</sup> )
α (1/s)	4.90 x 10 <sup>-4</sup> (2.82-6.98 x 10 <sup>-4</sup> )	1.76 x 10 <sup>-4</sup> (1.48-2.05 x 10 <sup>-4</sup> )
λ (1/s)	7.31 x 10 <sup>-4</sup> (6.65-7.97 x 10 <sup>-4</sup> )	8.52 x 10 <sup>-4</sup> (5.24-11.8 x 10 <sup>-4</sup> )
λ <sub>s</sub> (1/s)	1.73 x 10 <sup>-3</sup> (1.25-2.22 x 10 <sup>-3</sup> )	1.47x 10 <sup>-3</sup> (0-4.3 x 10 <sup>-3</sup> )
	Reach 1	Reach 2
Parameters	Injection B	Injection B
D (m <sup>2</sup> /s)	8.07 x 10 <sup>-1</sup> (4.58-11.6 x 10 <sup>-1</sup> )	3.71 x 10 <sup>-1</sup> (1.88-5.55 x 10 <sup>-1</sup> )
A (m <sup>2</sup> )	9.71 x 10 <sup>-1</sup> (8.82-10.6 x 10 <sup>-1</sup> )	1.63 (1.57-1.68)
A <sub>s</sub> (m <sup>2</sup> )	2.78 x 10 <sup>-1</sup> (2.0-3.58 x 10 <sup>-1</sup> )	9.06 x 10 <sup>-1</sup> (8.15-9.97 x 10 <sup>-1</sup> )
α (1/s)	2.97 x 10 <sup>-3</sup> (1.22-4.72 x 10 <sup>-3</sup> )	1.49 x 10 <sup>-4</sup> (1.15-1.85 x 10 <sup>-3</sup> )
λ (1/s)	3.92 x 10 <sup>-4</sup> (3.03-4.82 x 10 <sup>-4</sup> )	5.52 x 10 <sup>-4</sup> (3.23-7.81 x 10 <sup>-4</sup> )
λ <sub>s</sub> (1/s)	2.97 x 10 <sup>-4</sup> (0-7.26 x 10 <sup>-4</sup> )	1.83x 10 <sup>-4</sup> (0-12.1 x 10 <sup>-4</sup> )
Discharge [m <sup>3</sup> /s]	Lateral Inflow Reach 1 [m <sup>3</sup> /s·m]	Lateral Outflow Reach 2 [m <sup>3</sup> /s·m]
0.2984	0.0003967	0.00012039

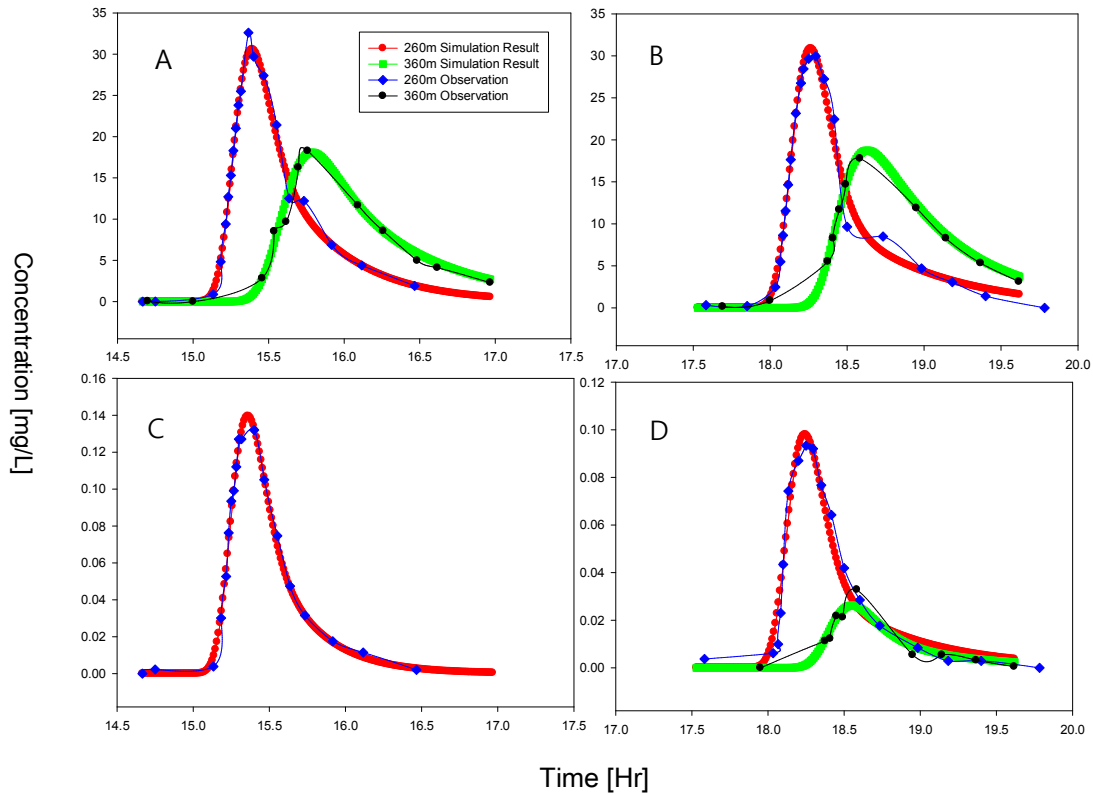


	Reach 1	Reach 2
Parameters	Injection A	Injection A
D (m <sup>2</sup> /s)	7.84 x 10 <sup>-1</sup> (6.78-8.9 x 10 <sup>-1</sup> )	7.33 x 10 <sup>-1</sup> (0-17.8 x 10 <sup>-2</sup> )
A (m <sup>2</sup> )	9.45 x 10 <sup>-1</sup> (9.19-9.72 x 10 <sup>-1</sup> )	1.1 (1.075-1.13)
A <sub>s</sub> (m <sup>2</sup> )	2.51 x 10 <sup>-1</sup> (2.2-2.8 x 10 <sup>-1</sup> )	2.6 x 10 <sup>-1</sup> (2.08-3.12 x 10 <sup>-1</sup> )
α (1/s)	5.58 x 10 <sup>-4</sup> (3.85-7.33 x 10 <sup>-4</sup> )	3.4 x 10 <sup>-4</sup> (2.34-4.46 x 10 <sup>-4</sup> )
λ (1/s)	4.49 x 10 <sup>-4</sup> (4.28-4.71 x 10 <sup>-4</sup> )	9.44 x 10 <sup>-4</sup> (9.35-9.53 x 10 <sup>-4</sup> )
λ <sub>s</sub> (1/s)	8.08 x 10 <sup>-4</sup> (4.5-11.7 x 10 <sup>-4</sup> )	4.25 x 10 <sup>-6</sup> (0-1.88 x 10 <sup>-3</sup> )
Parameters	Injection B	Injection B
D (m <sup>2</sup> /s)	8.74 x 10 <sup>-1</sup> (7.81-9.67 x 10 <sup>-1</sup> )	3.38 x 10 <sup>-1</sup> (1.83-5.55 x 10 <sup>-1</sup> )
A (m <sup>2</sup> )	9.63 x 10 <sup>-1</sup> (9.42-9.84 x 10 <sup>-1</sup> )	1.1 (1.06-1.13)
A <sub>s</sub> (m <sup>2</sup> )	2.71 x 10 <sup>-1</sup> (2.4-3.02 x 10 <sup>-1</sup> )	4.14 x 10 <sup>-1</sup> (3.47-4.82 x 10 <sup>-1</sup> )
α (1/s)	4.86 x 10 <sup>-4</sup> (3.7-6.03 x 10 <sup>-4</sup> )	5.96 x 10 <sup>-4</sup> (3.93-7.99 x 10 <sup>-4</sup> )
λ (1/s)	1.97 x 10 <sup>-4</sup> (1.59-2.35 x 10 <sup>-4</sup> )	2.04 x 10 <sup>-4</sup> (1.46-2.62 x 10 <sup>-4</sup> )
λ <sub>s</sub> (1/s)	8.74 x 10 <sup>-5</sup> (0-4.98 x 10 <sup>-4</sup> )	1.17x 10 <sup>-4</sup> (0-1.85 x 10 <sup>-3</sup> )
Discharge [m <sup>3</sup> /s]	Lateral Inflow Reach 1 [m <sup>3</sup> /s·m]	Lateral Outflow Reach 2 [m <sup>3</sup> /s·m]
0.1844	1.9673 E-05	2.671 E-05

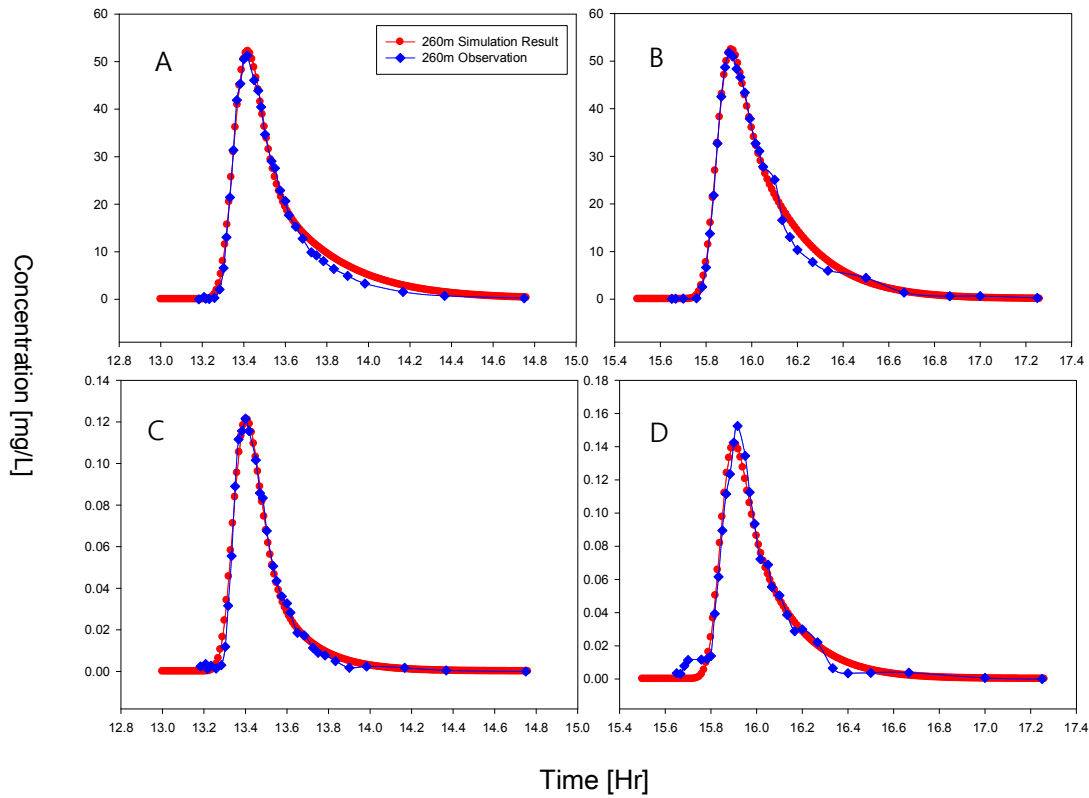


	Reach 1	Reach 2
Parameters	Injection A	Injection A
D (m <sup>2</sup> /s)	5.97 x 10 <sup>-1</sup> (4.68-7.26 x 10 <sup>-1</sup> )	3.79 x 10 <sup>-1</sup> (0-8.95 x 10 <sup>-1</sup> )
A (m <sup>2</sup> )	8.28 x 10 <sup>-1</sup> (7.92-8.63 x 10 <sup>-1</sup> )	1.074 (0.95-1.20)
A <sub>s</sub> (m <sup>2</sup> )	3.08 x 10 <sup>-1</sup> (2.78-3.38 x 10 <sup>-1</sup> )	6.46 x 10 <sup>-1</sup> (2.41-10.5 x 10 <sup>-1</sup> )
α (1/s)	9.15 x 10 <sup>-4</sup> (6.21-12.1 x 10 <sup>-4</sup> )	86.06 x 10 <sup>-4</sup> (0-12.3 x 10 <sup>-4</sup> )
λ (1/s)	4.28 x 10 <sup>-4</sup> (3.96-4.6 x 10 <sup>-4</sup> )	5.33 x 10 <sup>-4</sup> (3.98-6.67 x 10 <sup>-4</sup> )
λ <sub>s</sub> (1/s)	8.80 x 10 <sup>-4</sup> (5.57-12.0 x 10 <sup>-4</sup> )	5.42 x 10 <sup>-4</sup> (0-2.08 x 10 <sup>-3</sup> )
	Reach 1	Reach 2
Parameters	Injection B	Injection B
D (m <sup>2</sup> /s)	2.28 x 10 <sup>-1</sup> (0.89-3.68 x 10 <sup>-1</sup> )	1.008 (0-2.96)
A (m <sup>2</sup> )	7.64 x 10 <sup>-1</sup> (7.17-8.1 x 10 <sup>-1</sup> )	1.395 (0.78-2.00)
A <sub>s</sub> (m <sup>2</sup> )	3.3 x 10 <sup>-1</sup> (2.83-3.77 x 10 <sup>-1</sup> )	1.49 x 10 <sup>-1</sup> (0-1.36)
α (1/s)	1.625 x 10 <sup>-3</sup> (0.94-2.31 x 10 <sup>-3</sup> )	9.84 x 10 <sup>-5</sup> (0-1.76 x 10 <sup>-3</sup> )
λ (1/s)	5.16 x 10 <sup>-4</sup> (4.4-5.91 x 10 <sup>-4</sup> )	4.95 x 10 <sup>-4</sup> (0.84-9.06 x 10 <sup>-4</sup> )
λ <sub>s</sub> (1/s)	4.11 x 10 <sup>-5</sup> (0-3.06 x 10 <sup>-4</sup> )	1.15 x 10 <sup>-3</sup> (0-3.03 x 10 <sup>-3</sup> )
Discharge [m <sup>3</sup> /s]	Lateral Outflow Reach 1 [m <sup>3</sup> /s·m]	Lateral Outflow Reach 2 [m <sup>3</sup> /s·m]
0.153	1.633 E-05	5.242 E-06

- I8OUT/2011/06/10 [STREAM/YYYY/MM/DD]

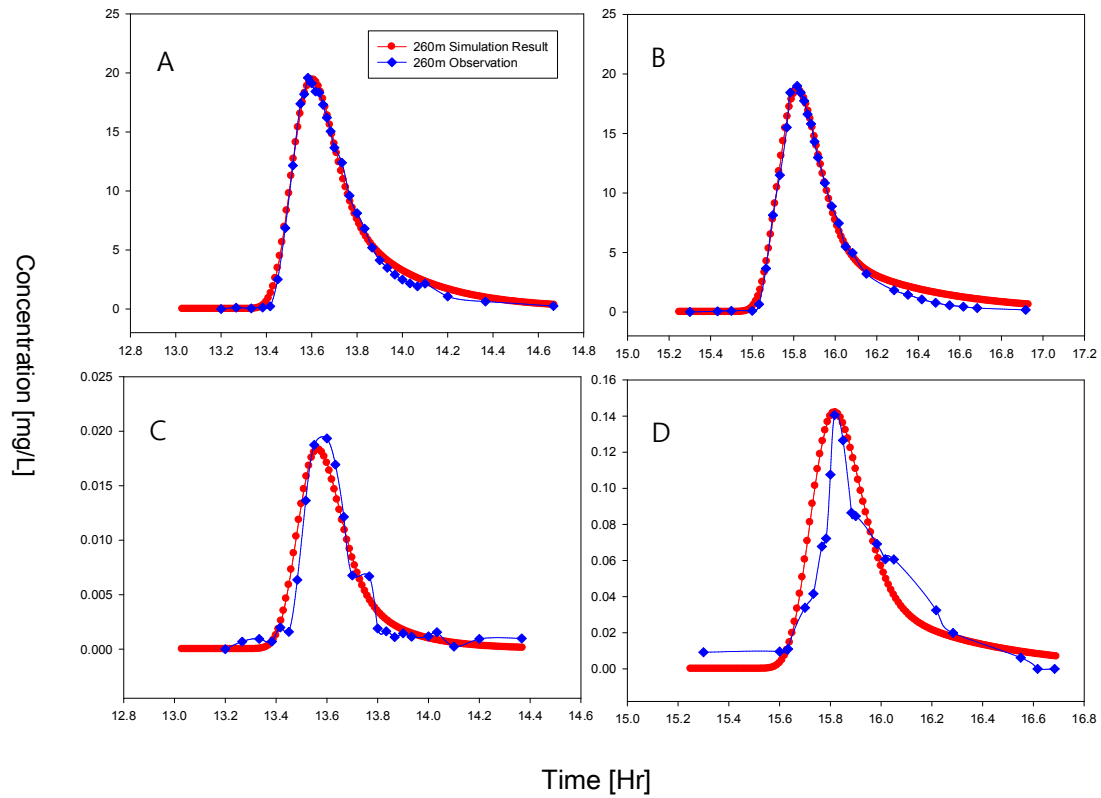


	Reach 1	Reach 2
Parameters	Injection A	Injection A
D (m <sup>2</sup> /s)	3.65 x 10 <sup>-1</sup> (2.99-4.31 x 10 <sup>-1</sup> )	6.29 x 10 <sup>-1</sup> (2.40-10.19 x 10 <sup>-1</sup> )
A (m <sup>2</sup> )	7.72 x 10 <sup>-1</sup> (7.46-7.97 x 10 <sup>-1</sup> )	1.16 (1.04-1.27)
A <sub>s</sub> (m <sup>2</sup> )	2.49 x 10 <sup>-1</sup> (2.12-2.85 x 10 <sup>-1</sup> )	9.73 x 10 <sup>-1</sup> (0-3.46)
α (1/s)	3.21 x 10 <sup>-4</sup> (2.13-4.28 x 10 <sup>-4</sup> )	1.10 x 10 <sup>-4</sup> (0-2.71 x 10 <sup>-4</sup> )
λ (1/s)	4.27 x 10 <sup>-4</sup> (4.01-4.54 x 10 <sup>-4</sup> )	
λ <sub>s</sub> (1/s)	1.18 x 10 <sup>-3</sup> (8.32-15.4 x 10 <sup>-4</sup> )	
Parameters	Injection B	Injection B
D (m <sup>2</sup> /s)	3.88 x 10 <sup>-1</sup> (3.15-4.61 x 10 <sup>-1</sup> )	1.305 x 10 <sup>-1</sup> (0-1.03)
A (m <sup>2</sup> )	8.03 x 10 <sup>-1</sup> (7.74-8.33 x 10 <sup>-1</sup> )	7.51 x 10 <sup>-1</sup> (3.45-11.6 x 10 <sup>-1</sup> )
A <sub>s</sub> (m <sup>2</sup> )	3.21 x 10 <sup>-1</sup> (2.21-4.21 x 10 <sup>-1</sup> )	5.46 x 10 <sup>-1</sup> (4.61-10.88 x 10 <sup>-1</sup> )
α (1/s)	2.51 x 10 <sup>-4</sup> (1.51-3.51 x 10 <sup>-4</sup> )	1.5 x 10 <sup>-3</sup> (0-4.43 x 10 <sup>-3</sup> )
λ (1/s)	3.55 x 10 <sup>-4</sup> (3.25-3.87 x 10 <sup>-4</sup> )	6.31 x 10 <sup>-4</sup> (2.95-9.68 x 10 <sup>-4</sup> )
λ <sub>s</sub> (1/s)	4.11 x 10 <sup>-4</sup> (0.5-3.06 x 10 <sup>-4</sup> )	1.15 x 10 <sup>-3</sup> (0-3.03 x 10 <sup>-3</sup> )
Discharge [m <sup>3</sup> /s]	Lateral Inflow Reach 1 [m <sup>3</sup> /s·m]	Lateral Outflow Reach 2 [m <sup>3</sup> /s·m]
0.0704	2.3035 E-05	3.8861 E-05



	Reach 1	Reach 2
Parameters	Injection A	Injection A
D (m <sup>2</sup> /s)	6.57 x 10 <sup>-1</sup> (5.84-7.30 x 10 <sup>-1</sup> )	
A (m <sup>2</sup> )	8.01 x 10 <sup>-1</sup> (7.87-8.15 x 10 <sup>-1</sup> )	
A <sub>s</sub> (m <sup>2</sup> )	3.3 x 10 <sup>-1</sup> (3.03-3.57x 10 <sup>-1</sup> )	
α (1/s)	5.75 x 10 <sup>-4</sup> (4.93-6.57 x 10 <sup>-4</sup> )	
λ (1/s)	6.92 x 10 <sup>-4</sup> (6.67-7.18 x 10 <sup>-4</sup> )	
λ <sub>s</sub> (1/s)	6.67 x 10 <sup>-4</sup> (4.29-9.06 x 10 <sup>-4</sup> )	
	Reach 1	Reach 2
Parameters	Injection B	Injection B
D (m <sup>2</sup> /s)	5.47 x 10 <sup>-1</sup> (4.55-6.39 x 10 <sup>-1</sup> )	
A (m <sup>2</sup> )	7.63 x 10 <sup>-1</sup> (7.43-7.84 x 10 <sup>-1</sup> )	
A <sub>s</sub> (m <sup>2</sup> )	2.85 x 10 <sup>-1</sup> (2.63-3.07 x 10 <sup>-1</sup> )	
α (1/s)	8.12 x 10 <sup>-4</sup> (6.47-9.77 x 10 <sup>-4</sup> )	
λ (1/s)	5.27 x 10 <sup>-4</sup> (4.92-5.63 x 10 <sup>-4</sup> )	
λ <sub>s</sub> (1/s)	2.52 x 10 <sup>-4</sup> (0.49-4.54 x 10 <sup>-4</sup> )	
Discharge [m <sup>3</sup> /s]	Lateral Inflow Reach 1 [m <sup>3</sup> /s·m]	Lateral Outflow Reach 2 [m <sup>3</sup> /s·m]
0.1332	4.06192 E-05	9.80409 E-05

- I8OUT/2011/07/16 [STREAM/YYYY/MM/DD]

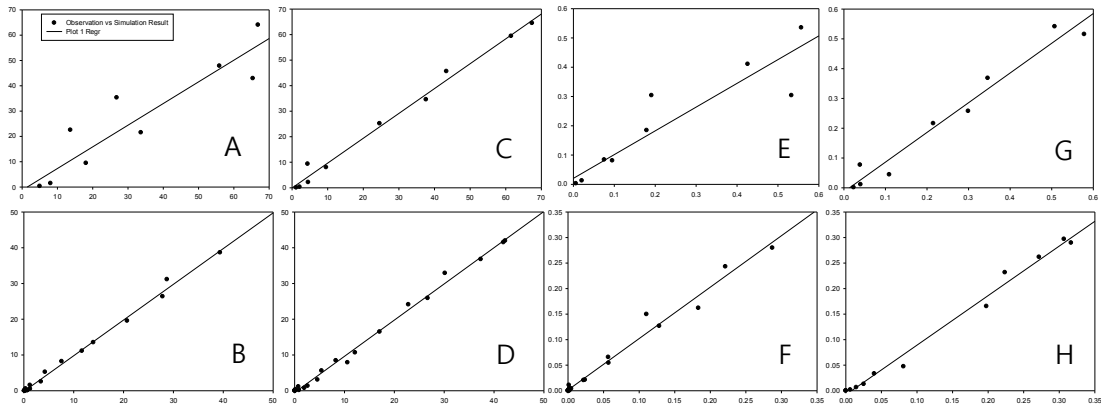


	Reach 1	Reach 2
Parameters	Injection A	Injection A
D (m <sup>2</sup> /s)	54.49 x 10 <sup>-1</sup> (3.96-5.03 x 10 <sup>-1</sup> )	
A (m <sup>2</sup> )	7.84 x 10 <sup>-1</sup> (7.70-7.98 x 10 <sup>-1</sup> )	
A <sub>s</sub> (m <sup>2</sup> )	1.89 x 10 <sup>-1</sup> (1.66-2.14 x 10 <sup>-1</sup> )	
α (1/s)	3.07 x 10 <sup>-4</sup> (2.38-3.76 x 10 <sup>-4</sup> )	
λ (1/s)	1.27 x 10 <sup>-3</sup> (1.21-1.34 x 10 <sup>-3</sup> )	
λ <sub>s</sub> (1/s)	26.37 x 10 <sup>-4</sup> (0-1.47 x 10 <sup>-3</sup> )	
Parameters	Injection B	Injection B
D (m <sup>2</sup> /s)	5.2 x 10 <sup>-1</sup> (4.61-5.79 x 10 <sup>-1</sup> )	
A (m <sup>2</sup> )	57.94 x 10 <sup>-1</sup> (7.79-8.07 x 10 <sup>-1</sup> )	
A <sub>s</sub> (m <sup>2</sup> )	2.57 x 10 <sup>-1</sup> (2.12-3.03 x 10 <sup>-1</sup> )	
α (1/s)	2.5 x 10 <sup>-4</sup> (1.94-3.06 x 10 <sup>-4</sup> )	
λ (1/s)	4.912 x 10 <sup>-5</sup> (4.89-4.93 x 10 <sup>-5</sup> )	
λ <sub>s</sub> (1/s)	4.39 x 10 <sup>-5</sup> (0-1.474 x 10 <sup>-3</sup> )	
Discharge [m <sup>3</sup> /s]	Lateral Inflow Reach 1 [m <sup>3</sup> /s·m]	Lateral Outflow Reach 2 [m <sup>3</sup> /s·m]
0.1002	1.4303 E-05	

## Appendix 2 Linear Regression result of parameter estimation

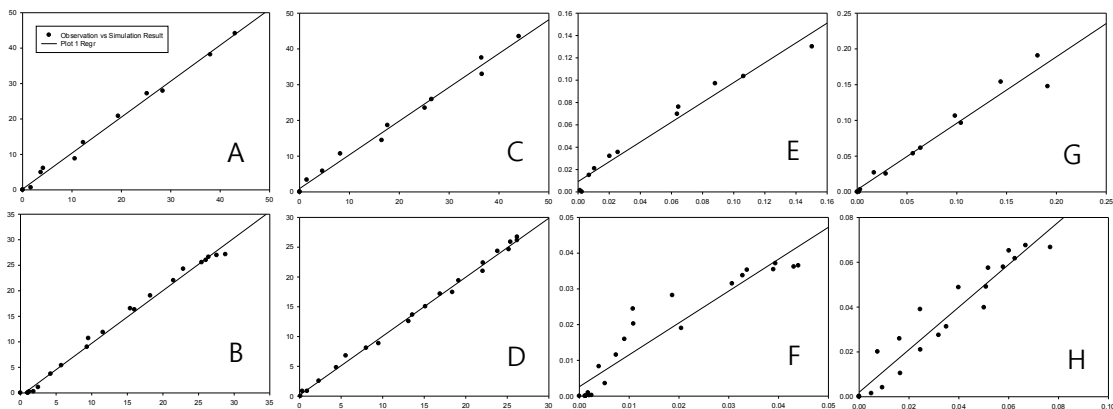
- I8IN/2010/07/21 [STREAM/YYYY/MM/DD]

A	Cl Injection A Reach1	C	Cl injection B Reach1	E	PO <sub>4</sub> Injection A Reach1	G	NH <sub>4</sub> injection B Reach1
B	Cl Injection A Reach2	D	Cl injection B Reach2	F	PO <sub>4</sub> Injection A Reach2	H	NH <sub>4</sub> injection B Reach2



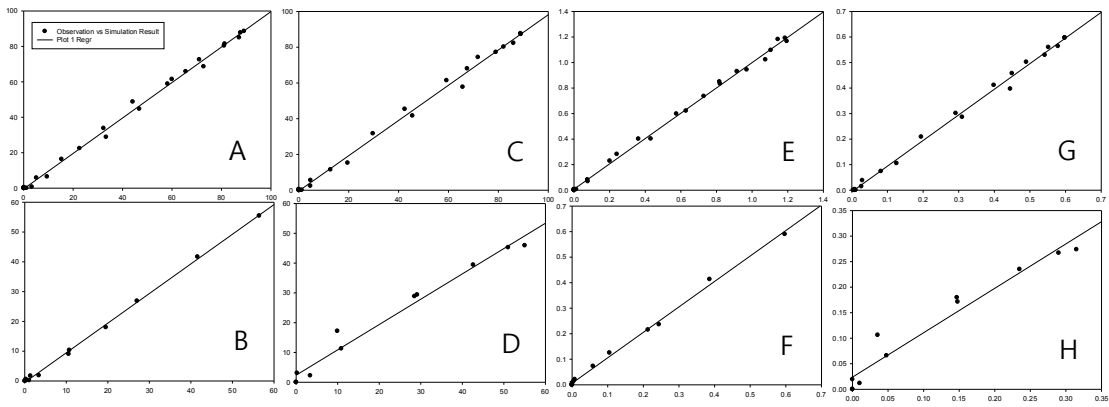
	A	B	C	D	E	F	G	H
R <sup>2</sup>	0.8846	0.9947	0.9817	0.9950	0.9287	0.9799	0.9803	0.9963

- I8IN/2010/07/28 [STREAM/YYYY/MM/DD]



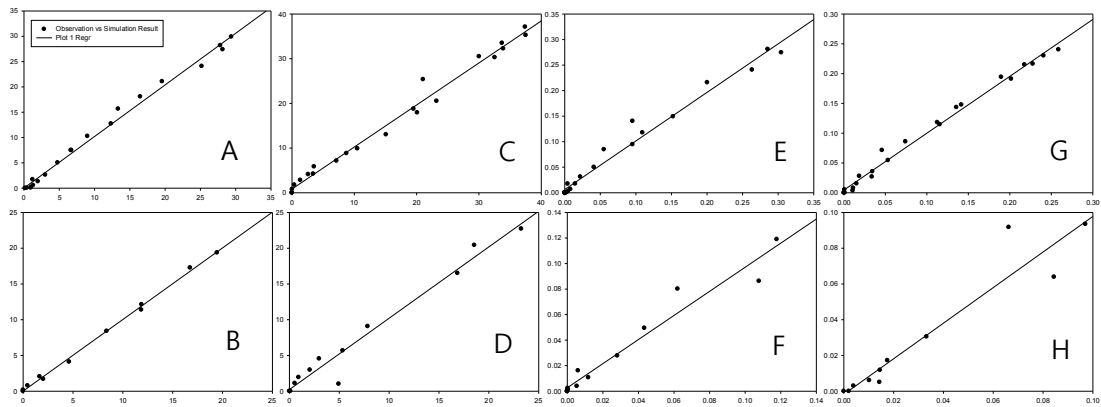
	A	B	C	D	E	F	G	H
R <sup>2</sup>	0.9935	0.9981	0.9932	0.9966	0.9896	0.8746	0.9613	0.9394

- 18IN/2010/09/18 [STREAM/YYYY/MM/DD]



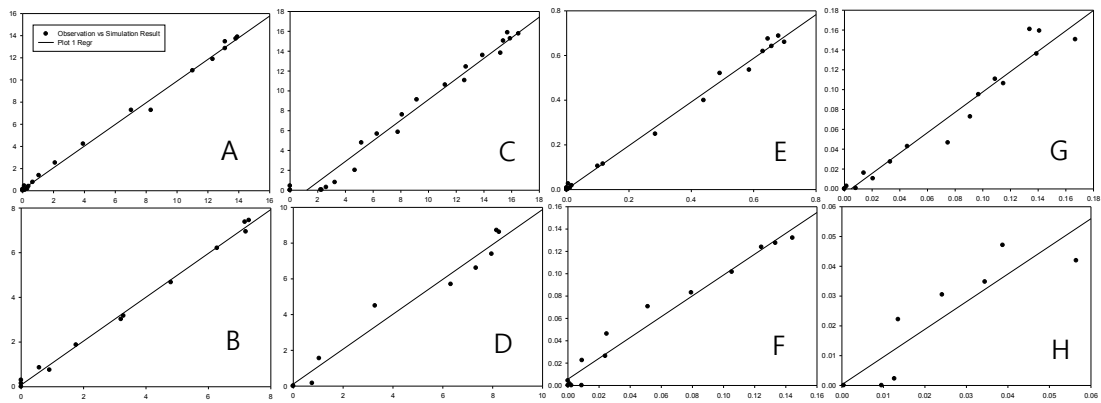
	A	B	C	D	E	F	G	H
$R^2$	0.9968	0.9985	0.9969	.0.9981	0.9974	0.9964	0.987	0.9969

- 18IN/2010/09/25 [STREAM/YYYY/MM/DD]



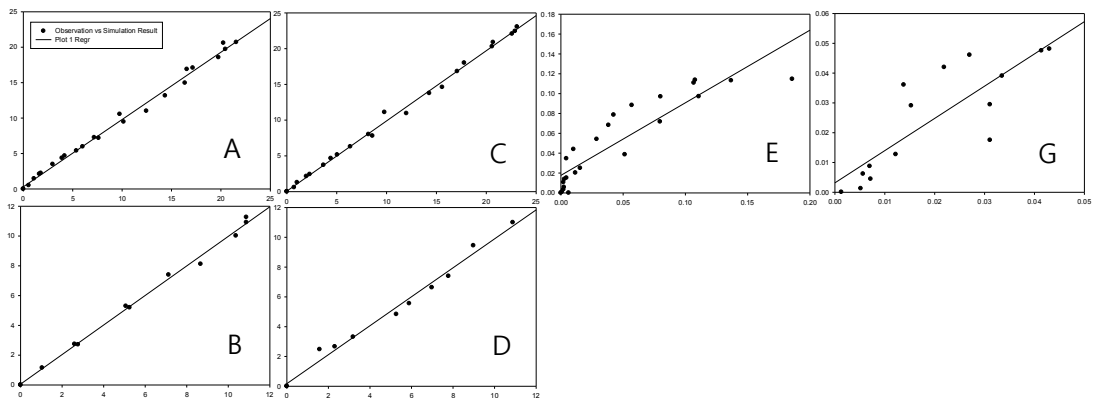
	A	B	C	D	E	F	G	H
$R^2$	0.9963	0.9961	0.9899	0.9736	0.9831	0.962	0.9806	0.9553

- I8IN/2011/06/06 [STREAM/YYYY/MM/DD]



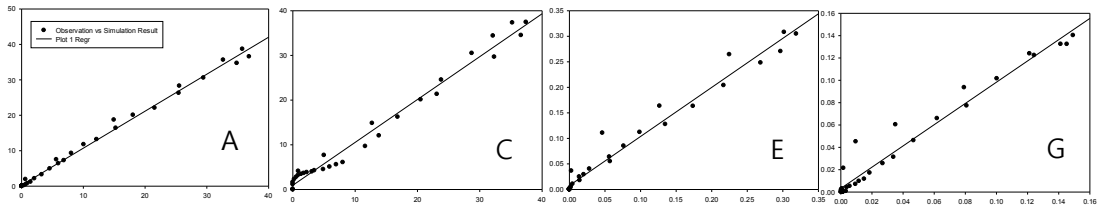
	A	B	C	D	E	F	G	H
R <sup>2</sup>	0.9967	0.9963	0.9868	0.9739	0.9941	0.9647	0.9537	0.7278

- I8IN/2011/06/12 [STREAM/YYYY/MM/DD]



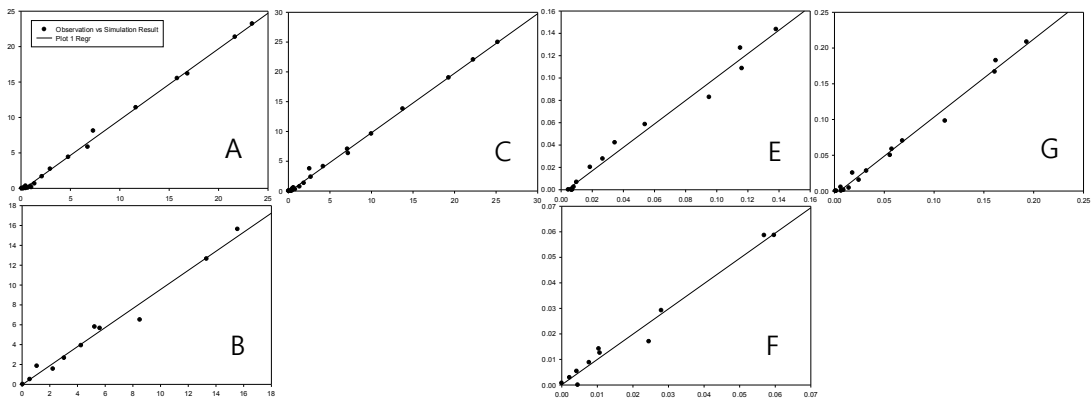
	A	B	C	D	E	F	G	H
R <sup>2</sup>	0.9959	0.9661	0.9966	0.9875	0.8041		0.7023	

- I8IN/2011/07/19 [STREAM/YYYY/MM/DD]



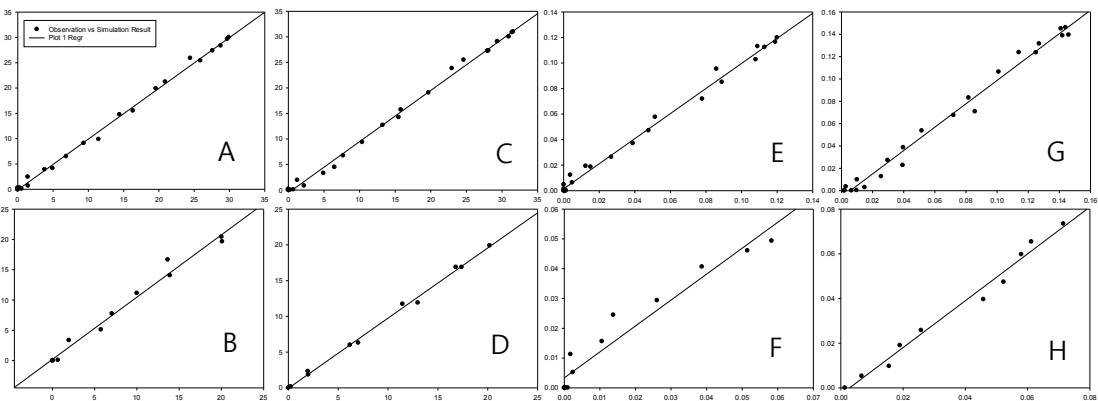
	A	B	C	D	E	F	G	H
R <sup>2</sup>	0.9943		.9837		0.9845		0.9654	

- I8OUT/2010/07/19 [STREAM/YYYY/MM/DD]



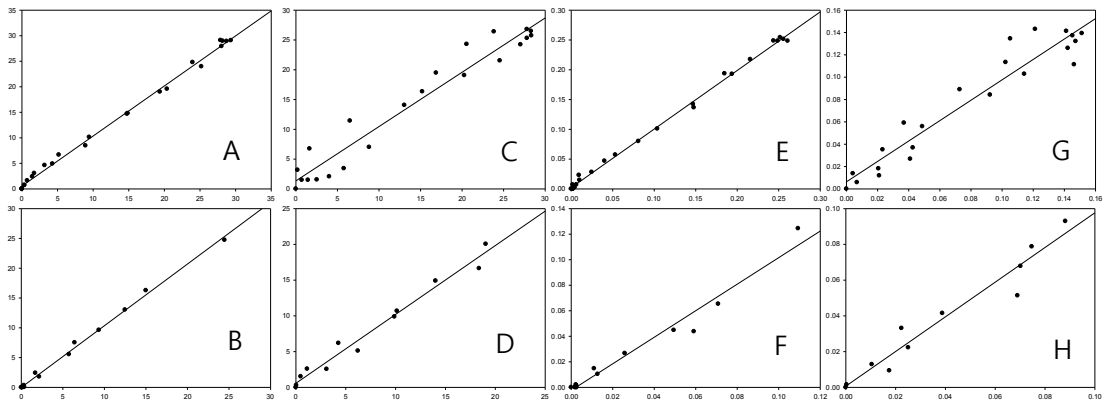
	A	B	C	D	E	F	G	H
R <sup>2</sup>	0.9978	0.9798	0.9975		0.9840	0.9776	0.9901	

- I8OUT/2010/07/26 [STREAM/YYYY/MM/DD]



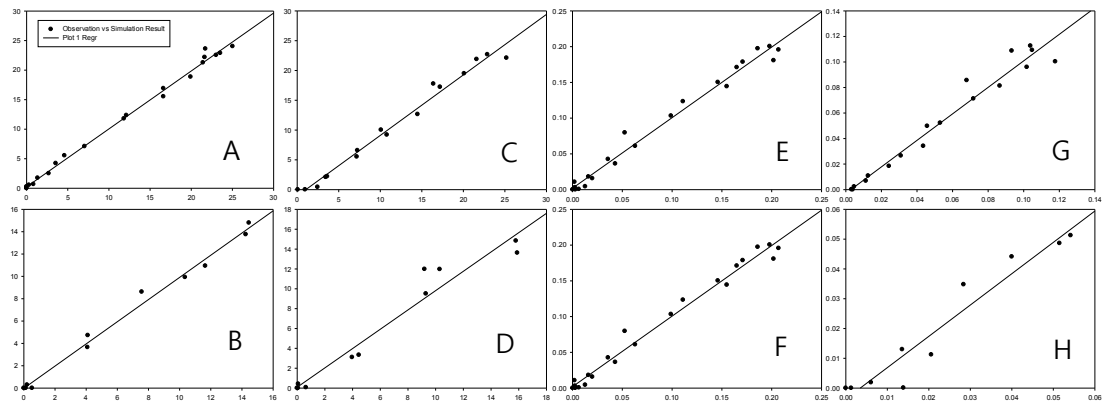
	A	B	C	D	E	F	G	H
R <sup>2</sup>	0.9975	0.9980	0.9963	0.9969	0.9929	0.9723	0.9878	0.9845

- I8OUT/2010/09/16 [STREAM/YYYY/MM/DD]



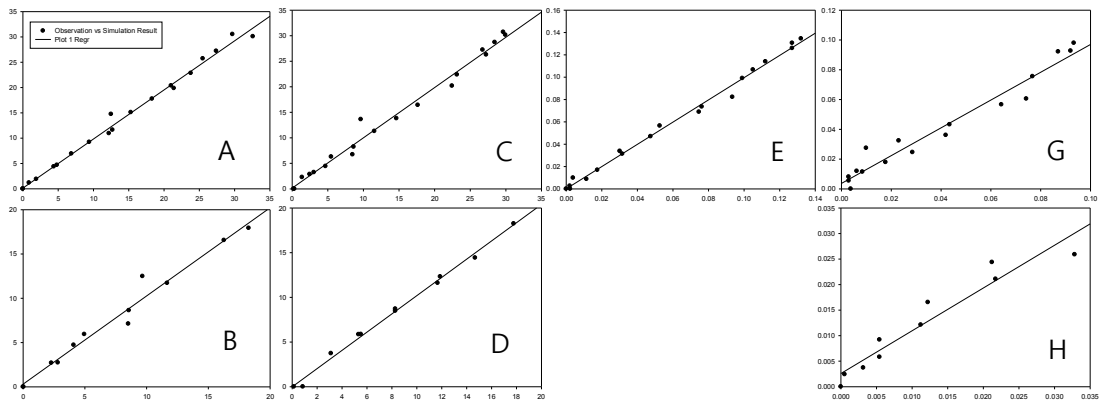
	A	B	C	D	E	F	G	H
R <sup>2</sup>	0.9959	0.9988	0.9969	0.9991	0.9959	0.9633	0.9805	0.9349

- I8OUT/2011/06/04 [STREAM/YYYY/MM/DD]



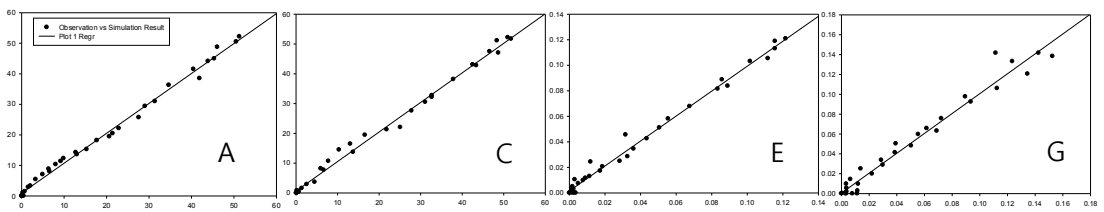
	A	B	C	D	E	F	G	H
R <sup>2</sup>	0.9949	0.9911	0.9840	0.9494	0.9833	0.9859	0.9614	0.9336

- I8OUT/2011/06/10 [STREAM/YYYY/MM/DD]



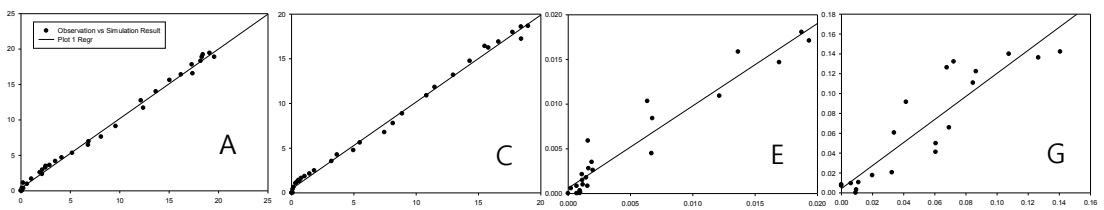
	A	B	C	D	E	F	G	H
R <sup>2</sup>	0.9925	0.9779	0.9861	0.9945	0.9589		0.9579	0.9213

- I8OUT/2011/07/16 [STREAM/YYYY/MM/DD]



	A	B	C	D	E	F	G	H
R <sup>2</sup>	0.9941		0.9934		0.9858		0.9237	

- I8OUT/2011/09/02 [STREAM/YYYY/MM/DD]



	A	B	C	D	E	F	G	H
R <sup>2</sup>	0.9955		0.9957		0.9237		0.8222	

### Appendix 3 Result of Metrics

Stream	Date	Injection	qs [m3s-1m-1]		ts [s]		Ls [m]		RSF		As/A	
			R1	R2	R1	R2	R1	R2	R1	R2	R1	R2
I8In	20100721	A	0.005971	0.0024	55.00024	174.4485	124.9867	310.9796	0.126979	0.125427	0.248	0.215
		B	0.009962	0.00606	33.595	87.34331	74.91807	123.1619	0.120031	0.064576	0.277	0.264
	20100728	A	0.001342	0.000488	114.4698	513.5019	138.641	381.0212	0.281181	0.147022	0.193	0.223
		B	0.000386	0.000193	340.7286	49220.73	481.2807	965.0483	0.240823	0.768134	0.167	8.697
	20100918	A	0.001869	0.000922	87.99975	227.3368	126.3439	256.0688	0.088497	0.086602	0.195	0.166
		B	0.001725	0.001199	93.77263	207.155	136.8646	196.824	0.002072	0.024979	0.190	0.200
	20100925	A	0.000156	0.000172	729.2711	62201.17	705.0804	641.069	0.87949	0.1285	0.106	9.320
		B	0.001645	0.00089	108.3666	322.4433	66.87907	123.5957	0.002149	0.025735	0.239	0.319
	20110606	A	0.000199	0.000117	396.6792	11450.13	340.748	581.2459	0.377167	6.428664		
		B	0.000203	0.000312	376.0209	586.9006	333.4601	216.9276	0.020416	0.293698	0.131	2.334
	20110612	A	5.28E-05	4.32E-05	1340.517	10673.06	538.7223	658.0294	0.063019		0.122	0.316
		B	6.12E-05	7.43E-05	1091.092	8245.275	464.1732	382.6753	0.028171		0.139	0.891
	20110719	A	0.000505		271.7232		388.2897		0.408307		0.127	1.226
		B	0.000334		1920.218		588.3495		2.179094		0.169	
I8OUT	20100719	A	0.000927	0.001565	234.4568	258.8562	269.5661	159.7688	0.067307	0.170648	0.729	
		B	0.001046		194.8075		238.9479	none	0.044455			
	20100726	A	0.002493	0.002227	110.2735	393.9184	132.2756	148.0523	0.375578	0.390733	0.227	0.408
		B	0.002883	0.00244	96.77846	371.538	114.3778	135.1205	0.065477	0.050278	0.221	
	20100916	A	0.000528	0.000376	475.2446	692.3577	354.1661	498.1234	0.282138	0.000592	0.281	0.530
		B	0.000469	0.000655	578.4271	632.6165	399.2677	285.5119	0.032941	0.026076	0.287	0.556
	20110604	A	0.000757	0.000652	406.7281	991.1326	198.0138	230.0622	0.470082	0.233488	0.266	0.235
		B	0.001241	0.000137	265.9661	1085.767	120.8009	1092.186	0.128229	0.01213	0.281	0.377
	20110610	A	0.000248	0.000128	1004.231	7628.102	294.2576	571.6138	1.050488			
		B	0.000202	0.001131	1594.058	483.5796	361.5876	64.50473	0.047144	0.865701	0.372	0.601
	20110716	A	0.000461		716.3286		295.9229		0.419907		0.432	0.107
		B	0.00062		460.472		220.1123		0.13711		0.322	0.840
	20110902	A	0.000241		788.1633		272.1445		0.480077		0.400	0.727
		B	0.000198		1297.353		330.2805		0.044884		0.412	

### Appendix 4 Result of the ratio of nutrient to tracer masses

Stream	Date @ Reach	Inj Mass	Sim Mass	OBS Mass	SIM / INJ	OBS / SIM	Inj Mass	Sim Mass	OBS Mass	SIM / INJ	OBS / SIM
		Ratio of PO <sub>4</sub> _P : Cl					Ratio of NH <sub>4</sub> _N : Cl				
18In	20100721 @ R1	0.009298	0.005533	0.00772	0.595098295	0.83019885	0.008392	0.007464	0.008553	0.889413	1.019199
	20100721 @ R2	0.009298	0.005431	0.00631	0.584125901	0.678562857	0.008392	0.007033	0.009264	0.838041	1.103899
	20100728 @ R1	0.005848	0.002749	0.002819	0.470015736	0.482020478	0.005315	0.003658	0.003997	0.688176	0.752078
	20100728 @ R2	0.005848	0.001387	0.001228	0.237239626	0.209908963	0.005315	0.002438	0.002185	0.458723	0.411076
	20100918 @ R1	0.015747	0.012824	0.012238	0.814393523	0.777184735	0.006917	0.006533	0.006868	0.944434	0.992985
	20100918 @ R2	0.015747	0.009826	0.008833	0.624031341	0.560936693	0.006917	0.005511	0.005171	0.796746	0.747634
	20100925 @ R1	0.015899	0.007549	0.006863	0.474803835	0.431641691	0.006877	0.006694	0.00641	0.973372	0.932022
	20100925 @ R2	0.015899	0.005286	0.004853	0.332436952	0.305207977	0.006877	0.004493	0.003988	0.653349	0.57993
	20110606 @ R1	0.0878	0.040079	0.048961	0.456480498	0.557643502	0.020755	0.01195	0.00926	0.575781	0.446162
	20110606 @ R2	0.0878	0.013518	0.014612	0.153968259	0.166428558	0.020755	0.004606	0.005212	0.221921	0.251102
	20110612 @ R1	0.029017	0.004646	0.004602	0.160120341	0.158613724	0.007715	0.001785	0.002044	0.231388	0.264941
	20110612 @ R2										
	20110719 @ R1	0.015095	0.006535	0.006536	0.432911028	0.433000806	0.007106	0.002621	0.003218	0.368878	0.452892
	20110719 @ R2										
	20100719 @ R1	0.013983	0.005603	0.007665	0.400686938	0.548146023	0.017397	0.007895	0.008237	0.453819	0.473482
20100719 @ R2	0.013983	0.003499	0.003679	0.25025542	0.263090691						
20100726 @ R1	0.007539	0.003304	0.003365	0.438282602	0.446396587	0.006364	0.00452	0.004955	0.710276	0.778662	
20100726 @ R2	0.007539	0.001924	0.001708	0.255182869	0.226615839	0.006364	0.003362	0.003564	0.528285	0.559968	
20100916 @ R1	0.015493	0.007082	0.007622	0.45712313	0.491958146	0.006798	0.005102	0.006215	0.750528	0.914311	
20100916 @ R2	0.015493	0.004157	0.005913	0.26828056	0.381631851	0.006798	0.004451	0.004717	0.654823	0.69384	
20110604 @ R1	0.015731	0.006138	0.006689	0.390181692	0.42523851	0.008899	0.00412	0.004069	0.463016	0.457241	
20110604 @ R2	0.015731	0.003733	0.004393	0.237336505	0.279263385	0.008899	0.002608	0.004145	0.293116	0.465759	
20110610 @ R1	0.017327	0.003357	0.003792	0.193740477	0.218840038	0.007831	0.00295	0.002967	0.376692	0.378886	
20110610 @ R2						0.007831	0.001063	0.001168	0.135755	0.149117	
20110716 @ R1	0.006241	0.001728	0.001845	0.276873689	0.295600773	0.005609	0.002364	0.002471	0.421471	0.440629	
20110716 @ R2											
20110902 @ R1	0.007289	0.000712	0.000753	0.097682819	0.10325885	0.008397	0.00724	0.00755	0.862215	0.899099	
20110902 @ R2											